SOUND PROPAGATION IN SMALL DIAMETER TUBES

Thesis by
Everett Truman Eiselen

In Partial Fulfillment of the Requirements
For the Degree of
Doctor of Philosophy

California Institute of Technology
Pasadena, California
1962

ACKNOWLEDGEMENTS

The author wishes to express his appreciation to Dr. T. K. Caughey for his many helpful suggestions and his encouragement during the course of this work.

He is grateful to the Shell Oil Company and the National Science Foundation for their financial support of part of this study.

The computational work was done at the Western Data Processing Center at UCLA, whose facilities made this investigation possible.

He also wishes to thank Barbara Rickert for typing the manuscript, and Beverly McAllister for helping with the preparation of the data and figures.

ABSTRACT

A detailed study of the propagation of sound in small diameter tubes has been made. The physical configuration studied, is typical of instrument systems. The transient response has been determined in addition to the frequency response. The solutions have been programmed on a high speed digital computer and evaluated.

Several approximate solutions have been compared. Iberall's results have been expanded to provide a solution of the transient problem. The range of applicability of the various approximations, and their deviation from the more precise solution including heat conduction, has been determined. A detailed analysis of the restrictions that are made on the more precise solution is given.

The results have been put in a dimensionless form to provide more general applicability. The proper parameter to describe the damping of the tube has been determined. A knowledge of this parameter and the volume on the end of the tube permits a quite accurate prediction of the response of the system. The value of this parameter required for optimization has been found.

TABLE OF CONTENTS

LIST OF FIGURES

NOTATION

A, B, C = constants

E = internal energy

F = a forcing function

$H(\tau)$ = the Heaviside step function

L = length of the tube

Q = assumed solution of equation 2.32; also the part of that solution that is a function of r alone

Q_1, Q_2 = the two solutions of equation 2.21; also the part of those solutions that is a function of r alone

R = inside radius of the tube

$\mathcal{R}$ = gas constant

T = absolute temperature

V = instrument volume at the end of the tube

X = body force acting on fluid in the x direction

a = area of the tube = πR^2

b = Newton velocity of sound = $\sqrt{p_o/\rho_o}$

c = Laplace velocity of sound = $\sqrt{\gamma p_o/\rho_o}$

c_T = velocity of sound appropriate to the polytropic process in the tube

c_I = velocity of sound appropriate to the polytropic process in the instrument volume

c_p = specific heat at constant pressure

c_v = specific heat at constant volume

f_{px} = force in x direction due to the variation of the pressure as a function of x

f_{fx} = force in x direction due to the viscous friction

i = $\sqrt{-1}$

k = thermal conductivity

m = mass

p = absolute pressure

$\tilde{p}$ = dimensionless pressure = $(p-p_o)/p_o$, sometimes used to represent only the r-dependent part of the pressure

q = particle velocity in the radial direction

q_h = the part of the radial velocity that comes from solving the homogeneous equation

r = radial coordinate

$\tilde{r}$ = dimensionless radial coordinate = r/R

s = Laplace transform variable

$\tilde{s}$ = dimensionless Laplace transform variable = sL/c_T

s = condensation

t = time

u = average velocity in the x direction

$\tilde{u}$ = dimensionless average velocity in the x direction

$$= \frac{u\mu L}{p_o R^2} = \frac{uc_T}{\psi b^2}$$

v = particle velocity in the x direction

$\tilde{v}$ = dimensionless particle velocity in the x direction

$$= \frac{v\mu L}{p_o R^2} = \frac{vc_T}{\psi b^2}$$

v_h = the part of the particle velocity in the x direction that comes from solving the homogeneous equation

x = axial coordinate

Φ = the dissipation function

Γ = dimensionless function that includes the effects of heat conduction

a = a real number

β = dimensionless coefficient = $\sqrt{\zeta\zeta'}/\psi$

γ = ratio of the specific heats = c_p/c_v

δ = $d\zeta/d\xi$

δ_L = low-frequency approximation of δ

δ_F = full-frequency expression for δ

δ_H = high-frequency approximation of δ

ζ = dimensionless specific acoustic impedance per unit length, the subscripts L, F and H have the same meaning as above

η_1, η_2 = the two roots of equation 2.24

θ = temperature excess

$\tilde{\theta}$ = dimensionless temperature excess = $\theta c_v/b^2$, sometimes used to represent only the r-dependent part of the temperature excess

κ = thermal diffusivity = $k/\rho c_v$

λ = coefficient giving the x dependence of p, θ, etc.

$\tilde{\lambda}$ = dimensionless coefficient = λL

μ = coefficient of absolute viscosity

μ' = second coefficient of absolute viscosity

ν = coefficient of kinematic viscosity

ν' = second coefficient of kinematic viscosity

ν^o = $(\frac{1}{3}\nu + \nu')$

ξ = dimensionless Laplace transform variable = $\frac{R^2 s}{\nu} = \psi\tilde{s}$

ρ = density

σ = Prandtl's number = $\mu c_p/k$

τ = dimensionless time = tc_T/L

υ = dimensionless instrument volume = Vc_T^2/aLc_I^2

ϕ = angular coordinate in a cylindrical system

χ = dimensionless axial coordinate = x/L

ψ = dimensionless tube parameter = $R^2 c_T/\nu L$

ω = angular frequency

A subscript zero on a symbol indicates the initial, quiescent value of the quantity represented by that symbol.

for example:

T_o, p_o, ρ_o, etc.

An asterisk * after a symbol indicates the Laplace transform of that symbol.

$$v^* = \int_0^\infty ve^{-st}\,dt$$

for example:

p^*, $\vec{v}^*$; θ^*, u^*, s^*, F^*, etc.

An arrow $\rightarrow$ over a symbol indicates that the symbol is a vector which includes all three space components. The same symbol without the arrow represents the x component of that vector.

for example:

$\vec{v}$, v, $\vec{v}_o$, v_o, $\vec{X}$, X, etc.

Wherever possible, the following representations are used to distinguish the curves obtained by using the various approximations.

low-frequency approximation (LF) ——— · ——— · ———

full-frequency approximation (FF) —— —— —— —— —— ——

high-frequency approximation (HF) — — — — — — — — — — —

theory with heat conduction (HC) ————————————

modified low-frequency approximation (MLF) ——— ·· ———

Optimum Response:

For the purposes of this work, optimum response is arbitrarily defined as that response which rises to 99% of its final value in a minimum time, and has less than 1% overshoot when a pressure step is applied to the end of the tube.

COMMENTS ON THE NOTATION

The quantities $\tilde{s}$, τ, ψ and υ, as defined here are used in both the first and the second sections of the Analysis. In Section One, the parameter c_T can take on any value between b and c, the Newton and Laplace velocities of sound, respectively. This permits the investigation of the results of considering the process in the tube as polytropic. However, in Section Two, since heat conduction in the tube is rigorously taken into account, c_T must be set equal to c. If it is desired to consider the process in the instrument volume as polytropic, c_I can be adjusted to take this into account in either Section One or Section Two. In general c_I would not equal c_T because of the different geometries involved.

VALUES OF THE PHYSICAL PARAMETERS USED

For the purpose of numerical calculations, it was assumed that the sound was being propagated through air under the conditions:

pressure,

$$p_o = 1 \text{ atm} = 760 \text{ mm Hg}$$

temperature,

$$T_o = 300^{\circ}\text{K} .$$

Air under these conditions has the following properties (9).

$$c = 1,139.5 \text{ ft/sec} = 13,674 \text{ in/sec}$$

$$\mu = 2.678 \times 10^{-9} \text{ lb-sec/in}^2$$

$$\rho_o = 1.101 \times 10^{-7} \text{ lb-sec}^2/\text{in}^4$$

$$\nu = 2.432 \times 10^{-2} \text{ in}^2/\text{sec}$$

$$\gamma = 1.4017$$

$$\sigma = 0.708$$

In figure 12, data for Argon, under the same conditions as above, are given. The pertinent properties (9) are:

$$\gamma = 1.670$$

$$\sigma = 0.677.$$

Where the orders of magnitude of the various approximations are calculated, it is assumed that the tube has the inside radius:

$$R = 0.1 \text{ in.}$$

Of course, accurate results can be obtained, using the methods presented here, even when the tube under consideration has a radius differing greatly from that assumed above.

I. INTRODUCTION

In recent years, engineers have been faced more and more often with the problem of measuring rapidly fluctuating pressures. As a result, the manufacturers of pressure transducers have developed a wide variety of devices with very short response times. However, it is not always possible for the engineer to place the transducer at the point where the pressure is to be measured. A tube is then used to connect the transducer to the measuring point. When this is done, the effect of the tube on the overall response of the measuring system must be investigated.

To date, the engineer has had little analytical help in designing an optimum system. Previous papers have generally considered only special elementary cases. Delio, Schwent and Cesaro (1) treated the case where the tube and transducer can be reduced to a lumped constant system. Taback (2), and Rohmann and Grogan (3) gave frequency response data for tubes using the electrical transmission line analogy, accurate only for low frequencies. If the engineer was forced to design a system where these restricted analyses did not hold, and little was said about the range of applicability, he was at a loss. Crandall (4) discussed the specific acoustic impedance of a tube, giving both high frequency and low frequency approximations, but did not apply his results to a measuring system. He does quote some experimental results verifying his expressions for the high frequency approximation.

Iberall (5), in his now classic paper of 1950, provided a complete analysis, accurate to very high frequencies. He also included the effects of heat conduction. He gave frequency response data for a high frequency approximation as well as for a low frequency approximation. He also presented some data in the middle range (see Appendix B of this work). The expressions he obtained, however, were just too complicated to be evaluated with a reasonable amount of labor.

For the problem of the transient response, Schuder and Binder (6) added the time solution for a step input using the low frequency approximation. The low frequency approximation corresponds to the problem of electrical transmission along a line without leakage. An excellent and complete discussion of transmission line theory is given by Weber (7). In fact, the problem that Schuder solved is the analog of problem 8.12 in Weber.

The traveling wave solution for the high frequency approximation given in Appendix A of this work is shown on page 377 of Weber to give results similar to those obtained in the electrical analogy of a transmission line including skin effects and corona. A traveling wave solution, corresponding to the low frequency approximation is also given in Weber, page 383, but it is not as useful as the high frequency case, because it requires graphical or numerical evaluation.

With the advent of high speed digital computers, the computational difficulties of Iberall's expressions vanish. Complete frequency response data can be obtained easily in all ranges of the frequency spectrum. The results of the various approximations can be compared.

Of even more interest, the transient response for a step input can be obtained, and again the various approximations can be compared. This permits an easy and accurate method of determining the regions in which the approximations are valid, and how much they differ from the more precise solution.

Using the results of the computer, an optimization has been achieved, and because the expressions in this work have been put in dimensionless form, the results can be applied to general problems.

The physical arrangement that is discussed in this work is that of a tube connecting the point at which the measurement is to be made, to a volume associated with the transducer, (fig. 1). It is assumed that the motions of the diaphragm of the transducer are sufficiently small so that they do not affect the size of the instrument volume.

More complicated systems are considered by Taback (2), and Reid and Kops (8) that may be used to obtain the damping necessary for optimization. However, these systems are beyond the scope of this work and empirical data must be used in designs involving them.

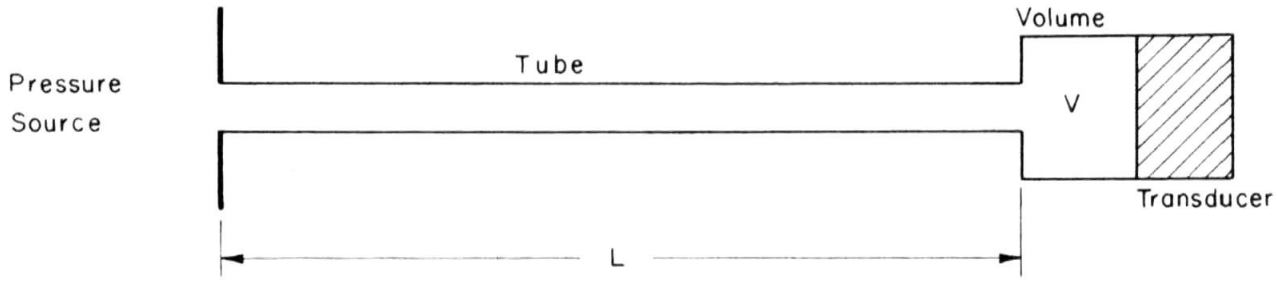

Figure 1. Tube and Transducer System.

II. ANALYSIS

The analysis is broken down into three sections. Section One presents a simple theory to give a feel for the concepts involved in the problem and the sort of results to be expected. In the simple theory, the momentum equation is obtained by an intuitive treatment of the forces on the fluid. The continuity equation considers only the average velocity across the tube. The pressure is assumed constant over a cross section. The effects of heat conduction in the tube are incorporated by the stratagem of considering the process in the tube as being polytropic. Two approximate solutions are obtained for the extreme cases by taking a two term expansion of the general solution.

In Section Two, a more precise derivation is presented. The starting point is the equations of fluid mechanics in their most general form. The results are made manageable, so that useful engineering information can be obtained, by imposing restrictions on the solutions. A detailed analysis is given of the effects of these restrictions. It is shown that the assumptions of Section One are justified. In fact, the more precise solution obtained here reduces to the general solution obtained before if the tube is made of an insulating material.

The end results of Sections One and Two are the Laplace transforms of the pressure at the end of the tube. Section Three presents and compares the methods used to obtain the time solutions from these expressions.

SECTION ONE

SIMPLE THEORY

A first approximation to the problem of sound propagating in a small diameter tube is obtained under the assumptions:

1. The medium through which the sound is propagating is a perfect gas.
2. The ratio of the particle velocity to the velocity of sound is small.
3. The pressure variation is independent of the radius r, i.e., it is a function only of time and axial position along the tube.
4. The radial velocity is zero.
5. The problem is axially symmetric, i.e., there is no dependence on ϕ.
6. The process in the tube is polytropic. The velocity of sound associated with the polytropic constant is c_T. In the limits, if $c_T = c$, the process is adiabatic; if $c_T = b$, the process is isothermal.
7. The process in the instrument volume is polytropic. The velocity of sound associated with this polytropic constant is c_I. In general c_I would not equal c_T because of the different geometries.
8. The pressure is uniform throughout the instrument volume, and therefore a function only of time.

The assumptions 3 and 4 will be justified in Section Two. A precise definition of "small" will also be given.

Momentum Equation

In order to derive the proper form of the momentum equation consistent with the above assumptions, a tubular element of fluid is considered, (fig. 2). The mass of the tube is

$$dm = \rho 2\pi r dr dx$$

The net pressure force is

$$f_{px} = -\frac{\partial p}{\partial x} dx\, 2\pi r dr$$

The net force acting in the x direction on the cylindrical surfaces of the tube, due to viscous friction is

$$f_{fx} = 2\pi \mu \frac{\partial}{\partial r}\left(r \frac{\partial v}{\partial r} \right) dr dx$$

Setting the forces equal to the mass times the acceleration produces

$$\frac{1}{r}\frac{\partial}{\partial r}\left(r \frac{\partial v}{\partial r}\right) = \frac{1}{\mu}\frac{\partial p}{\partial x} + \frac{\rho}{\mu}\frac{\partial v}{\partial t}$$

This equation is written in the dimensionless form,

$$\frac{1}{\tilde{r}}\frac{\partial}{\partial \tilde{r}}\left(\tilde{r}\frac{\partial \tilde{v}}{\partial \tilde{r}}\right) = \frac{\partial \tilde{p}}{\partial \chi} + \psi \frac{\partial \tilde{v}}{\partial \tau} \qquad (1.1)$$

by the substitutions:

$$\tilde{r} = r/R$$

$$\tilde{v} = v c_T / \psi b^2$$

$$\tilde{p} = (p - p_o)/p_o$$

$$\psi = R^2 c_T / \nu L$$

$$\tau = t c_T / L$$

$$\chi = x/L$$

The Laplace transform of equation 1.1 is formed by multiplying both sides by $e^{\tilde{s}\tau} d\tau$ and integrating from zero to infinity. The Laplace transform

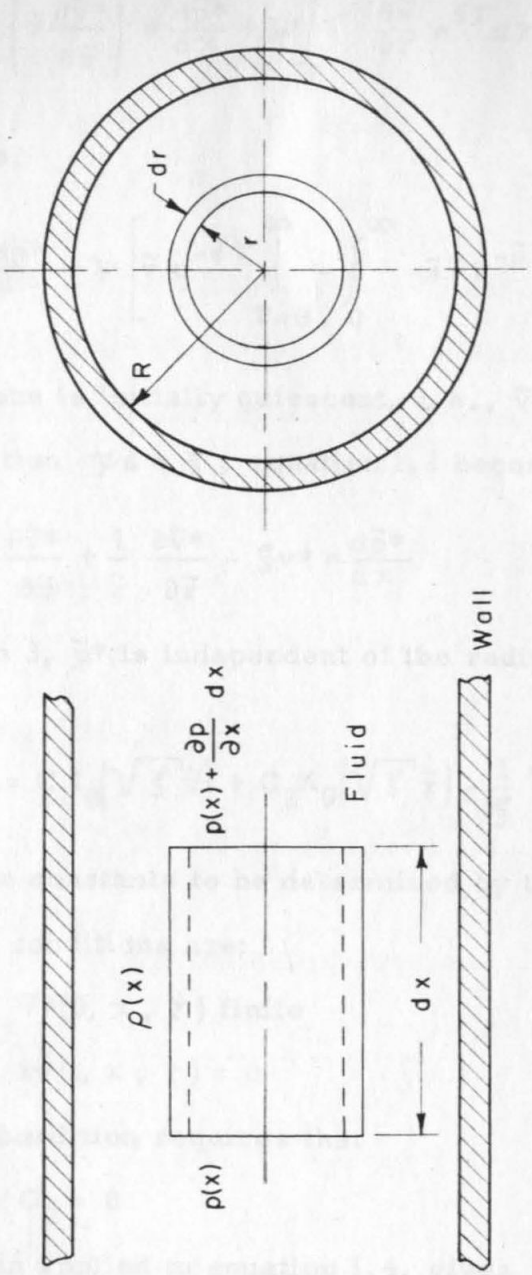

Figure 2. Tubular Element of Fluid

of a variable is denoted by an asterisk.

$$\frac{1}{\tilde{r}} \frac{\partial}{\partial \tilde{r}} \left(\tilde{r} \frac{\partial \tilde{v}^*}{\partial \tilde{r}} \right) = \frac{d\tilde{p}^*}{d\tilde{\chi}} + \psi \int_0^\infty \frac{\partial \tilde{v}}{\partial \tilde{\tau}} e^{\tilde{s}\tilde{\tau}} d\tilde{\tau}$$

Integrating by parts,

$$\frac{1}{\tilde{r}} \frac{\partial}{\partial \tilde{r}} \left(\tilde{r} \frac{\partial \tilde{v}^*}{\partial \tilde{r}} \right) = \frac{d\tilde{p}^*}{d\tilde{\chi}} + \psi \left[\tilde{v} e^{-\tilde{s}\tilde{\tau}} \Big|_{\tau=0}^{\infty} - \int_0^\infty -\tilde{s}\tilde{v} e^{-\tilde{s}\tilde{\tau}} d\tilde{\tau} \right] \tag{1.2}$$

and assuming the tube is initially quiescent, i.e., $\tilde{v}(\tilde{r}, \chi, 0) = 0$, and making the substitution $\psi\tilde{s} = \xi$, equation 1.2 becomes

$$\frac{\partial \tilde{v}^*}{\partial \tilde{r}} + \frac{1}{\tilde{r}} \frac{\partial \tilde{v}^*}{\partial \tilde{r}} - \xi v^* = \frac{d\tilde{p}^*}{d\tilde{\chi}} \tag{1.3}$$

Since by assumption 3, $\tilde{p}^*$ is independent of the radius $\tilde{r}$, the solution of equation 1.3 is

$$\tilde{v}^* = C_1 I_0\left(\sqrt{\xi}\,\tilde{r}\right) + C_2 K_0\left(\sqrt{\xi}\,\tilde{r}\right) - \frac{1}{\xi} \frac{dp^*}{d\chi} \tag{1.4}$$

where C_1 and C_2 are constants to be determined by the boundary conditions.

The boundary conditions are:

$$\tilde{v}^*(0, \chi, \tau) \text{ finite}$$

$$\tilde{v}^*(1, \chi, \tau) = 0$$

The first boundary condition requires that

$$C_2 = 0$$

and the second, when applied to equation 1.4, gives

$$0 = C_1 I_0\left(\sqrt{\xi}\right) - \frac{1}{\xi} \frac{d\tilde{p}^*}{d\chi}$$

hence

$$C_1 = \frac{1}{\xi I_0\left(\sqrt{\xi}\right)} \frac{d\tilde{p}^*}{d\chi}$$

Upon substitution of these values for the constants, equation 1.4 becomes

$$\tilde{v}^* = -\frac{1}{\xi} \frac{d\tilde{p}^*}{d\chi}\left[1 - \frac{I_0\left(\sqrt{\xi}\,\tilde{r}\right)}{I_0\left(\sqrt{\xi}\right)}\right] \tag{1.5}$$

The detailed velocity profile is not important in this problem in light of the assumption that the pressure is independent of the radius $\tilde{r}$. Therefore in the discussion that follows, the average velocity across the tube is used.

$$\tilde{u}^* = \frac{1}{\pi}\int_0^1 \tilde{v}^*\, 2\pi\tilde{r}d\tilde{r} = -\frac{2}{\xi} \frac{d\tilde{p}^*}{d\chi}\int_0^1 \left[\tilde{r} - \frac{\tilde{r}I_0\left(\sqrt{\xi}\,\tilde{r}\right)}{I_0\left(\sqrt{\xi}\right)}\right] d\tilde{r}$$

Carrying out the integration,

$$\tilde{u}^* = -\frac{2}{\xi} \frac{d\tilde{p}^*}{d\chi}\left[\frac{\tilde{r}^2}{2} - \frac{\tilde{r}}{\sqrt{\xi}} \frac{I_1\left(\sqrt{\xi}\,\tilde{r}\right)}{I_0\left(\sqrt{\xi}\right)}\right]_0^1$$

evaluating at the limits and rearranging produces

$$\frac{d\tilde{p}^*}{d\chi} = \frac{-\xi\tilde{u}^*}{1 - \frac{2}{\sqrt{\xi}} \frac{I_1\left(\sqrt{\xi}\right)}{I_0\left(\sqrt{\xi}\right)}} \tag{1.6}$$

or, to simplify the notation,

$$\frac{d\tilde{p}^*}{d\chi} = -\varsigma\tilde{u}^* \tag{1.7}$$

where

$$\varsigma = \frac{\xi}{1 - \frac{2}{\sqrt{\xi}} \frac{I_1\left(\sqrt{\xi}\right)}{I_0\left(\sqrt{\xi}\right)}}$$

The quantity ζ is a specific acoustic impedance per unit length, in dimensionless form. Since $\xi = R^2 s/\nu$, if s is replaced by $i\omega$, it is permissible to speak about equation 1.8 in terms of frequency. Three cases will be considered in this work. If the frequencies of interest are low, ξ will be small and the Bessel functions can be expanded in a power series. If the frequencies of interest are high, ξ will be large and the Bessel functions can be expanded in an asymptotic series. In the more general case, where the frequencies of interest cover the whole spectrum, the complete full-frequency expression of equation 1.8 must be used. The results of these approximations are as follows:

$$\zeta_L = 8 + \frac{4}{3}\xi \qquad \xi < 1$$

$$\zeta_F = \frac{\xi}{1 - \frac{2}{\sqrt{\xi}} \frac{I_1(\sqrt{\xi})}{I_0(\sqrt{\xi})}} \tag{1.9}$$

$$\zeta_H = \xi + 2\sqrt{\xi} \qquad \xi > 100$$

These three cases are compared in figures 3 and 4. The curves are plotted as a function of ξ, for ξ purely imaginary, the real part of ζ in figure 3, the imaginary part of ζ in figure 4.

Continuity Equation

The continuity equation can be derived by considering a cylindrical element of fluid, dx in length, (fig. 5). In this analysis, the average velocity across the tube is used.

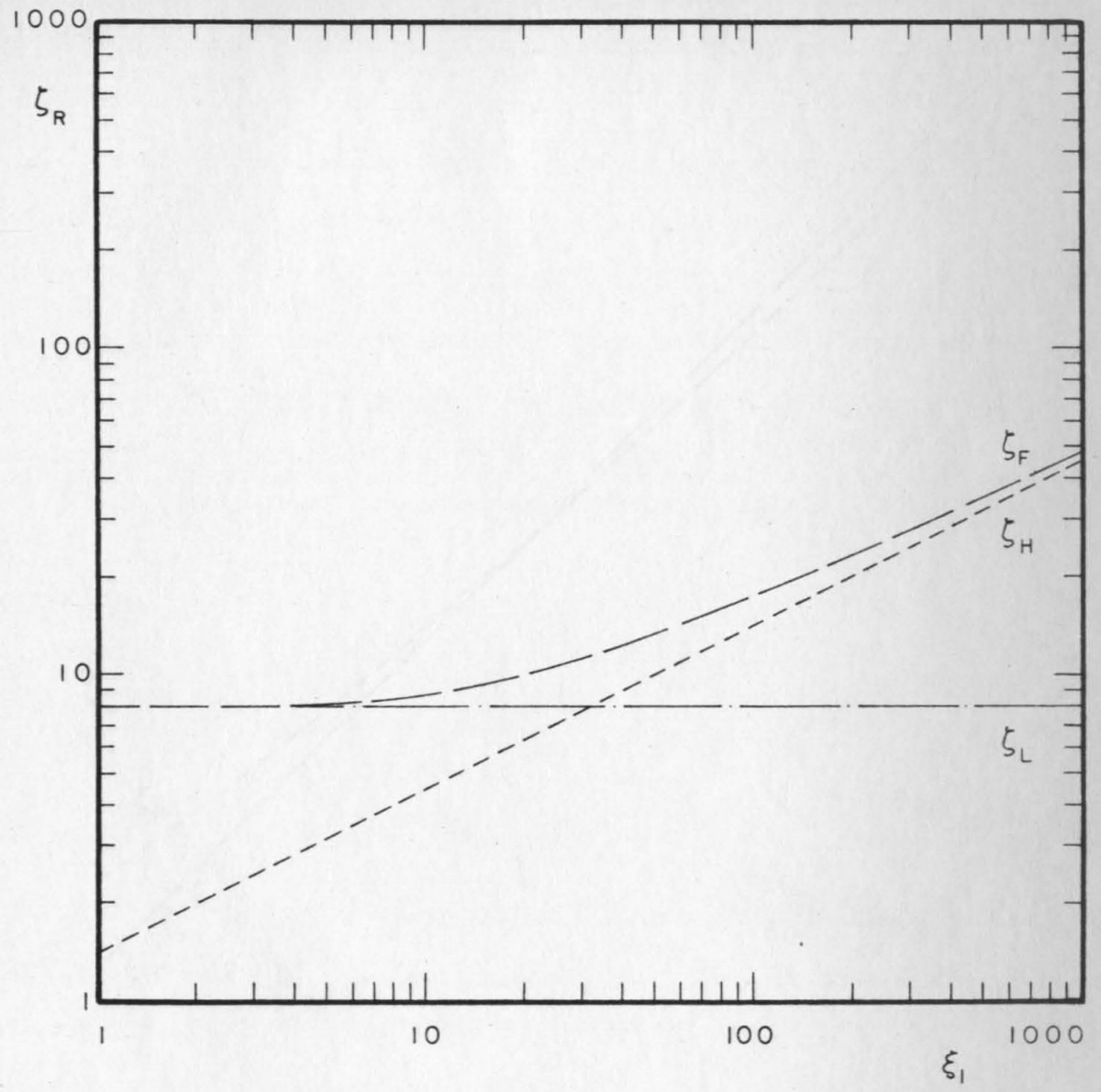

Figure 3. Specific Acoustic Impedance per Unit Length - Real

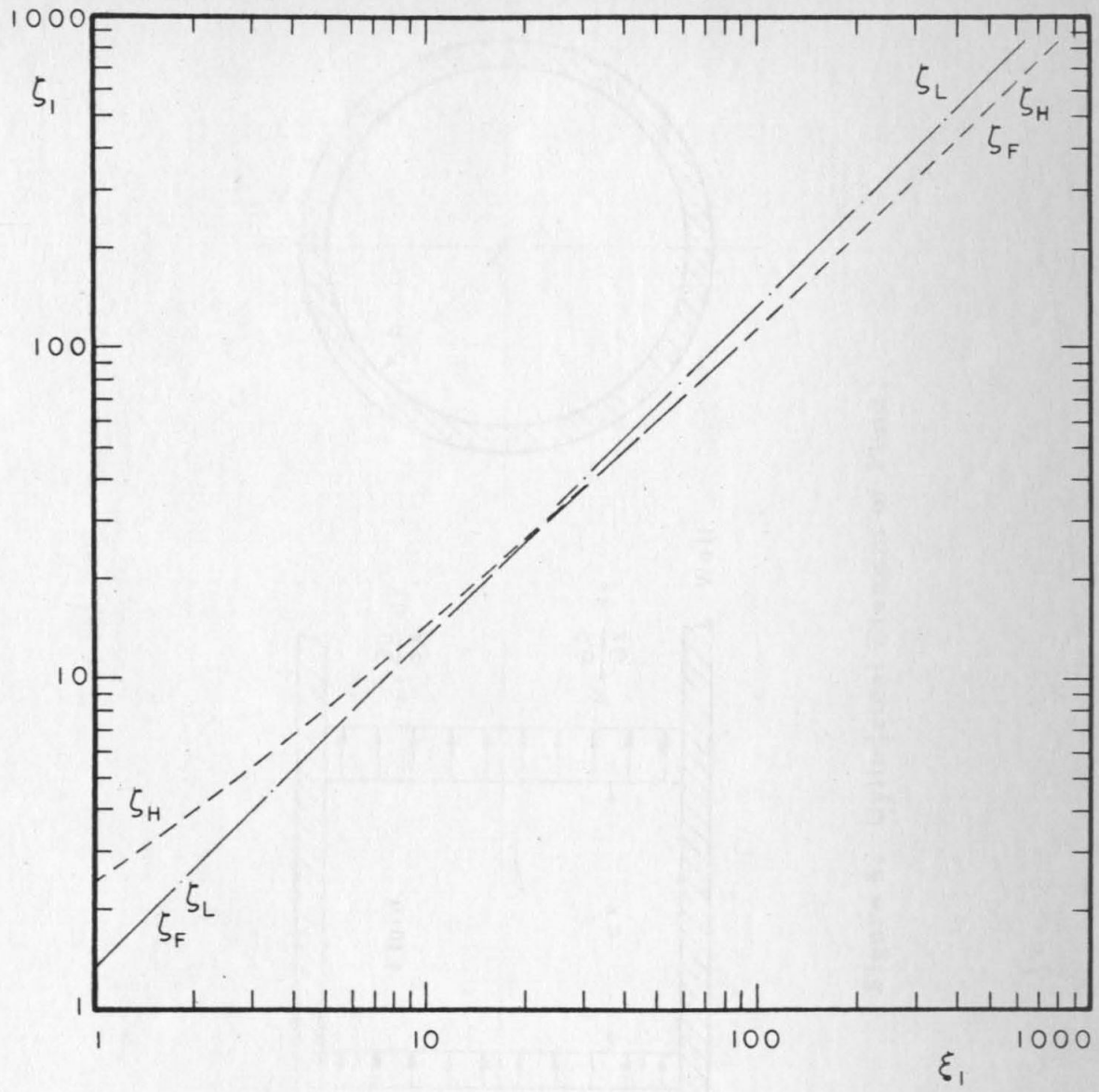

Figure 4. Specific Acoustic Impedance per Unit Length - Imaginary

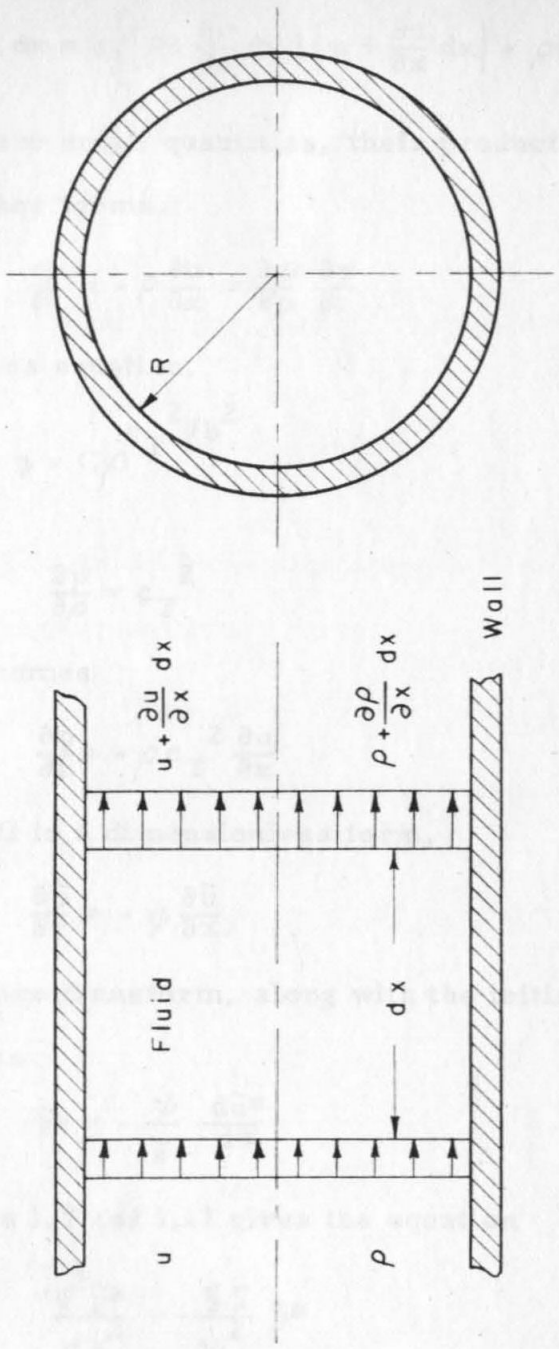

Figure 5. Cylindrical Element of Fluid

The rate of increase of mass in the element is equal to the net rate at which mass flows into the element.

$$-a \frac{\partial \rho}{\partial t} dx = a\left[\left(\rho + \frac{\partial \rho}{\partial x} dx\right)\left(u + \frac{\partial u}{\partial x} dx\right) - \rho u\right]$$

Since u and $\partial \rho / \partial x$ are small quantities, their product can be neglected compared to the other terms.

$$\frac{\partial \rho}{\partial t} = -\rho \frac{\partial u}{\partial x} = \frac{\partial \rho}{\partial p} \frac{\partial p}{\partial t} \tag{1.10}$$

The assumed process equation,

$$p = C\rho^{c_T^2/b^2}$$

implies that,

$$\frac{\partial p}{\partial \rho} = c_T^2$$

so equation 1.10 becomes

$$\frac{\partial p}{\partial t} = -\rho c_T^2 \frac{\partial u}{\partial x} \tag{1.11}$$

Writing equation 1.11 in a dimensionless form,

$$\frac{\partial \tilde{p}}{\partial \tau} = -\psi \frac{\partial \tilde{u}}{\partial \chi}$$

and taking the Laplace transform, along with the initial condition $\tilde{p}(\chi, 0) = 0$, produces

$$\tilde{p}^* = -\frac{\psi}{\tilde{s}} \frac{d\tilde{u}^*}{d\chi} \tag{1.12}$$

Combining equations 1.7 and 1.12 gives the equation

$$\frac{d^2 \tilde{p}^*}{d\chi^2} = \frac{\tilde{s}\tilde{s}}{\psi^2} \tilde{p}^* \tag{1.13}$$

The solution of equation 1.13 is

$$\tilde{p}^* = C_1 e^{+\beta x} + C_2 e^{-\beta x} \tag{1.14}$$

where

$$\beta = \frac{1}{\psi}\sqrt{\zeta\zeta}$$

The real and imaginary parts of β are plotted, for the three different ζ's, in figures 6 and 7, respectively. The independent variable is a purely imaginary ζ, and ψ is set equal to unity.

The constants C_1 and C_2 in equation 1.14 are determined by the boundary conditions on the tube.

$$\tilde{p}(0, \tau) = H(\tau) \tag{1.15}$$

where

$H(\tau)$ is the Heaviside step function.

The Laplace transform of equation 1.15 is

$$\tilde{p}^*(0, \tilde{s}) = \frac{1}{\tilde{s}} \tag{1.16}$$

At $x = 1$ the mass flow rate into the terminal volume equals the rate of mass increase within the volume.

$$\rho a u = V \frac{d\rho}{dt} \tag{1.17}$$

The assumed process equation,

$$p = C\rho^{c_I^2/b^2}$$

implies that

$$\frac{\partial p}{\partial \rho} = c_I^2$$

so that equation 1.17 becomes

$$u = \frac{V}{\rho a c_I^2}\frac{dp}{dt} \tag{1.18}$$

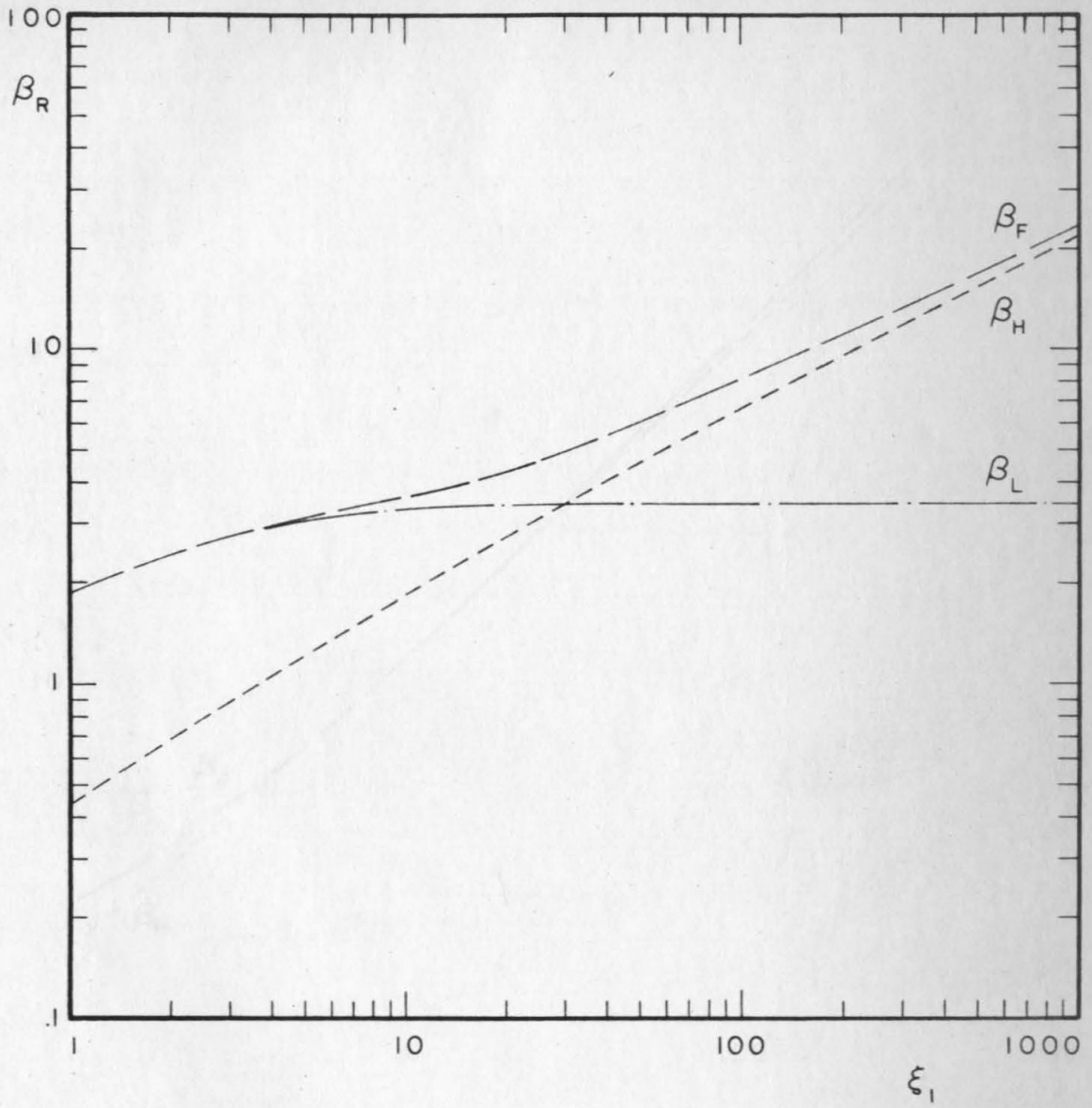

Figure 6. Beta - Real

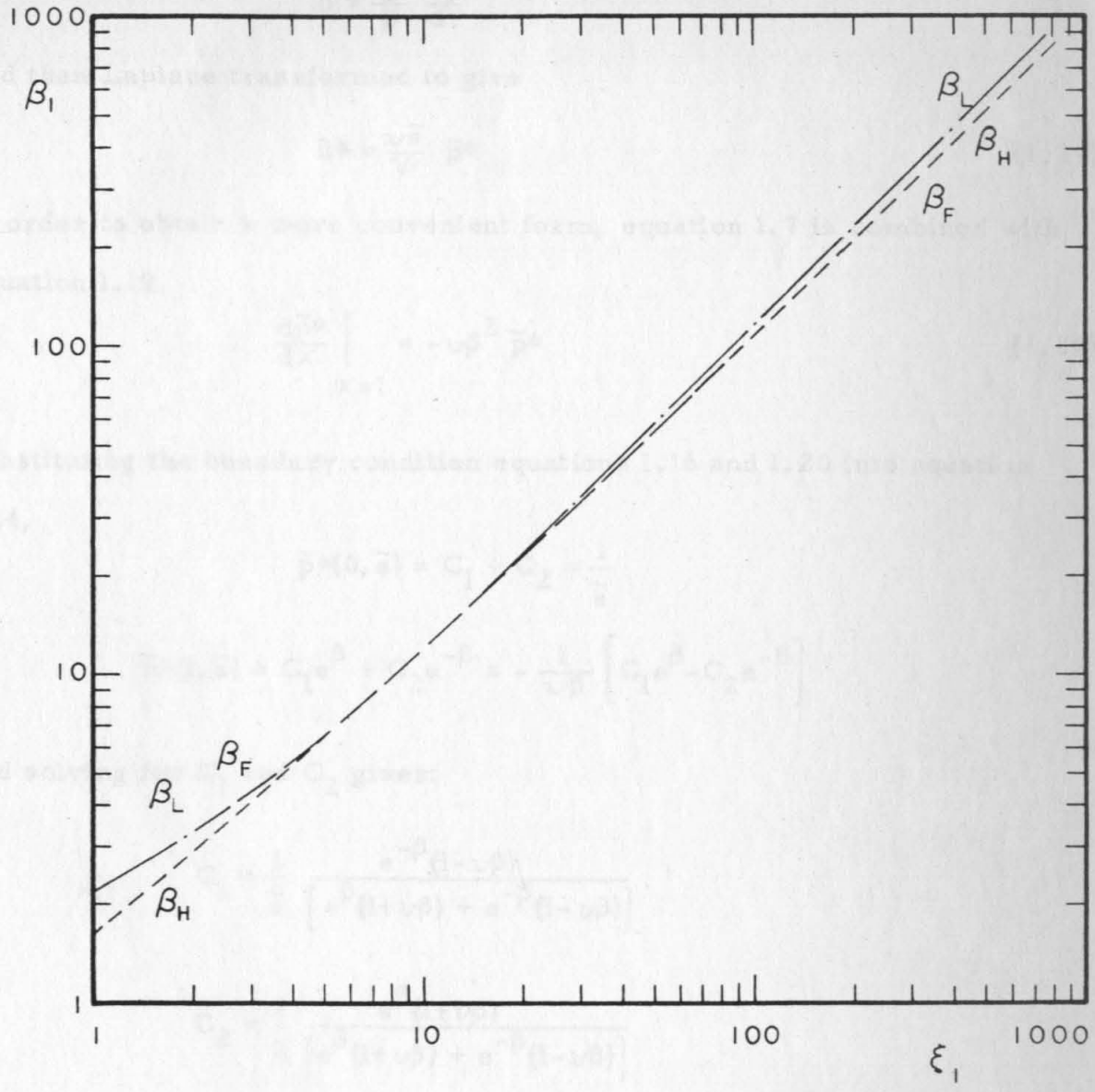

Figure 7. Beta - Imaginary

Equation 1.18 is written in dimensionless form,

$$\tilde{u} = \frac{\nu}{\psi} \frac{d\tilde{p}}{d\tau}$$

and then Laplace transformed to give

$$\tilde{u}^* = \frac{\nu \tilde{s}}{\psi} \tilde{p}^* \tag{1.19}$$

In order to obtain a more convenient form, equation 1.7 is combined with equation 1.19.

$$\left.\frac{d\tilde{p}^*}{dx}\right|_{x=1} = -\nu\beta^2 \tilde{p}^* \tag{1.20}$$

Substituting the boundary condition equations 1.16 and 1.20 into equation 1.14,

$$\tilde{p}^*(0, \tilde{s}) = C_1 + C_2 = \frac{1}{\tilde{s}}$$

$$\tilde{p}^*(1, \tilde{s}) = C_1 e^{\beta} + C_2 e^{-\beta} = -\frac{1}{\nu\beta}\left[C_1 e^{\beta} - C_2 e^{-\beta}\right]$$

and solving for C_1 and C_2 gives:

$$C_1 = \frac{1}{\tilde{s}} \frac{e^{-\beta}(1-\nu\beta)}{\left[e^{\beta}(1+\nu\beta) + e^{-\beta}(1-\nu\beta)\right]}$$

$$C_2 = \frac{1}{\tilde{s}} \frac{e^{\beta}(1+\nu\beta)}{\left[e^{\beta}(1+\nu\beta) + e^{-\beta}(1-\nu\beta)\right]}$$

The pressure at the end of the tube is

$$\tilde{p}^*(1, \tilde{s}) = \frac{2}{\tilde{s}\left[e^{\beta}(1+\nu\beta) + e^{-\beta}(1-\nu\beta)\right]}$$

or

$$\tilde{p}^*(1, \tilde{s}) = \frac{1}{\tilde{s}\left[\cosh\beta + \nu\beta \sinh\beta\right]} \tag{1.21}$$

The frequency response is found by substituting $i\omega$ for s in the expression,

$$\tilde{p}\ (1, \omega) = \frac{1}{\cosh\beta + \nu\beta \sinh\beta} \tag{1.22}$$

where

β is a complex function of ω.

SECTION TWO

THEORY INCLUDING HEAT CONDUCTION

In this section a more precise formulation of the problem is considered. Heat conduction is also included. The only restriction on the motion of the fluid is that the ratio of the particle velocity to the velocity of sound be small compared to unity so that the square of this quantity can be neglected. This implies that the variations in the pressure, density and temperature are also small, compared to their static values, so that products of these terms can be neglected. The physical properties of the medium are functions of the temperature and pressure, but since the variation of these quantities is small, it is assumed that the properties are constant.

The analysis given here from equation 2.11 through equation 2.46 follows very closely the derivation given in Rayleigh (10), sections 348 and 350. It is reproduced here for continuity. Changes have been made in the notation (see Table 1) to make it consistent with other parts of this work. The first part of the analysis is carried out using general vector notation so that the results are independent of the coordinate system chosen.

The equations of motion of the fluid are derived, starting with the equations of fluid mechanics in their most general form (11) consistent with the above assumptions.

Continuity Equation

$$\frac{D\rho}{Dt} = -\rho \nabla \cdot \vec{v}$$

where

$$\frac{D}{Dt} = \frac{\partial}{\partial t} + \vec{v} \cdot \nabla$$

Table 1

Rayleigh	This Work
θ'	$\tilde{\theta}$
s	$\mathcal{s}$
u	v
u'	v_h
q'	q_h
α	$1/T_o$
β	b^2/c_v
μ'	ν
μ''	ν^o
ν	κ
λ	η
m	λ
a	c
h	s
P	F

Other symbols are the same in both works.

Let $\rho = \rho_o(1+\Delta)$. Then, since Δ and $\vec{v}$ are small so that second order terms can be neglected, and dividing by ρ_o,

$$\frac{\partial \Delta}{\partial t} = - \nabla . \vec{v} \tag{2.1}$$

Momentum Equation

$$\rho \frac{D\vec{v}}{Dt} = \rho \vec{X} - \nabla p + (\frac{1}{3}\mu + \mu') \nabla (\nabla . \vec{v}) + \mu \nabla^2 \vec{v} \tag{2.2}$$

It is assumed in this equation that μ and μ' are constants. For the problem under consideration in this work, the body force $\vec{X}$ can be set equal to zero. Using the above assumption and equation 2.1, equation 2.2 becomes

$$\frac{\partial \vec{v}}{\partial t} = - \frac{1}{\rho_o} \nabla p - (\frac{1}{3}\nu + \nu') \nabla \frac{\partial \Delta}{\partial t} + \nu \nabla^2 \vec{v} \tag{2.3}$$

Energy Equation

$$\rho \frac{DE}{Dt} = -p \nabla . \vec{v} + \Phi + k \nabla^2 T \tag{2.4}$$

where Φ is called the dissipation function. It is a quadratic term in the velocities and so may be neglected compared with the other terms in the equation. Substituting into equation 2.4 the equation for the internal energy,

$$E = c_v T$$

and equation 2.1, gives

$$c_v \rho_o \frac{\partial T}{\partial t} = p_o \frac{\partial \Delta}{\partial t} + k \nabla^2 T \tag{2.5}$$

Let θ equal the temperature excess, then equation 2.5 becomes

$$\frac{\partial \theta}{\partial t} = \frac{p_o}{\rho_o c_v} \frac{\partial \Delta}{\partial t} + \frac{k}{\rho_o c_v} \nabla^2 \theta \tag{2.6}$$

Equation of State

$$p = \rho \mathcal{R} T \tag{2.7}$$

In differential form equation (2.7) is

$$\frac{dp}{p} = \frac{d\rho}{\rho} + \frac{dT}{T}$$

then rearranging terms and applying the small variation assumptions

$$dp = p_o \left(\mathcal{s} + \frac{\theta}{T_o} \right)$$

but

$$p = p_o + dp$$

therefore

$$p = p_o \left(1 + \mathcal{s} + \frac{\theta}{T_o} \right) \tag{2.8}$$

Let

$$\tilde{\theta} = \frac{c_v}{b^2} \theta$$

then equation 2.6 becomes

$$\frac{\partial \tilde{\theta}}{\partial t} = \frac{\partial \mathcal{s}}{\partial t} + \kappa \nabla^2 \tilde{\theta} \tag{2.9}$$

where

$$\kappa = \frac{k}{\rho_o c_v}$$

and with the substitution

$$\frac{b^2}{T_o c_v} = \frac{p_o \mathcal{R}}{\mathcal{R} \rho_o T_o c_v} = \frac{\mathcal{R}}{c_v} = (\gamma - 1)$$

equation 2.8 becomes

$$p = p_o \left[1 + \mathcal{s} + (\gamma - 1) \tilde{\theta} \right] \tag{2.10}$$

Combining equations 2.3, 2.9 and 2.10 gives

$$\frac{\partial \vec{v}}{\partial t} + b^2 \nabla \mathcal{A} + (c^2 - b^2) \nabla \tilde{\theta} = \nu \nabla^2 \vec{v} - \nu^o \nabla \frac{\partial \mathcal{A}}{\partial t} \tag{2.11}$$

where

$$\nu^o = \left(\frac{1}{3}\nu + \nu'\right)$$

Rayleigh, following arguments by Stokes, set ν' equal to zero. Quantum mechanics indicates that ν' should not, in general, be set equal to zero (12).

Equations 2.1, 2.9 and 2.11 are Laplace transformed assuming the initial conditions:

$$\tilde{\theta}(0) = 0$$

$$\vec{v}(0) = 0$$

$$\mathcal{A}(0) = 0$$

thus:

$$s \mathcal{A}^* = - \nabla \cdot \vec{v}^* \tag{2.12}$$

$$(s - \kappa \nabla^2)\tilde{\theta}^* = s \mathcal{A}^* \tag{2.13}$$

$$s\vec{v}^* + b^2 \nabla \mathcal{A}^* + (c^2 - b^2) \nabla \tilde{\theta}^* = \nu \nabla^2 \vec{v}^* - \nu^o s \nabla \mathcal{A}^* \tag{2.14}$$

where the Laplace transform of a variable is indicated by an asterisk.

Let

$$F^* = (b^2 + \nu^o s) \mathcal{A}^* + (c^2 - b^2) \tilde{\theta}^* \tag{2.15}$$

so equation 2.14 can be written in a simpler form.

$$s\vec{v}^* - \nu \nabla^2 \vec{v}^* = - \nabla F^* \tag{2.16}$$

Using equation 2.13 to eliminate $\mathcal{A}^*$ from equations 2.12 and 2.15,

$$(s - \kappa \nabla^2) \tilde{\theta}^* = - \nabla \cdot \vec{v}^* \tag{2.17}$$

$$F^* = (b^2+\nu^o s)\left(1 - \frac{\kappa}{s}\nabla^2\right)\tilde{\theta}^* + (c^2-b^2)\tilde{\theta}^* \tag{2.18}$$

and by rearranging terms, equation 2.18 becomes

$$F^* = (c^2+\nu^o s)\tilde{\theta}^* - \frac{\kappa}{s}(b^2+\nu^o s)\nabla^2\tilde{\theta}^* \tag{2.19}$$

Taking the divergence of equation 2.16,

$$s\nabla\cdot\vec{\tilde{v}}^* - \nu\nabla\cdot(\nabla^2\vec{\tilde{v}}^*) = -\nabla^2 F^* \tag{2.20}$$

using the identity,

$$\nabla\cdot(\nabla^2\vec{w}) = \nabla^2(\nabla\cdot\vec{w})$$

and substituting equations 2.17 and 2.19 into equation 2.20 gives:

$$(s-\nu\nabla^2)(s-\kappa\nabla^2)\tilde{\theta}^* = \nabla^2\left[(c^2+\nu^o s) - \frac{\kappa}{s}(b^2+\nu^o s)\nabla^2\right]\tilde{\theta}^*$$

or

$$\frac{\kappa}{s}\left[b^2+s(\nu+\nu^o)\right]\nabla^4\tilde{\theta}^* - \left[c^2+s(\nu+\nu^o+\kappa)\right]\nabla^2\tilde{\theta}^* + s^2\tilde{\theta}^* = 0 \tag{2.21}$$

The solution of equation 2.21 can be written in the form

$$\tilde{\theta}^* = A_1 Q_1 + A_2 Q_2 \tag{2.22}$$

where

$$\begin{aligned}\nabla^2 Q_1 &= \eta_1 Q_1 \\ \nabla^2 Q_2 &= \eta_2 Q_2\end{aligned} \tag{2.23}$$

and where A_1 and A_2 are arbitrary constants to be determined by the boundary conditions, and η_1 and η_2 are the roots of the equation

$$s^2 - \left[c^2+s(\nu+\nu^o+\kappa)\right]\eta + \frac{\kappa}{s}\left[b^2+s(\nu+\nu^o)\right]\eta^2 = 0 \tag{2.24}$$

Assume for the velocity, the solution

$$\vec{v}_p^* = \nabla(B_1 Q_1 + B_2 Q_2) \tag{2.25}$$

where B_1 and B_2 are constants and $\vec{v}_p^*$ is a particular solution. Substituting this in equation 2.17 gives

$$\nabla^2(B_1 Q_1 + B_2 Q_2) + (s - \kappa\nabla^2)(A_1 Q_1 + A_2 Q_2) = 0$$

then by equation 2.23

$$B_1 \eta_1 Q_1 + B_2 \eta_2 Q_2 + (s - \kappa\eta_1)A_1 Q_1 + (s - \kappa\eta_2)A_2 Q_2 = 0$$

and solving for B_1 and B_2:

$$B_1 = A_1\left(\kappa - \frac{s}{\eta_1}\right) \qquad B_2 = A_2\left(\kappa - \frac{s}{\eta_2}\right) \tag{2.26}$$

Equations 2.25 and 2.26 provide a particular solution to equation 2.16. The part of the velocity corresponding to the homogeneous solution, denoted by $\vec{v}_h^*$, is the solution of equation 2.16 with the right-hand side set equal to zero.

$$\nabla^2 \vec{v}_h^* = \frac{s}{\nu} \vec{v}_h^* \tag{2.27}$$

Therefore, the total velocity is given by

$$\vec{v}^* = \vec{v}_h^* + \nabla(B_1 Q_1 + B_2 Q_2) \tag{2.28}$$

By substituting equation 2.28 into equation 2.17 and then making use of equation 2.26, it is seen that

$$\nabla \cdot \vec{v}_h^* = 0 \tag{2.29}$$

The above equations have been derived in a form applicable to any coordinate system by the use of general vector notation. Their solution is now obtained for the special case of a cylindrical tube. The method of separation of variables can be applied to equation 2.23. When this is done, it is desirable to change the notation so that the Q's represent the r-dependent function, and the x dependence is given by $e^{\lambda x}$, where λ is a complex coefficient to be determined presently. In the following discussion, $\tilde{p}$ and $\tilde{\theta}$ will likewise represent the r-dependent part of the solution.

$$\frac{\partial^2 Q_1}{\partial r^2} + \frac{1}{r}\frac{\partial Q_1}{\partial r} = (\eta_1 - \lambda^2) Q_1 \tag{2.30}$$

$$\frac{\partial^2 Q_2}{\partial r^2} + \frac{1}{r}\frac{\partial Q_2}{\partial r} = (\eta_2 - \lambda^2) Q_2 \tag{2.31}$$

Let v^* represent to total particle velocity in the x direction, and v_h^* the homogeneous part, corresponding to $\tilde{v}_h^*$, of that velocity. Similarly, let q^* represent the total velocity, and q_h^* the homogeneous part of that velocity, in the radial direction.

Writing equation 2.27 explicitly gives,

$$\frac{\partial^2 v_h^*}{\partial r^2} + \frac{1}{r}\frac{\partial v_h^*}{\partial r} = \left(\frac{s}{\nu} - \lambda^2\right) v_h^* \tag{2.32}$$

$$\frac{\partial^2 q_h^*}{\partial r^2} + \frac{1}{r}\frac{\partial q_h^*}{\partial r} = \left(\frac{s}{\nu} - \lambda^2\right) q_h^* \tag{2.33}$$

and equation 2.29 becomes

$$\lambda v_h^* + \frac{\partial q_h^*}{\partial r} + \frac{q_h^*}{r} = 0 \tag{2.34}$$

These equations can be solved by first differentiating equation 2.34 with respect to r, and then subtracting the result from equation 2.33.

$$q_h^* = \frac{-\lambda}{\frac{s}{\nu} - \lambda^2} \frac{\partial v_h^*}{\partial r} \tag{2.35}$$

Assume a solution of the form

$$v_h^* = AQ(r)$$

so that equation 2.32 becomes

$$\frac{\partial^2 Q}{\partial r^2} + \frac{1}{r} \frac{\partial Q}{\partial r} = \left(\frac{s}{\nu} - \lambda^2 \right) Q \tag{2.36}$$

Combining equations 2.26, 2.28 and 2.35 gives

$$v^* = AQ - A_1 \lambda \left(\frac{s}{\eta_1} - K \right) Q_1 - A_2 \lambda \left(\frac{s}{\eta_2} - K \right) Q_2 \tag{2.37}$$

$$q^* = \frac{-\lambda A}{\frac{s}{\nu} - \lambda^2} \frac{\partial Q}{\partial r} - A_1 \left(\frac{s}{\eta_1} - K \right) \frac{\partial Q_1}{\partial r} - A_2 \left(\frac{s}{\eta_2} - K \right) \frac{\partial Q_2}{\partial r} \tag{2.38}$$

$$\tilde{\theta}^* = A_1 Q_1 + A_2 Q_2 \tag{2.39}$$

For one boundary condition, it is assumed that v^*, q^* and $\tilde{\theta}^*$ are finite at r = 0. This boundary condition, along with equations 2.30, 2.31 and 2.36, gives

$$\begin{aligned} Q &= I_0 \left(r \sqrt{\frac{s}{\nu} - \lambda^2} \right) \\ Q_1 &= I_0 \left(r \sqrt{\eta_1 - \lambda^2} \right) \\ Q_2 &= I_0 \left(r \sqrt{\eta_2 - \lambda^2} \right) \end{aligned} \tag{2.40}$$

For the second boundary condition, it is assumed that $v^* = q^* = \tilde{\theta}^* = 0$ at the wall, $r = R$, since the velocity is zero and the temperature remains constant. This condition requires that the determinant of the coefficients of the A's in equations 2.37, 2.38 and 2.39 must vanish when the functions Q, Q_1 and Q_2, and their derivatives, are evaluated at $r = R$. Multiplying out the determinant and dividing by $-Q_1Q_2Q_3$ gives

$$\left[\frac{\lambda^2 s}{\frac{s}{\nu} - \lambda^2} \left(\frac{1}{\eta_1} - \frac{1}{\eta_2} \right) \frac{1}{Q} \frac{\partial Q}{\partial r} + \left(\frac{s}{\eta_1} - K \right) \frac{1}{Q_1} \frac{\partial Q_1}{\partial r} - \left(\frac{s}{\eta_2} - K \right) \frac{1}{Q_2} \frac{\partial Q_2}{\partial r} \right]_{r=R} = 0 \tag{2.41}$$

Equation 2.41 determines λ, the two η's being determined by equation 2.24 and the Q's given by equation 2.40.

By using the second boundary condition, the three constants in equations 2.37, 2.38 and 2.39 can be reduced to one. From equation 2.39

$$A_2 Q_2(R) = -A_1 Q_1(R) \tag{2.42}$$

From equations 2.37 and 2.42,

$$0 = AQ(R) - A_1 \lambda \left(\frac{s}{\eta_1} - K \right) Q_1(R) + A_1 Q_1(R) \lambda \left(\frac{s}{\eta_2} - K \right)$$

and solving for $A_1 Q_1(R)$

$$A_1 Q_1(R) = \frac{AQ(R)}{\lambda s \left(\frac{1}{\eta_1} - \frac{1}{\eta_2} \right)} \tag{2.43}$$

Let $B = A_1 Q_1(R)$, and then using the above results

$$v^* = B \left[\lambda s \left(\frac{1}{\eta_1} - \frac{1}{\eta_2} \right) \frac{Q(r)}{Q(R)} - \lambda \left(\frac{s}{\eta_1} - K \right) \frac{Q_1(r)}{Q_1(R)} + \lambda \left(\frac{s}{\eta_2} - K \right) \frac{Q_2(r)}{Q_2(R)} \right] \tag{2.44}$$

$$q^* = B\left[\frac{\lambda^2 s\left(\frac{1}{\eta_1}-\frac{1}{\eta_2}\right)\frac{\partial Q}{\partial r}}{\left(\frac{s}{\nu}-\lambda^2\right)Q(R)} - \frac{\left(\frac{s}{\eta_1}-K\right)\frac{\partial Q_1}{\partial r}}{Q_1(R)} + \frac{\left(\frac{s}{\eta_2}-K\right)\frac{\partial Q_2}{\partial r}}{Q_2(R)}\right] \tag{2.45}$$

$$\tilde{\theta}^* = B\left[\frac{Q_1(r)}{Q_1(R)} - \frac{Q_2(r)}{Q_2(R)}\right] \tag{2.46}$$

The pressure is found by taking the Laplace transform of equation 2.10, along with the initial condition $p(0) = 0$. Using the dimensionless notation

$$\tilde{p} = \frac{p-p_o}{p_o}$$

$$\tilde{p}^* = \mathcal{A}^* + (\gamma-1)\,\tilde{\theta}^* \tag{2.47}$$

By equation 2.13,

$$\mathcal{A}^* = \left(1 - \frac{K}{s}\nabla^2\right)\tilde{\theta}^*$$

where $\tilde{\theta}^*$ is given in equation 2.46, but from equation 2.23,

$$\nabla^2 Q_1 = \eta_1 Q_1$$

$$\nabla^2 Q_2 = \eta_2 Q_2$$

so that

$$\tilde{p}^* = B\left[\left(\gamma - \frac{K}{s}\eta_1\right)\frac{Q_1(r)}{Q_1(R)} - \left(\gamma - \frac{K}{s}\eta_2\right)\frac{Q_2(r)}{Q_2(R)}\right] \tag{2.48}$$

Up to this point the only restrictions that have been made are:

1. The fractional pressure variation $\tilde{p}$ is small compared to unity.

In this context, a small quantity is taken to be on the order of 10^{-4}, or less.

This number was chosen because a fractional pressure variation of this value is usually taken as the limit of classical acoustics, and it is also of the same order as terms neglected later.

2. The ratio of the particle velocity to the velocity of sound is small compared to unity.

3. The condensation s is small compared to unity.

4. The medium can be described by parameters that are constants with respect to time and position.

Although the above restrictions are listed separately to be more explicit, they are all consequences of the general restriction that only small amplitude waves are being considered.

The two η's can be determined from equation 2.24 exactly. In principle, equation 2.41 can be solved for λ, to any desired degree of accuracy, by an iteration procedure. However, such an approach would completely obscure the effects of the physical processes that occur in the tube.

In order to make the above equations manageable, the following restrictions are made:

$$\left| \frac{s\nu}{c2} \right| = \left| \xi \left(\frac{\nu}{Rc} \right)^2 \right| \leq O(10^{-6}) \tag{2.49}$$

$$\left| \frac{\nu}{Rc} \xi^{3/4} \right| \leq O(10^{-2}) \tag{2.50}$$

where for the purpose of evaluating the restrictions it is assumed that the tube has a radius of 0.1 inch, so that,

$$\frac{\nu}{Rc} \leq O(10^{-5}) \tag{2.51}$$

Combining inequality 2.51 with restriction 2.50 gives

$$\xi \leq O(10^4) \tag{2.52}$$

The specific orders of magnitude are given so that the effect of the restrictions on the various equations can be seen, and so that a consistant set of approximations can be made. Since ν, ν^o and K are all the same size, and c^2 is the same order of magnitude as b^2, expressions similar to restriction 2.49 also hold for these quantities.

The limitation on the size of s, or equivalently ξ, means that it is impossible to get a wave-front expansion while observing these restrictions. However, under normal circumstances, (i.e., with ψ less than about 30) the solutions to the transient response problem, obtained by the methods developed here, differ from the exact solutions, near the wave front, by an amount that cannot be plotted on the scale used in this work.

It should be noted that the form of restriction 2.50 differs from, but is not incompatible with, the form stated by Iberall. (See ref. 6 equation 76. (The line above equation 76 should read, "Equations 74 and 75...) .) As the necessity for restrictions 2.49 and 2.50 is developed in the following equations, it will be seen that the form of restriction 2.50 given here is the more directly applicable.

The solution of equation 2.24 is

$$\eta = \frac{sc^2\left[1+\frac{s}{c^2}(\nu+\nu^o+K)\right]}{2Kb^2\left[1+\frac{s}{b^2}(\nu+\nu^o)\right]}\left\{1 \pm \sqrt{1-\frac{4sKb^2\left[1+\frac{s}{b^2}(\nu+\nu^o)\right]}{c^4\left[1+\frac{s}{c^2}(\nu+\nu^o+K)\right]^2}}\right\} \tag{2.53}$$

The smaller η is denoted by η_1, the larger by η_2. Applying restriction 2.49 to equation 2.53, taking the minus sign, and using the first three terms in the expansion of the square root produces

$$\eta_1 = \frac{s^2}{c^2}\left[1 - \frac{s}{c^2}\left[\nu+\nu^o+(\gamma-1)\frac{\kappa}{\gamma}\right]\right] \tag{2.54}$$

Taking the plus sign, and only the first two terms of the square root expansion gives

$$\eta_2 = \frac{s\gamma}{\kappa}\left[1 - \frac{s}{c^2}(\gamma-1)\left[\nu+\nu^o-\frac{\kappa}{\gamma}\right]\right] \tag{2.55}$$

Both restrictions 2.49 and 2.50 are used in the determination of λ. Equation 2.41 is repeated here for convenience.

$$\left[\frac{\lambda^2 s}{\frac{s}{\nu}-\lambda^2}\left(\frac{1}{\eta_1}-\frac{1}{\eta_2}\right)\frac{1}{Q}\frac{\partial Q}{\partial r}+\left(\frac{s}{\eta_1}-\kappa\right)\frac{1}{Q_1}\frac{\partial Q_1}{\partial r}-\left(\frac{s}{\eta_2}-\kappa\right)\frac{1}{Q_2}\frac{\partial Q_2}{\partial r}\right]_{r=R}=0 \tag{2.56}$$

Since for plane waves traveling in free space $\lambda^2=s^2/c^2$, it is assumed here that the value of λ determined from equation 2.56 is of this order of magnitude. Using the above assumption and restriction 2.49, the following substitutions can be made:

$$\frac{s}{\nu}-\lambda^2 \approx \frac{s}{\nu}\left(1-\frac{s\nu}{c^2}\right)\approx\frac{s}{\nu}$$

$$\left(\frac{1}{\eta_1}-\frac{1}{\eta_2}\right)\approx\frac{s^2}{c^2}\left(1-\frac{\kappa s}{\gamma c^2}\right)\approx\frac{c^2}{s^2}$$

$$\left(\frac{s}{\eta_1}-\kappa\right)\approx\frac{c^2}{s}\left(1-\frac{s\kappa}{c^2}\right)\approx\frac{c^2}{s}$$

$$\left(\frac{s}{\eta_2}-\kappa\right)\approx\left(\frac{s\kappa}{s\gamma}-\kappa\right)=\frac{\kappa}{\gamma}(1-\gamma)$$

$$(\eta_2 - \lambda^2) \approx \frac{\gamma s}{K}\left(1 - \frac{s K}{\gamma_c{}^2}\right) \approx \frac{\gamma s}{K}$$

$$Q = I_0\left(r\sqrt{\frac{s}{\nu} - \lambda^2}\right) \approx I_0\left(r\sqrt{\frac{s}{\nu}}\right)$$

$$Q_1 = I_0\left(r\sqrt{\eta_1 - \lambda^2}\right) \approx I_0\left(r\sqrt{\frac{s^2}{c^2} - \lambda^2}\right)$$

$$Q_2 = I_0\left(r\sqrt{\eta_2 - \lambda^2}\right) \approx I_0\left(r\sqrt{\frac{\gamma s}{K}}\right)$$

To first order, $\eta_1 - \lambda^2 = 0$ so it will be assumed that

$$\left|R\sqrt{\eta_1 - \lambda^2}\right| \leq O(10^{-2}) \tag{2.57}$$

so that

$$I_0\left(R\sqrt{\eta_1 - \lambda^2}\right) \approx 1 \tag{2.58}$$

and

$$\frac{1}{Q_1}\frac{\partial Q_1}{\partial r}\bigg|_{r=R} \approx \frac{1}{2} R\left(\frac{s^2}{c^2} - \lambda^2\right) \tag{2.59}$$

The validity of assumption 2.57 will have to be verified after λ has been determined. Making the above substitutions, and using the above assumptions, equation 2.30 becomes

$$\lambda^2 \nu\left(\frac{c^2}{s}\right)\sqrt{\frac{s}{\nu}}\,\frac{I_1\left(R\sqrt{\frac{s}{\nu}}\right)}{I_0\left(R\sqrt{\frac{s}{\nu}}\right)} + \frac{c^2}{s}\,\frac{1}{2} R\left(\frac{s^2}{c^2} - \lambda^2\right) + \frac{K}{\gamma}(\gamma - 1)\sqrt{\frac{\gamma s}{K}}\,\frac{I_1\left(R\sqrt{\frac{\gamma s}{K}}\right)}{I_0\left(R\sqrt{\frac{\gamma s}{K}}\right)} = 0 \tag{2.60}$$

and solving for λ^2 gives

$$\lambda^2 = \frac{\frac{s^2}{c^2}\left[1 + \frac{2(\gamma-1)}{R\sqrt{\frac{\gamma s}{\kappa}}} \frac{I_1\left(R\sqrt{\frac{\gamma s}{\kappa}}\right)}{I_0\left(R\sqrt{\frac{\gamma s}{\kappa}}\right)}\right]}{1 - \frac{2}{R\sqrt{\frac{s}{\nu}}} \frac{I_1\left(R\sqrt{\frac{s}{\nu}}\right)}{I_0\left(R\sqrt{\frac{s}{\nu}}\right)}} \tag{2.61}$$

To simplify the verification of the restriction 2.57, equation 2.61 is put in dimensionless form. Making the substitutions:

$$\xi = R^2 \frac{s}{\nu}$$

$$\tilde{s} = \frac{sL}{c} = \frac{\xi}{\psi}$$

where

$$\psi = \frac{R^2 c}{\nu L}$$

and

$$\sigma\xi = \frac{\gamma s}{\kappa}$$

where

σ is Prandtl's number,

equation 2.61 is written

$$\lambda^2 L^2 = \tilde{\lambda}^2 = \frac{\xi^2\left[1 + \frac{2(\gamma-1)\, I_1(\sqrt{\sigma\xi})}{\sqrt{\sigma\xi}\, I_0(\sqrt{\sigma\xi})}\right]}{\psi^2\left[1 - \frac{2}{\sqrt{\xi}} \frac{I_1(\sqrt{\xi})}{I_0(\sqrt{\xi})}\right]} \tag{2.62}$$

In dimensionless form, inequality 2.57 becomes

$$\left| \frac{R}{L} \sqrt{\frac{s^2 L^2}{c^2} - \lambda^2 L^2} \right| \leq O(10^{-2}) \tag{2.63}$$

Using the above substitutions plus

$$\frac{R}{L\psi} = \frac{\nu}{Rc}$$

inequality 2.63 is, when written out explicitly,

$$\left| \left(\frac{\nu}{Rc}\right) \xi \sqrt{1 - \frac{1 + \frac{2(\gamma-1) I_1(\sqrt{\sigma \xi})}{\sqrt{\sigma \xi}\, I_0(\sqrt{\sigma \xi})}}{1 - \frac{2 I_1(\sqrt{\xi})}{\sqrt{\xi} I_0(\sqrt{\xi})}}} \right| \leq O(10^{-2}) \tag{2.64}$$

An order of magnitude estimate of the quantity in the radical is obtained by setting Prandtl's number equal to unity. For ξ small compared to unity, the Bessel functions are expanded in power series, and inequality 2.64 becomes,

$$\left| \left(\frac{\nu}{Rc}\right) \xi \sqrt{1 - \frac{\left[1 + (\gamma-1)\left(1 - \frac{1}{8}\xi\right)\right]}{\frac{1}{8}\xi}} \right| \leq O(10^{-2}) \tag{2.65}$$

or by keeping only the most important terms

$$\left| \left(\frac{\nu}{Rc}\right) \xi^{1/2} \right| \leq O(10^{-2}) \tag{2.66}$$

Since by inequality 2.51

$$\left(\frac{\nu}{Rc}\right) \leq O(10^{-5})$$

and ξ was, by assumption, small compared to unity, inequality 2.66 is obviously satisfied for small ξ.

For ξ large, the Bessel functions are expanded in the asymptotic series. Inequality 2.64 then gives

$$\left| \left(\frac{\nu}{Rc}\right) \xi \sqrt{\frac{1 + \frac{2}{\sqrt{\xi}}}{1 - \frac{2}{\sqrt{\xi}}}} \right| \leq O(10^{-2}) \qquad (2.67)$$

or, since $2/\sqrt{\xi}$ is small compared to unity, inequality 2.67 can be reduced to

$$\left| \left(\frac{\nu}{Rc}\right) \xi \sqrt{1 - 1 + \frac{4}{\sqrt{\xi}}} \right| \leq O(10^{-2})$$

or simply

$$\left| \left(\frac{\nu}{Rc}\right) \xi^{3/4} \right| \leq O(10^{-2}) \qquad (2.68)$$

Clearly, any difficulty that might be encountered would be for large ξ, so that inequality 2.68, which is just a repeat of inequality 2.50, is the expression that should be taken for the second restriction. Combining inequalities 2.50 and 2.51 gives inequality 2.52,

$$\xi \leq O(10^4)$$

If the tube is made of an insulating material, the boundary condition at the wall is

$$v^* = q^* = \frac{\partial \tilde{\theta}^*}{\partial r} = 0$$

For the purpose of evaluating the determinant to obtain an expression analogous to equation 2.41, equation 2.39 is replaced by

$$\frac{\partial \tilde{\theta}^*}{\partial r} = A_1 \frac{\partial Q_1}{\partial r} + A_2 \frac{\partial Q_2}{\partial r} \qquad (2.69)$$

Multiplying out the determinant of equations 2.37, 2.38 and 2.69, and dividing by

$$-\frac{\partial Q}{\partial r}\,\frac{\partial Q_1}{\partial r}\,\frac{\partial Q_2}{\partial r}$$

gives

$$\left[s\left(\frac{1}{\eta_1}-\frac{1}{\eta_2}\right)\frac{Q}{\frac{\partial Q}{\partial r}} + \frac{\lambda^2}{\frac{s}{\nu}-\lambda^2}\left\{\left(\frac{s}{\eta_1}-K\right)\frac{Q_1}{\frac{\partial Q_1}{\partial r}} - \left(\frac{s}{\eta_2}-K\right)\frac{Q_2}{\frac{\partial Q_2}{\partial r}}\right\}\right]_{r=R} = 0 \qquad (2.70)$$

Equation 2.70 can be put in a more convenient form by making the same approximations as before, and rearranging terms.

$$\frac{\frac{s^2}{c^2}-\lambda^2}{1+\left(\frac{s^2}{c^2}-\lambda^2\right)\frac{K^2}{c^2\gamma^2}(\gamma-1)\,\frac{R\sqrt{\frac{\gamma s}{K}}}{2}\,\frac{I_0\left(R\sqrt{\frac{\gamma s}{K}}\right)}{I_1\left(R\sqrt{\frac{\gamma s}{K}}\right)}} = \frac{-\lambda^2 2}{R\sqrt{\frac{s}{\nu}}}\,\frac{I_1\left(R\sqrt{\frac{s}{\nu}}\right)}{I_0\left(R\sqrt{\frac{s}{\nu}}\right)} \qquad (2.71)$$

It is desirable to obtain an order of magnitude estimate of the second term of the denominator on the left hand side to see if it is significant. Using the previous solution it is clear that

$$\left|\frac{s^2}{c^2}-\lambda^2\right| < \frac{s^2}{c^2}$$

Considering the factor

$$f = \frac{R\sqrt{\frac{\gamma s}{K}}}{2}\,\frac{I_0\left(R\sqrt{\frac{\gamma s}{K}}\right)}{I_1\left(R\sqrt{\frac{\gamma s}{K}}\right)}$$

for s small

$$f \longrightarrow 1$$

for s large

$$f \longrightarrow \frac{R\sqrt{\frac{\gamma s}{K}}}{2} = \frac{\sqrt{\sigma \xi}}{2}$$

The limit of large s will provide the greater contribution. Using these approximations, the second term becomes,

$$\frac{s^2 K^2}{c^4 \gamma^2} (\gamma - 1) \frac{\sqrt{\sigma \xi}}{2}$$

then the substitution $\sigma = \nu \gamma / K$ gives

$$\left(\frac{s\nu}{c^2}\right)^2 \frac{(\gamma - 1)}{\sigma^2} \frac{\sqrt{\sigma \xi}}{2}$$

Assuming $\sigma = 1$, and inserting the restrictions listed earlier, this term takes on a value of 10^{-10}, or less, which certainly can be neglected compared to unity.

Then the solution of equation 2.71, using dimensionless notation, is

$$\tilde{\lambda}^2 = \frac{\xi^2}{\psi^2 \left[1 - \frac{2}{\sqrt{\xi}} \frac{I_1(\sqrt{\xi})}{I_0(\sqrt{\xi})}\right]} = \beta \qquad (2.72)$$

where the β is the one given in Section One when the full-frequency approximation is used and c_T is set equal to c, the Laplace velocity of sound.

Considerable simplification occurs when the above restrictions are applied to equation 2.48 which is repeated here for convenience.

$$\tilde{p}^* = B \left[\gamma \left(1 - \frac{K}{\gamma s} \eta_1\right) \frac{Q_1(r)}{Q_1(R)} - \gamma \left(1 - \frac{K}{\gamma s} \eta_2\right) \frac{Q_2(r)}{Q_2(R)} \right] \qquad (2.73)$$

By substituting the previously determined values of η, and taking both terms in the approximation to η_2, this equation becomes

$$\tilde{p}^* = \gamma B \left[\left(1 - \frac{\kappa s}{\gamma c^2}\right) \frac{Q_1(r)}{Q_1(R)} + \frac{s}{c^2} (\gamma-1)(\nu+\nu^o - \frac{\kappa}{\gamma}) \frac{Q_2(r)}{Q_2(R)} \right] \qquad (2.74)$$

Applying restrictions 2.49 and 2.50 makes the first term equal to unity. The second term can be neglected compared to the first if it can be shown that the ratio of the Bessel functions is of order unity, or less, in all parts of the ξ plane where expressions that are derived from equation 2.74 are evaluated. This assumption is written explicitly, using restriction 2.49 and the notation,

$$\frac{\gamma s}{\kappa} = \sigma \xi$$

as

$$\left| \frac{I_0\left(\frac{r}{R}\sqrt{\sigma \xi}\right)}{I_0\left(\sqrt{\sigma \xi}\right)} \right| \leq O(1) \qquad (2.75)$$

For ξ along the imaginary axis, as would be the case in evaluating the frequency response, inequality 2.75 is valid. Normally, along the pole locus, i.e., the path the poles move along as a function of ψ_a (see Section Three), inequality 2.75 is also valid. Trouble would be anticipated only as ξ approached a zero of the denominator. This would occur only in the rare case where σ approaches unity and the residue is evaluated at the pole farther from the origin when ψ_a is small. However, the contribution of this residue becomes negligible faster than the violation of inequality 2.75 becomes significant.

Making the assumption that the second term can be neglected, equation 2.73 reduces to

$$\tilde{p}^* = \gamma B \tag{2.76}$$

Since the fractional pressure variation $\tilde{p}$ was small by assumption, B is small compared to unity. Equation 2.76 shows that $\tilde{p}$ is independent of the radius r, as was assumed in Section One.

When restrictions 2.49 and 2.50 are applied to equation 2.44, repeated here for convenience,

$$v^* = B\left[\lambda s\left(\frac{1}{\eta_1} - \frac{1}{\eta_2}\right)\frac{Q(r)}{Q(R)} - \lambda\left(\frac{s}{\eta_1} - K\right)\frac{Q_1(r)}{Q_1(R)} + \lambda\left(\frac{s}{\eta_1} - K\right)\frac{Q_2(r)}{Q_2(R)}\right] \tag{2.77}$$

it becomes

$$v^* = B\left[\frac{\lambda c^2}{s}\frac{I_0\left(r\sqrt{\frac{s}{\nu}}\right)}{I_0\left(R\sqrt{\frac{s}{\nu}}\right)} - \lambda\frac{c^2}{s} + \frac{\lambda c^2}{s}\left(\frac{K}{\gamma} - K\right)\frac{I_0\left(r\sqrt{\frac{\gamma s}{K}}\right)}{I_0\left(R\sqrt{\frac{\gamma s}{K}}\right)}\frac{s}{c^2}\right] \tag{2.78}$$

and then by the same arguments that lead to equation 2.75, equation 2.78 is reduced to

$$v^* = -\frac{\lambda c^2}{s} B\left[1 - \frac{I_0\left(r\sqrt{\frac{s}{\nu}}\right)}{I_0\left(R\sqrt{\frac{s}{\nu}}\right)}\right]$$

It should be noted that to a first approximation

$$\frac{\lambda c^2}{s} = c \tag{2.79}$$

Since B is small compared to unity, v is also small compared to c, as stated earlier.

Whenever the volume flow is considered, the average velocity across the tube is used.

$$u^* = -B\frac{\lambda c^2}{s}\frac{2}{R^2}\int_0^R \left[r - \frac{rI_0\left(r\sqrt{\frac{s}{\nu}}\right)}{I_0\left(R\sqrt{\frac{s}{\nu}}\right)}\right] dr \tag{2.80}$$

Which, when integrated and evaluated at the limits becomes

$$u^* = -B\frac{\lambda c^2}{s}\left[1 - \frac{2\ I_1\left(R\sqrt{\frac{s}{\nu}}\right)}{R\sqrt{\frac{s}{\nu}}\ I_0\left(R\sqrt{\frac{s}{\nu}}\right)}\right] \tag{2.81}$$

If equation 2.45, the equation for q^*, is evaluated at r = R, the resulting expression is just that from which λ^2 was determined.

$$q^* = B\left[\frac{\lambda^2 s\left(\frac{1}{\eta_1} - \frac{1}{\eta_2}\right)}{\left(\frac{s}{\nu} - \lambda^2\right) Q(R)}\ \frac{\partial Q}{\partial r} - \frac{\left(\frac{s}{\eta_1} - K\right)}{Q_1(R)}\ \frac{\partial Q_1}{\partial r} + \frac{\left(\frac{s}{\eta_2} - K\right)}{Q_2(R)}\ \frac{\partial Q_2}{\partial r}\right] \tag{2.82}$$

Using the same approximations that were used in determining λ^2, equation 2.82 becomes

$$q^* = B\left[\lambda^2 \nu \frac{c^2}{s^2}\sqrt{\frac{s}{\nu}}\ \frac{I_1\left(r\sqrt{\frac{s}{\nu}}\right)}{I_0\left(R\sqrt{\frac{s}{\nu}}\right)} + \frac{1}{2} r \frac{c^2}{s}\left(\frac{s^2}{c^2} - \lambda^2\right) + \frac{K}{\gamma}(\gamma - 1)\sqrt{\frac{\gamma s}{K}}\ \frac{I_1\left(r\sqrt{\frac{\gamma s}{K}}\right)}{I_0\left(R\sqrt{\frac{\gamma s}{K}}\right)}\right] \tag{2.83}$$

Considering only the middle term in equation 2.83, and putting it in a more useful form, it becomes

$$\frac{1}{2} r \frac{c^2}{s}\left(\frac{s^2}{c^2} - \lambda^2\right) = \frac{1}{2}\frac{r}{R^2}\ \frac{c^2}{s}\ \frac{R^2}{L^2}\left(\frac{s^2 L^2}{c^2} - \lambda^2 L^2\right) \tag{2.84}$$

In accordance with the derivation of inequality 2.68 from 2.63, equation 2.84 can be replaced, at least to an order of magnitude, by

$$\frac{1}{2} r \frac{c^2}{s}\left(\frac{s^2}{c^2} - \lambda^2\right) \sim \frac{1}{2} \frac{r}{R^2} \frac{c^2}{s} \left(\frac{\nu}{Rc}\right)^2 \xi^{3/2} \tag{2.85}$$

and using the substitution,

$$\xi = \frac{R^2 s}{\nu}$$

equation 2.84 becomes

$$\frac{1}{2} r \frac{c^2}{s}\left(\frac{s^2}{c^2} - \lambda^2\right) = O\left(\frac{1}{2} \frac{r}{R} \sqrt{s\nu}\right) \tag{2.86}$$

Using equation 2.86 and taking the first approximation $\lambda^2 = \frac{s^2}{c^2}$, equation 2.83 becomes

$$q^* = B\left[\sqrt{s\nu} \frac{I_1\left(r\sqrt{\frac{s}{\nu}}\right)}{I_0\left(R\sqrt{\frac{s}{\nu}}\right)} + O\left(\frac{1}{2} \frac{r}{R} \sqrt{s\nu}\right) + (\gamma-1)\sqrt{\frac{s\kappa}{\gamma}} \frac{I_1\left(r\sqrt{\frac{s\gamma}{\kappa}}\right)}{I_0\left(R\sqrt{\frac{s\gamma}{\kappa}}\right)}\right] \tag{2.87}$$

The two ratios of Bessel functions are of order unity, or less, except near zeros of the denominator. The only place, involved in the present analysis, where a zero occurs is for the pole farther from the origin when $\psi a = 0$. Since the contribution to the transient response is negligible near this point, it can be assumed that

$$\frac{r}{R}, \quad \frac{I_1\left(r\sqrt{\frac{s}{\nu}}\right)}{I_0\left(R\sqrt{\frac{s}{\nu}}\right)} \quad \text{and} \quad \frac{I_1\left(r\sqrt{\frac{\gamma s}{\kappa}}\right)}{I_0\left(R\sqrt{\frac{\gamma s}{\kappa}}\right)}$$

are all of order unity, or less.

Applying these results to equation 2.87

$$q^* = O\left(B\sqrt{s\nu}\right) \tag{2.88}$$

and then comparing q^* with u^*:

$$\frac{q^*}{u^*} = O\left(\frac{B\sqrt{s\nu}}{Bc}\right) = O\left(\sqrt{\frac{s\nu}{c^2}}\right) = O\,(10^{-3}) \tag{2.89}$$

Equation 2.89 justifies the assumption of zero radial velocity made in Section One.

Including the x dependence in $\tilde{p}^*$ explicitly,

$$\tilde{p}^* = B\,\gamma e^{\lambda x}$$

the derivative with respect to x is

$$\frac{d\tilde{p}^*}{dx} = B\,\gamma\lambda e^{\lambda x} \tag{2.90}$$

Combining equation 2.90 with equation 2.81 gives

$$\frac{d\tilde{p}^*}{dx} = \frac{su^*/b^2}{1 - \dfrac{2}{R\sqrt{\frac{s}{\nu}}}\dfrac{I_1\left(R\sqrt{\frac{s}{\nu}}\right)}{I_0\left(R\sqrt{\frac{s}{\nu}}\right)}}$$

or writing this in dimensionless form,

$$\frac{d\tilde{p}^*}{d\chi} = \frac{-\xi\tilde{u}^*}{1 - \dfrac{2}{\sqrt{\xi}}\dfrac{I_1(\sqrt{\xi})}{I_0(\sqrt{\xi})}}$$

where

$$\chi = \frac{x}{L}$$

$$\xi = R^2\frac{s}{\nu}$$

$$\tilde{u}^* = \frac{u^*\mu L}{p_o R^2} = \frac{u^* c}{\psi b^2}$$

which is just

$$\frac{d\tilde{p}^*}{d\chi} = -\xi_F\,\tilde{u}^* \tag{2.91}$$

where

$\mathcal{S}_F$ is the full-frequency expression for the specific acoustic impedance per unit length as defined in Section One.

Writing the full expression for the pressure in dimensionless form gives

$$\tilde{p}^* = C_1 e^{\tilde{\lambda} x} + C_2 e^{-\tilde{\lambda} x} \tag{2.92}$$

where C_1 and C_2 are constants determined by the boundary conditions on the tube, and

$$\tilde{\lambda}^2 = \frac{\mathcal{S}}{\psi^2} \left[\frac{\mathcal{S}}{1 - \frac{2}{\sqrt{\mathcal{S}}} \frac{I_1(\sqrt{\mathcal{S}})}{I_0(\sqrt{\mathcal{S}})}} \right] \left[1 + \frac{2(\gamma-1)}{\sqrt{\sigma \mathcal{S}}} \frac{I_1(\sqrt{\sigma \mathcal{S}})}{I_0(\sqrt{\sigma \mathcal{S}})} \right]$$

or in simpler notation

$$\tilde{\lambda}^2 = (\beta \Gamma)^2 \tag{2.93}$$

where

$$\Gamma^2 = \left[1 + \frac{2(\gamma-1)}{\sqrt{\sigma \mathcal{S}}} \frac{I_1(\sqrt{\sigma \mathcal{S}})}{I_0(\sqrt{\sigma \mathcal{S}})} \right]$$

is the factor that contains the effects of the heat conduction.

Note that equation 2.92 is of the same form as equation 1.14, Section One, but with β replaced by $\beta \Gamma$. Equation 2.91 is identical to equation 1.7, Section One, when the full-frequency form of $\mathcal{S}$ is used.

Because of the similarity of the expressions here to those in Section One, only the main points of the following analysis will be included.

As before, the boundary conditions are

$$\tilde{p}^*(0, \tilde{s}) = \frac{1}{\tilde{s}} \tag{2.94}$$

$$\left.\frac{d\tilde{p}^*}{dx}\right|_{x=1} = -\nu\beta^2 \tilde{p}^*$$

Because the β in the exponent is now replaced by $\beta\Gamma$, the expression analogous to equation 1.22 is:

$$\tilde{p}^*(1, \tilde{s}) = \frac{2}{\tilde{s}\left[e^{\beta\Gamma}\left(1 + \frac{\beta\nu}{\Gamma}\right) + e^{-\beta\Gamma}\left(1 - \frac{\beta\nu}{\Gamma}\right)\right]}$$

or

$$\tilde{p}^*(1, \tilde{s}) = \frac{1}{\tilde{s}\left[\cosh\beta\Gamma + \frac{\beta\nu}{\Gamma}\sinh\beta\Gamma\right]} \tag{2.95}$$

The frequency response can be found by substituting $i\omega$ for s in the expression

$$\tilde{p}(1, \omega) = \frac{1}{\cosh\beta\Gamma + \frac{\beta\nu}{\Gamma}\sinh\beta\Gamma} \tag{2.96}$$

where β and Γ are complex functions of ω.

SECTION THREE

INVERSION OF THE LAPLACE TRANSFORMS

In Sections One and Two the Laplace transform of the pressure at the end of the tube was derived for several approximations. In this section the methods used to invert these Laplace transforms, to obtain the pressure as a function of time, are described. Two techniques were used and the results compared to ensure accuracy. The method that turned out to be more useful centered on the evaluation of the residues. The second method was a direct numerical evaluation of the inversion integral.

Residue Theory

In the simple application of the residue theorem to the inversion of Laplace transforms, the path of integration consists of the Bromwich contour, and closure is by means of a semicircle in the left half plane. This simple contour is not applicable to all the approximations considered in this work, and must be modified for some cases. The modifications required will be discussed later in this section. However, the general process for the finding of the poles and the evaluation of the residues is essentially the same for all approximations. The initial discussion of the residues will pertain to the theory of Section One, and then the extensions that must be made to include heat conduction will be described.

Using the residue theorem, the part of the pressure at the end of the tube due to the contribution of the residues, takes on a relatively simple form,

$$\tilde{p}(1, \tau) = \sum_{n}^{\infty} \left(\frac{1}{g'(\tilde{s})} \right)_n e^{\tilde{s}_n \tau} \tag{3.1}$$

where

$$\frac{1}{g(\tilde{s})} = \tilde{p}^*(1, \tilde{s})$$

and the prime indicates the derivative with respect to $\tilde{s}$. The expression $1/g'(\tilde{s})$ is to be evaluated at each of the poles of $\tilde{p}^*(1, \tilde{s})$, which are denoted by $n = 0, 1, \ldots$, and then summed.

The poles of $\tilde{p}^*(1, \tilde{s})$ are found where

$$g(\tilde{s}) = \tilde{s}(\cosh\beta + \nu\beta \sinh\beta) = 0 \tag{3.2}$$

Obviously one solution of this equation is $\tilde{s} = 0$, which gives, by equation 3.1, the value unity for the first term of the summation. Attention is now restricted to the other poles, which are determined by

$$\cosh\beta + \nu\beta \sinh\beta = 0 \tag{3.3}$$

Let $\beta = i\alpha$, where α is a real number. Then equation 3.3 becomes

$$\beta \tanh\beta = -\frac{1}{\nu}$$

or

$$\alpha \tan\alpha = \frac{1}{\nu}$$

thus

$$\cot\alpha = \nu\alpha \tag{3.4}$$

An approximate solution of equation 3.4 can be found by plotting the functions on each side and finding their intersections, (fig. 8). More precise solutions can be found by numerical iterations. The variation of the first root as a function of ν is shown in figure 9. The ratio of higher roots to this first root is also given.

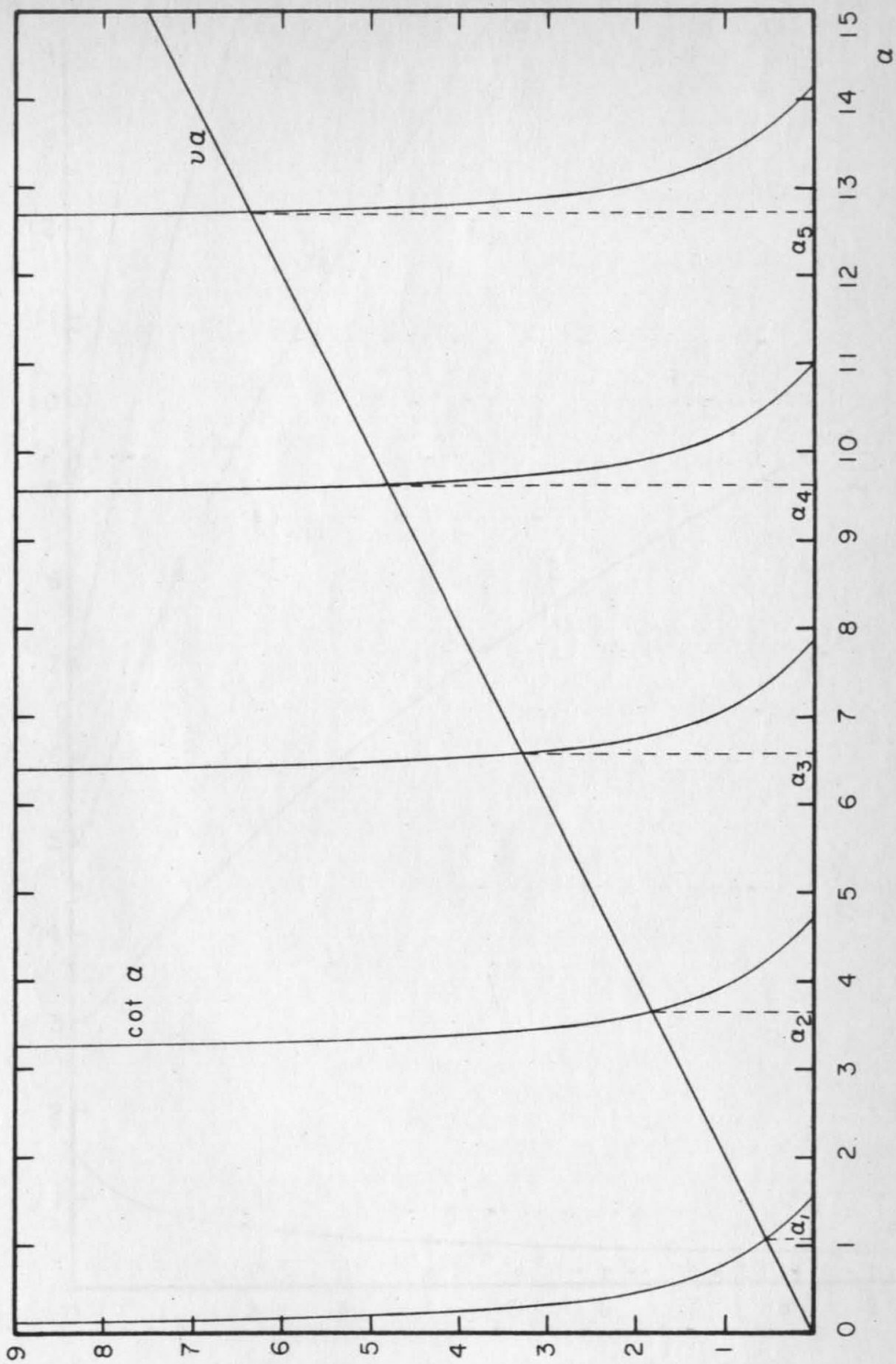

Figure 8. Determination of Alpha

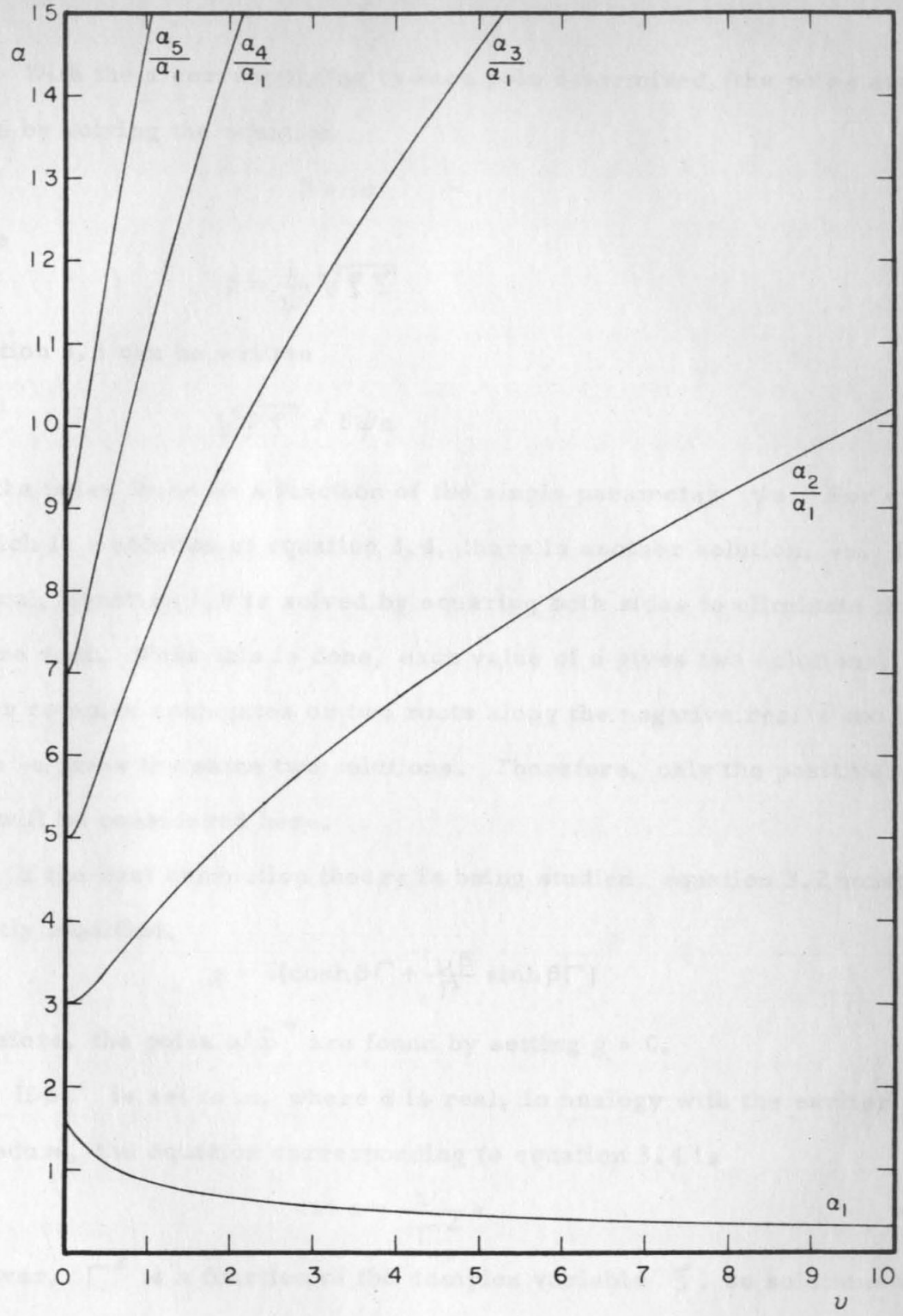

Figure 9. Alpha Ratios as a Function of Volume

With the α corresponding to each pole determined, the poles are found by solving the equation

$$\beta = i\alpha \tag{3.5}$$

Since

$$\beta = \frac{1}{\psi}\sqrt{\xi\zeta}$$

equation 3.5 can be written

$$\sqrt{\xi\zeta} = i\psi\alpha \tag{3.6}$$

and the poles found as a function of the single parameter $\psi\alpha$. For every α which is a solution of equation 3.4, there is another solution, $-\alpha$. In general, equation 3.6 is solved by squaring both sides to eliminate the square root. When this is done, each value of α gives two solutions, either complex conjugates or two roots along the negative real $\tilde{s}$ axis. The value $-\alpha$ gives the same two solutions. Therefore, only the positive values of α will be considered here.

If the heat conduction theory is being studied, equation 3.2 must be slightly modified.

$$g = \tilde{s}(\cosh\beta\Gamma + \frac{\nu\beta}{\Gamma}\sinh\beta\Gamma) \tag{3.7}$$

As before, the poles of $\tilde{p}^*$ are found by setting $g = 0$.

If $\beta\Gamma$ is set to $i\alpha$, where α is real, in analogy with the earlier procedure, the equation corresponding to equation 3.4 is

$$\cot\alpha = -\frac{\nu}{\Gamma^2}\alpha \tag{3.8}$$

However, Γ^2 is a function of the complex variable ξ, so solutions of this equation can be found with real α only when $\nu = 0$. In that case,

$$\alpha = \frac{\pi}{2}(2n-1) \qquad n = 1, 2, 3, \ldots \tag{3.9}$$

The motion of the poles as a function of $\psi\alpha$ is shown in figures 10 and 11. In figure 10, the motion near the origin is given. Figure 11 covers a larger range of $\psi\alpha$. These curves are referred to as pole loci. Both figures include the solutions for the three ζ's and also the case including heat conduction. Figure 12 shows the result of varying γ and σ.

When heat conduction is considered and ν is not equal to zero, the $i\alpha$ substitution is not useful; then the solution of equation 3.7 must be found by an iteration procedure. The information obtained by this method can be displayed best by plotting the case $\nu = 0$ as a starting curve, and then indicating the variation with ν by branches off this main curve for particular ψ's and for various n's, (fig. 13).

The motion of the poles along the negative real ζ-axis as a function of $\psi\alpha$ is shown in figure 14 for the case including heat conduction and the cases of β calculated using the low-frequency and the full-frequency expressions for ζ.

Iberall (6) has pointed out that for low frequencies the expression for λ including heat conduction reduces to the expression found by taking the low-frequency approximation of β and considering the polytropic process in the tube as being isothermal. This is achieved by setting $c_T = b$ in the definition of ψ. Or, alternatively, the isothermal ψ is obtained by multiplying the adiabatic ψ by the ratio of b/c.

$$\psi_{Is} = \psi_A \, b/c$$

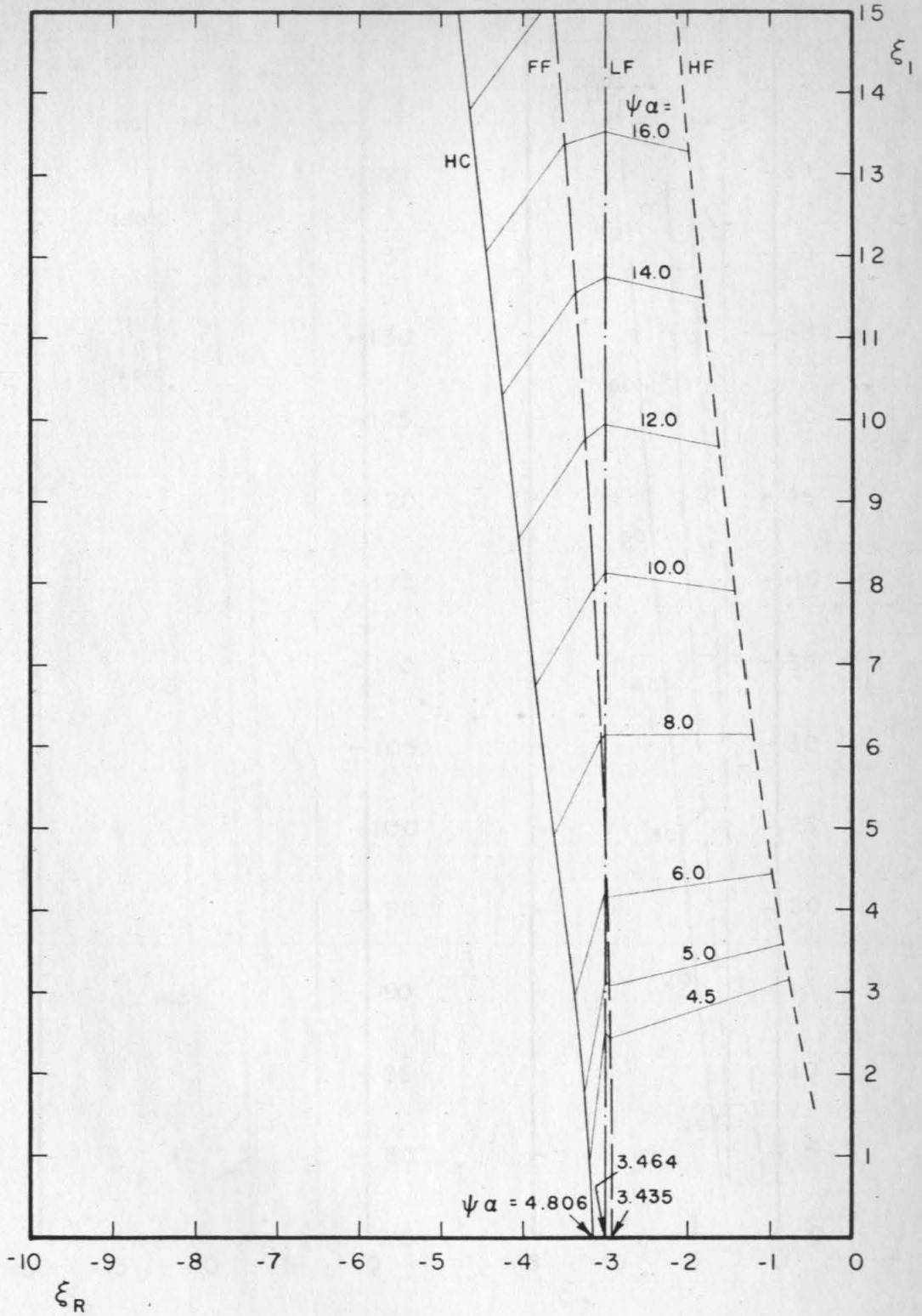

Figure 10. Pole Locus - Near Origin

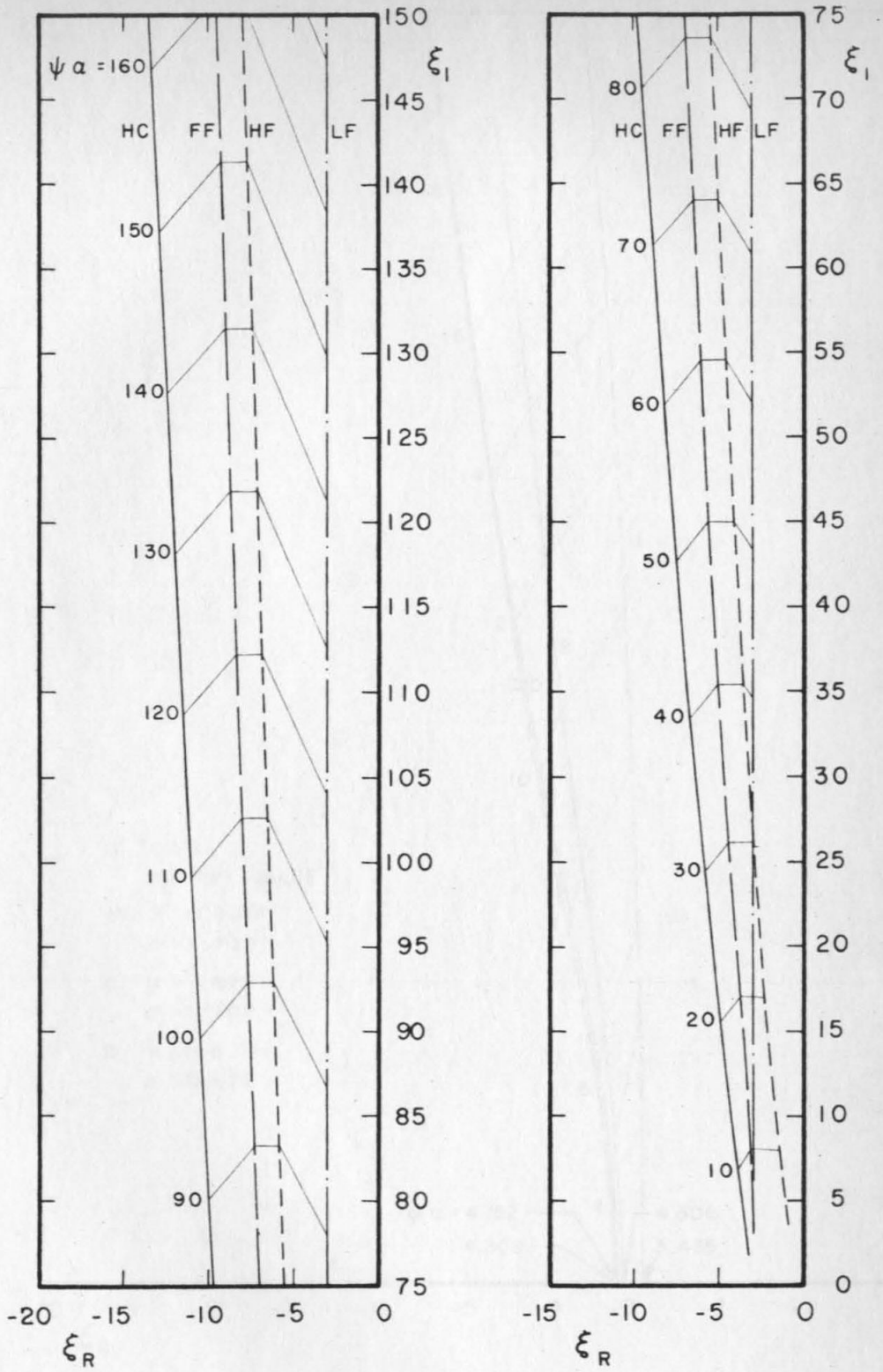

Figure 11. Pole Locus - Overall View

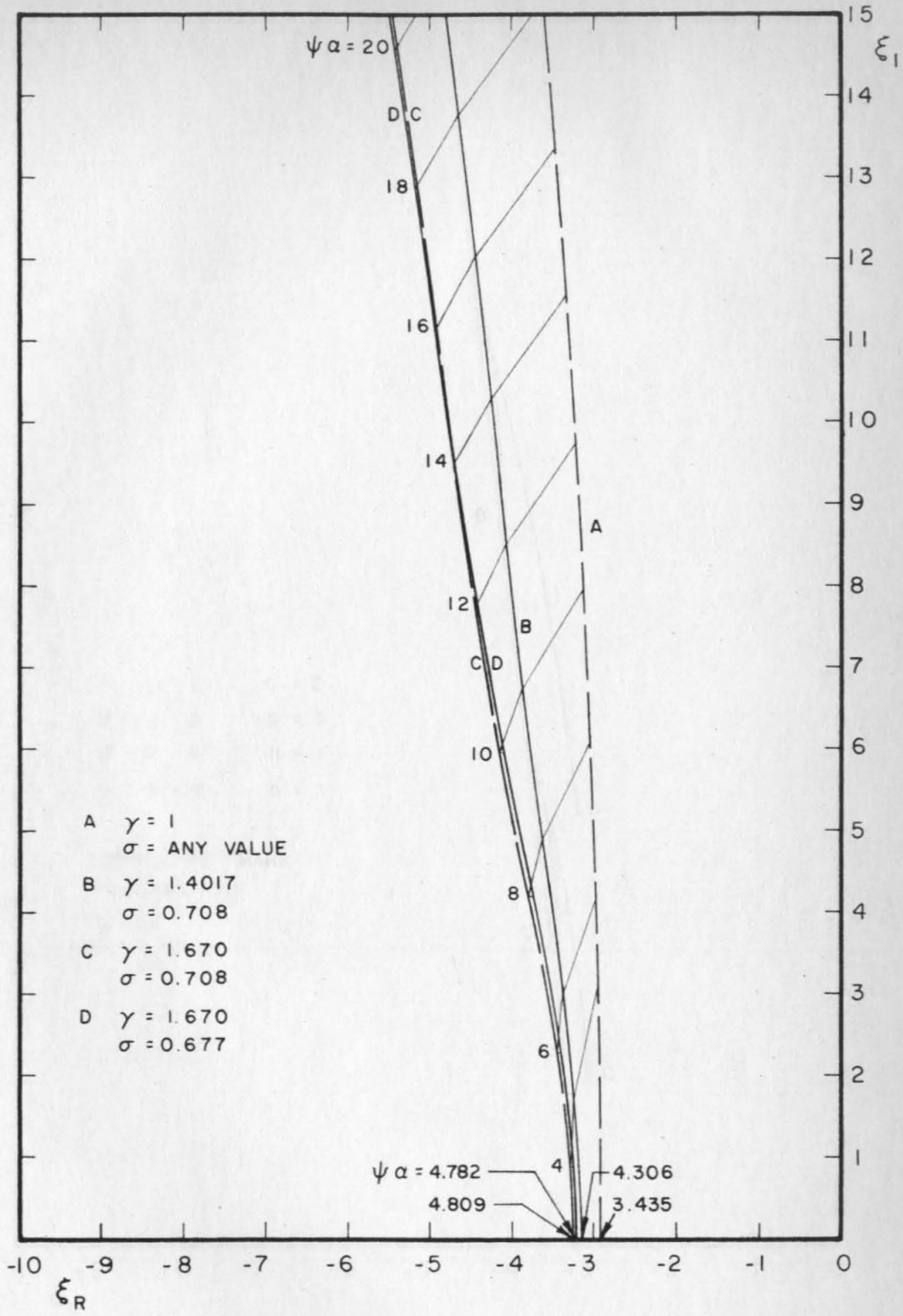

Figure 12. Pole Locus - Changes with γ and σ

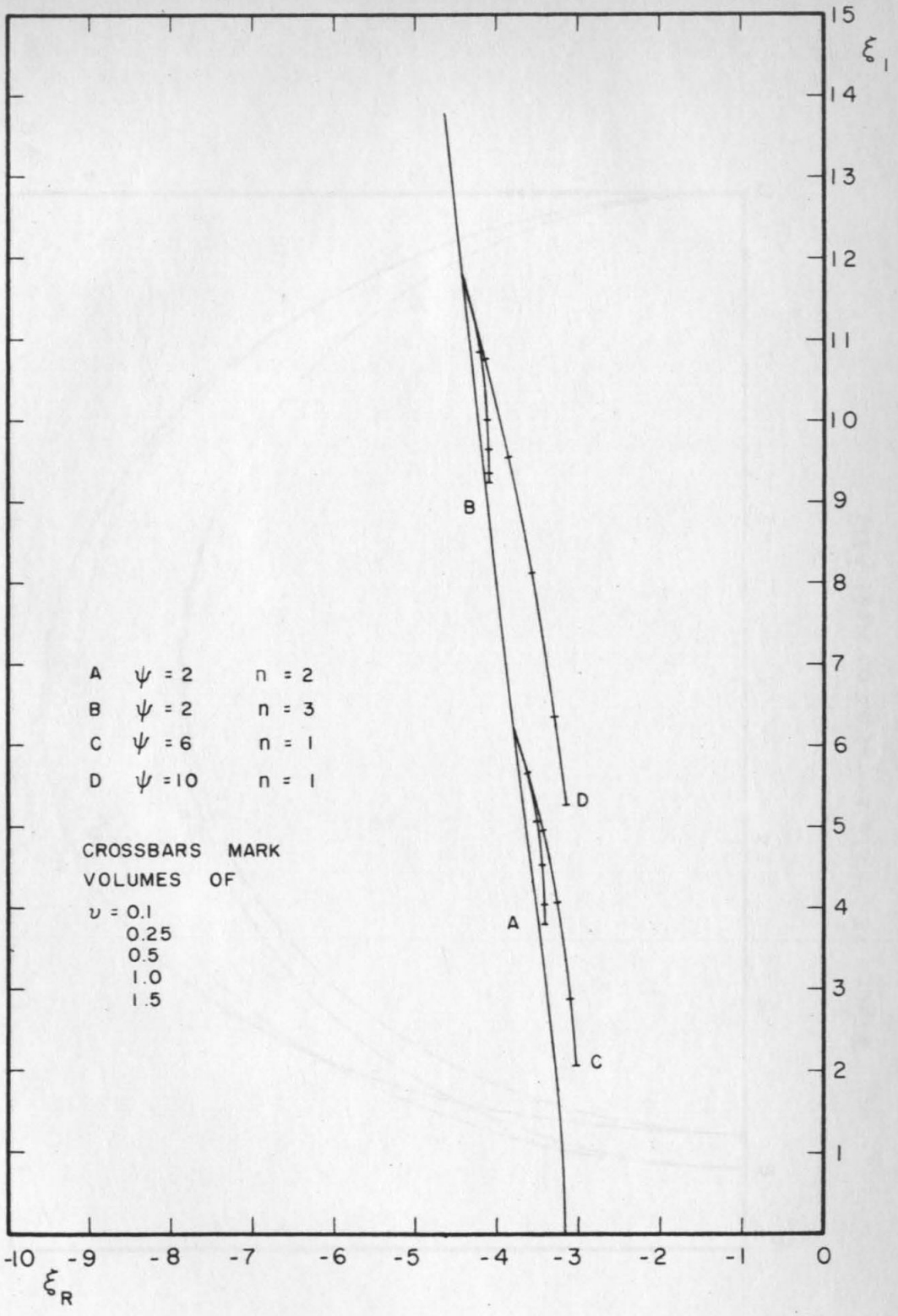

Figure 13. Pole Locus - Heat Conduction with Volume

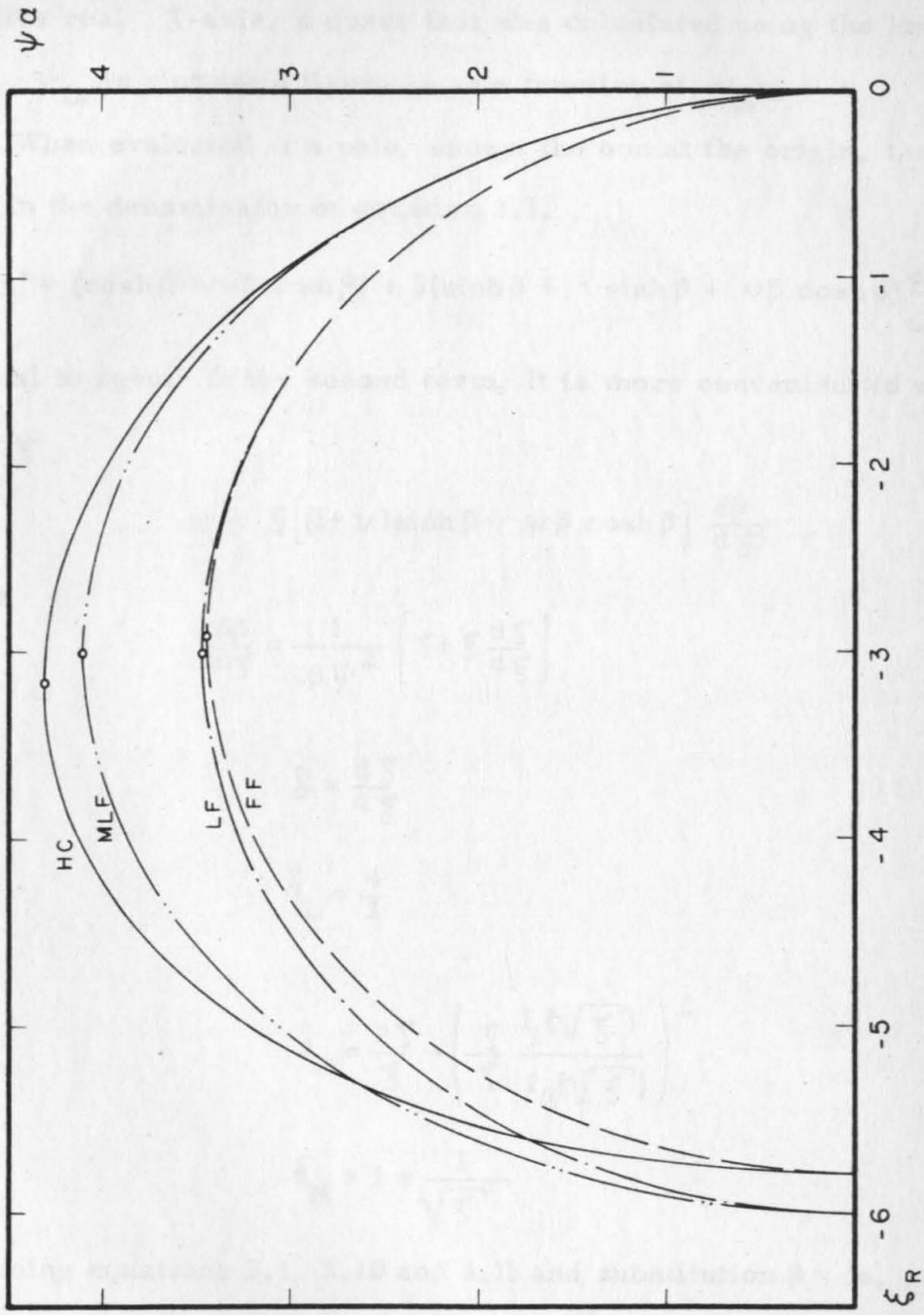

Figure 14. Pole Location on Real Axis

To determine the validity of Iberall's approximation along the negative real ξ-axis, a curve that was calculated using the low-frequency β and ψ_{Is} is plotted in figure 14 as a function of $\psi_A a$.

When evaluated at a pole, except the one at the origin, the first term in the denominator of equation 3.1,

$$g' = (\cosh\beta + \nu\beta \sinh\beta) + \tilde{s}(\sinh\beta + \nu\sinh\beta + \nu\beta \cosh\beta)\frac{d\beta}{d\tilde{s}}$$

is equal to zero. In the second term, it is more convenient to substitute $\psi \tilde{s} = \xi$.

$$g' = \xi\left[(1+\nu)\sinh\beta + \nu\beta \cosh\beta\right]\frac{d\beta}{d\xi} \tag{3.10}$$

where

$$\frac{d\beta}{d\xi} = \frac{1}{2\beta\psi^2}\left[\zeta + \xi\frac{d\zeta}{d\xi}\right] \tag{3.11}$$

Let

$$\delta = \frac{d\zeta}{d\xi}$$

then

$$\delta_L = \frac{4}{3}$$

$$\delta_F = \frac{2\zeta}{\xi} - \left(\frac{\zeta}{\xi}\frac{I_1(\sqrt{\xi})}{I_0(\sqrt{\xi})}\right)^2 \tag{3.12}$$

$$\delta_H = 1 + \frac{1}{\sqrt{\xi}}$$

Combining equations 3.1, 3.10 and 3.11 and substitution $\beta = ia$, produces

$$\tilde{p}(1, \tau) = 1 + \sum_{a_n} \frac{2ia_n\psi^2 \exp(\frac{\xi_n}{\psi}\tau)}{\xi_n\left[(1+\nu)\sinh ia_n + i\nu a_n \cosh ia_n\right]\left[\zeta_n + \xi_n \delta_n\right]}$$

or

$$\tilde{p}(1,\tau) = 1 + \sum_{a_n} \frac{2a_n \psi^2 e^{\frac{\xi_n}{\psi}\tau}}{\xi_n \left[(1+\nu)\sin a_n + \nu a_n \cos a_n\right]\left[\xi_n + \xi_n \delta_n\right]} \qquad (3.13)$$

$$n=1, 2, \ldots,$$

If heat conduction is included,

$$g' = \xi\left[\sinh\beta\Gamma + \frac{\nu\beta}{\Gamma}\cosh\beta\Gamma\right]\frac{d\beta\Gamma}{d\xi} + \frac{\nu}{\Gamma}\sinh\beta\Gamma\left(\frac{d\beta}{d\xi} - \frac{\beta}{\Gamma}\frac{d\Gamma}{d\xi}\right) \qquad (3.14)$$

where

$$\frac{d\Gamma^2}{d\xi} = \frac{(\gamma-1)}{\xi}\left[1 - \frac{I_1(\sqrt{\sigma\xi})}{I_0(\sqrt{\sigma\xi})}\left(\frac{2}{\sqrt{\sigma\xi}} + \frac{I_1(\sqrt{\sigma\xi})}{I_0(\sqrt{\sigma\xi})}\right)\right] \qquad (3.15)$$

In dimensionless form, the contribution of the residues to the pressure at the end of a tube resulting from the application of a pressure step at the other end is,

$$\tilde{p}(1,\tau) = 1 + \sum_{n} \frac{e^{\xi_n \frac{\tau}{\psi}}}{\left[\xi_n\left[\sinh\beta_n\Gamma_n + \frac{\nu\beta_n}{\Gamma_n}\cosh\beta_n\Gamma_n\right]\left(\frac{d\beta\Gamma}{d\xi}\right)_n + \frac{\nu}{\Gamma_n}\sinh\beta_n\Gamma_n\left[\left(\frac{d\beta}{d\xi}\right)_n - \frac{\beta_n}{\Gamma_n}\left(\frac{d\Gamma}{d\xi}\right)_n\right]\right]} \qquad (3.16)$$

$$n=1, 2, \ldots,$$

Other Contributions

The simple theory just outlined suffices for the low-frequency approximation, and the sum of the residues gives the total contribution to the pressure.

In the high-frequency approximation, branch character is introduced because the Bessel functions are replaced by a simple expression containing a square root.

$$\frac{2}{\sqrt{\xi}} \frac{I_1(\sqrt{\xi})}{I_0(\sqrt{\xi})} \approx \frac{2}{\sqrt{\xi}} \qquad \xi \text{ large}$$

The branch cut is taken along the negative real ξ-axis and the integration contour is distorted so that it does not cross the branch cut, (fig. 15). The contribution along the segments 3, 4 and 5 must be evaluated numerically. Since the modified contour cuts out the pole at the origin, whose contribution has already been included in the summation of the residues, it is necessary to subtract the value 1.0 from the integration results before they are added to the contribution of the residues. The integration contributions are small (see Table 2), but are non-vanishing for all the ψ's and for all the τ's considered in this work.

In the full-frequency and heat conduction approximations, a different difficulty arises. If β, or $\beta\Gamma$, is evaluated along the negative real ξ-axis, there are regions where it becomes imaginary, (see Table 3). In these regions, it is possible to find solutions to the equation

$$\beta = i\alpha \qquad \text{or } \beta\Gamma = i\alpha \tag{3.17}$$

respectively. The function β, or $\beta\Gamma$, takes on the value i-zero at the end of the region farther from the origin, and the value i-infinity at the end nearer the origin. Since α can take on an infinite number of values, there are an infinite number of solutions to equation 3.17, and therefore, an infinite number of poles in each region. The residue theorem requires a finite number of poles within the contour, so the contour must be distorted

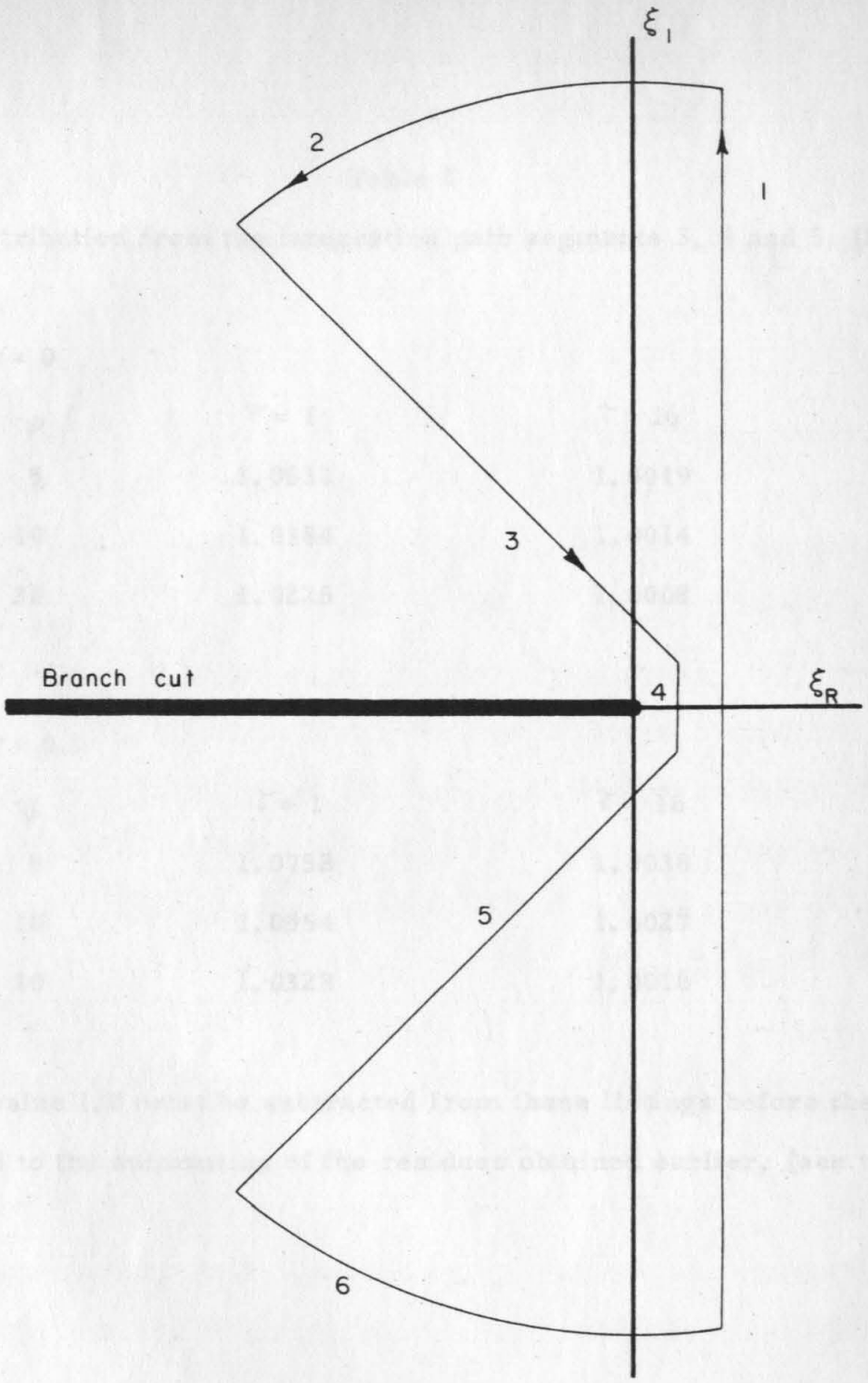

Figure 15. Integration Contour - High-frequency Approximation

Table 2

Contribution from the integration path segments 3, 4 and 5, (fig. 15).

$\upsilon = 0$

ψ	$\tau = 1$	$\tau = 16$
5	1.0532	1.0019
10	1.0384	1.0014
30	1.0225	1.0008

$\upsilon = 0.5$

ψ	$\tau = 1$	$\tau = 16$
5	1.0758	1.0038
10	1.0554	1.0027
30	1.0328	1.0016

The value 1.0 must be subtracted from these listings before they are added to the summation of the residues obtained earlier, (see text).

Table 3

Regions along the negative real ξ-axis containing an infinite number of poles.

β	$\beta\Gamma$
	-8.2 - 10.2
-26.4 - 30.5	-26.4 - 30.5
	-43.0 - 45.2
-70.8 - 74.9	-70.8 - 74.9
	-105.8 - 108.0
-135.0 - 139.1	-135.0 - 139.1
	-196.4 - 198.6
-218.9 - 222.9	-218.9 - 222.9
	-314.9 - 317.1

to eliminate these regions, (fig. 16). The contribution along the segments 3, 4 and 5 were not significant for all ψ, nor for all τ, (see Table 4). When the contributions along these path segments are added to the sum of the residues, the total pressure is obtained.

Integration

The numerical integration was carried out using the Gaussian integration formula. The infinite integral was broken down into small intervals which were integrated and then summed. As a check on the accuracy of the numerical evaluation, each interval was first integrated with a nine-point approximation, and then with an eight-point approximation, and the two answers compared. If the difference was greater than a given number, the size of the interval was cut; if smaller than a smaller number, the next interval was increased in size. The integration was truncated if the contribution of the absolute value of the integrand over a specified interval was less than a given amount. All of the above operations were performed automatically with the given numbers supplied as input that could be varied in an attempt to optimize the procedure. The path of integration was either a straight line parallel to the imaginary axis, or it took a jog to the left to take advantage of the exponential character of the integrand,(fig. 17). Since the integrand evaluated at a point in the lower half plane is the complex conjugate of the integrand evaluated at the conjugate point in the upper half plane, only one half of this path had to be integrated. The starting point along the real ξ-axis was determined by the minimum of the integrand along the real axis as long as that minimum

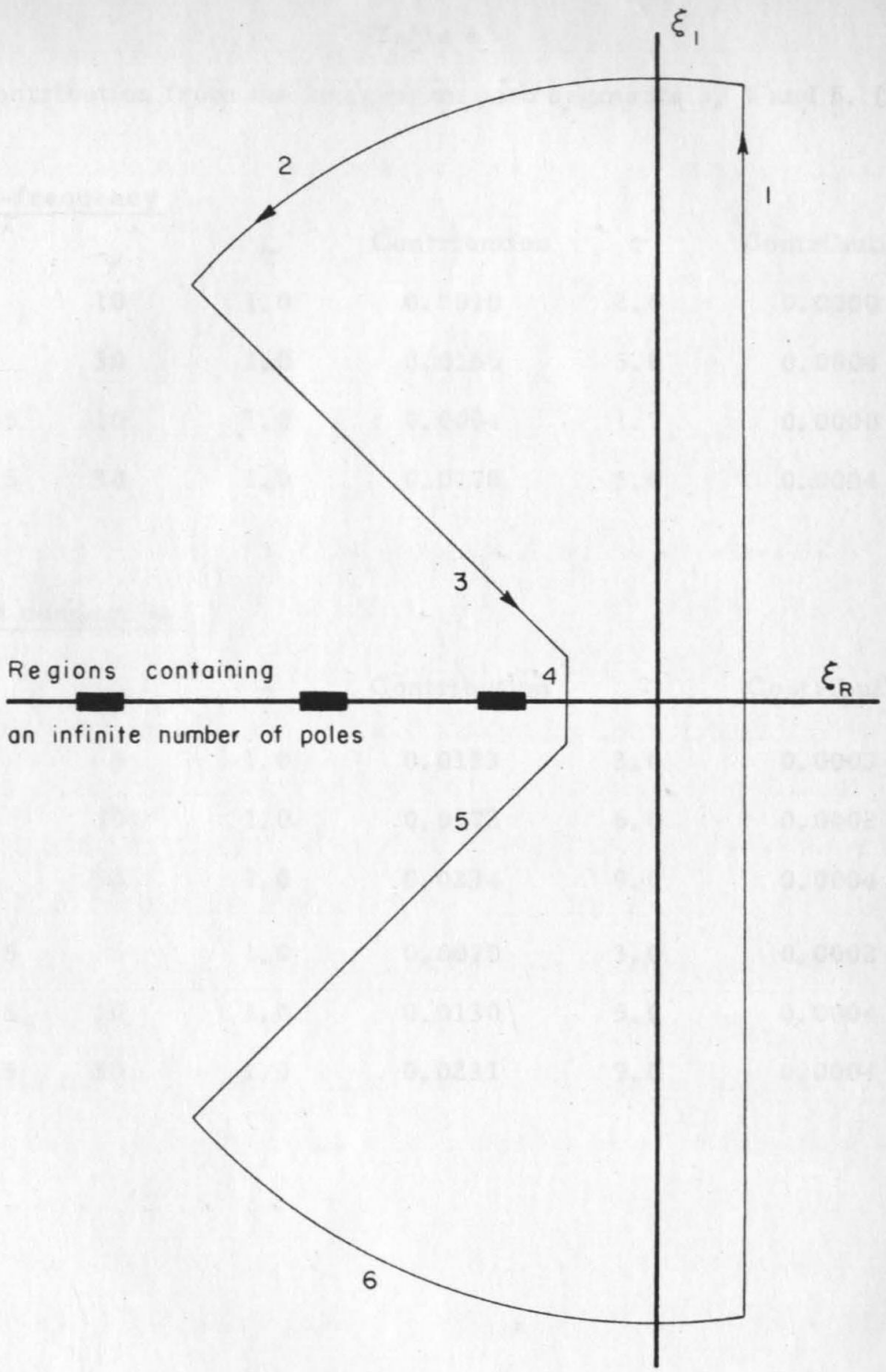

Figure 16. Integration Contour - Full-frequency and Heat Conduction

Table 4

Contribution from the integration path segments 3, 4 and 5, (fig. 16).

full-frequency

υ	ψ	τ	Contribution	τ	Contribution
0	10	1.0	0.0010	2.0	0.0000
0	30	1.0	0.0156	5.0	0.0004
0.5	10	1.0	0.0004	1.7	0.0000
0.5	30	1.0	0.0178	5.0	0.0004

heat conduction

υ	ψ	τ	Contribution	τ	Contribution
0	5	1.0	0.0133	3.0	0.0003
0	10	1.0	0.0172	6.0	0.0002
0	30	1.0	0.0234	9.0	0.0004
0.5	5	1.0	0.0070	3.0	0.0002
0.5	10	1.0	0.0130	5.0	0.0004
0.5	30	1.0	0.0231	9.0	0.0004

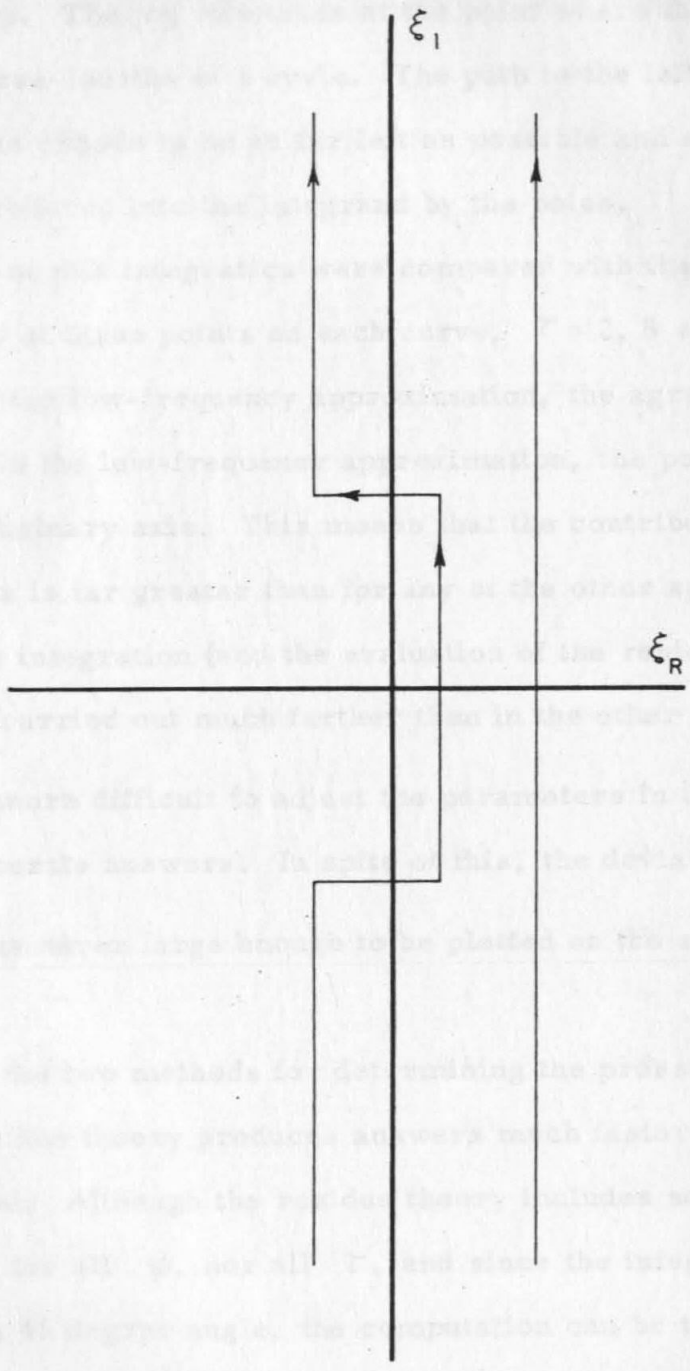

Figure 17. Integration Paths

was located at $\xi = 3.0$, or less. For small ψ and large τ this minimum became very sharp. The jog was taken at the point where the integrand had passed through three-fourths of a cycle. The path to the left of the imaginary axis was chosen to be as far left as possible and still avoid the irregularities introduced into the integrand by the poles.

The results of this integration were compared with the results of the residue theory at three points on each curve, $\tau = 2$, 8 and 14. In all cases, except for the low-frequency approximation, the agreement was within $\pm$ 0.0001. In the low-frequency approximation, the pole locus is parallel to the imaginary axis. This means that the contribution of the more distant poles is far greater than for any of the other approximations. Consequently, the integration (and the evaluation of the residues, see Results) must be carried out much farther than in the other cases. This meant it was far more difficult to adjust the parameters in the integration scheme to get accurate answers. In spite of this, the deviation from the residue theory was never large enough to be plotted on the scale used in this work.

Comparing the two methods for determining the pressure, it is found that the residue theory produces answers much faster than the integration method. Although the residue theory includes some integration, it is not required for all ψ, nor all τ, and since the integration path is off to the left at a 45 degree angle, the computation can be truncated very quickly because of the exponential character of the integrand. A rough estimate would say that, if it took two hours for the computer to find the

poles, evaluate the residues, and the integration contribution where necessary, it would probably take 80 hours to obtain the same data by direct integration. The above estimate is, of necessity, rough because of the very wide variation in the integrating time required as a function of ψ and τ.

III. RESULTS

The calculation procedures outlined in the Analysis were programmed for a high speed digital computer. The computer results, comparing the various approximations for several values of the parameters, are given here. The values of the parameters were chosen in an attempt to illustrate the range of validity of the different approximate theories.

All of the curves of this section have been drawn using the following representations to distinguish the curves obtained by using the various approximations.

low-frequency approximation (LF) ———·———·———·———

full-frequency approximation (FF) —— —— —— —— —— —— ——

high-frequency approximation (HF) — — — — — — — — — — — — —

theory with heat conduction (HC) ————————————————

modified low-frequency
approximation (see text) (MLF) ———··———··———··——

Frequency Response

Although the transient response curves were considered the more fundamentally useful, a few samples of frequency response curves are included for completeness. Figure 18 compares the various approximations for $\psi = 2.5$ which is the optimum* value for the low-frequency and the full-frequency approximations. In order to compare the various approximations for a tube with less damping, curves for $\psi = 10$ and

---

* See Notation for the definition of optinum response.

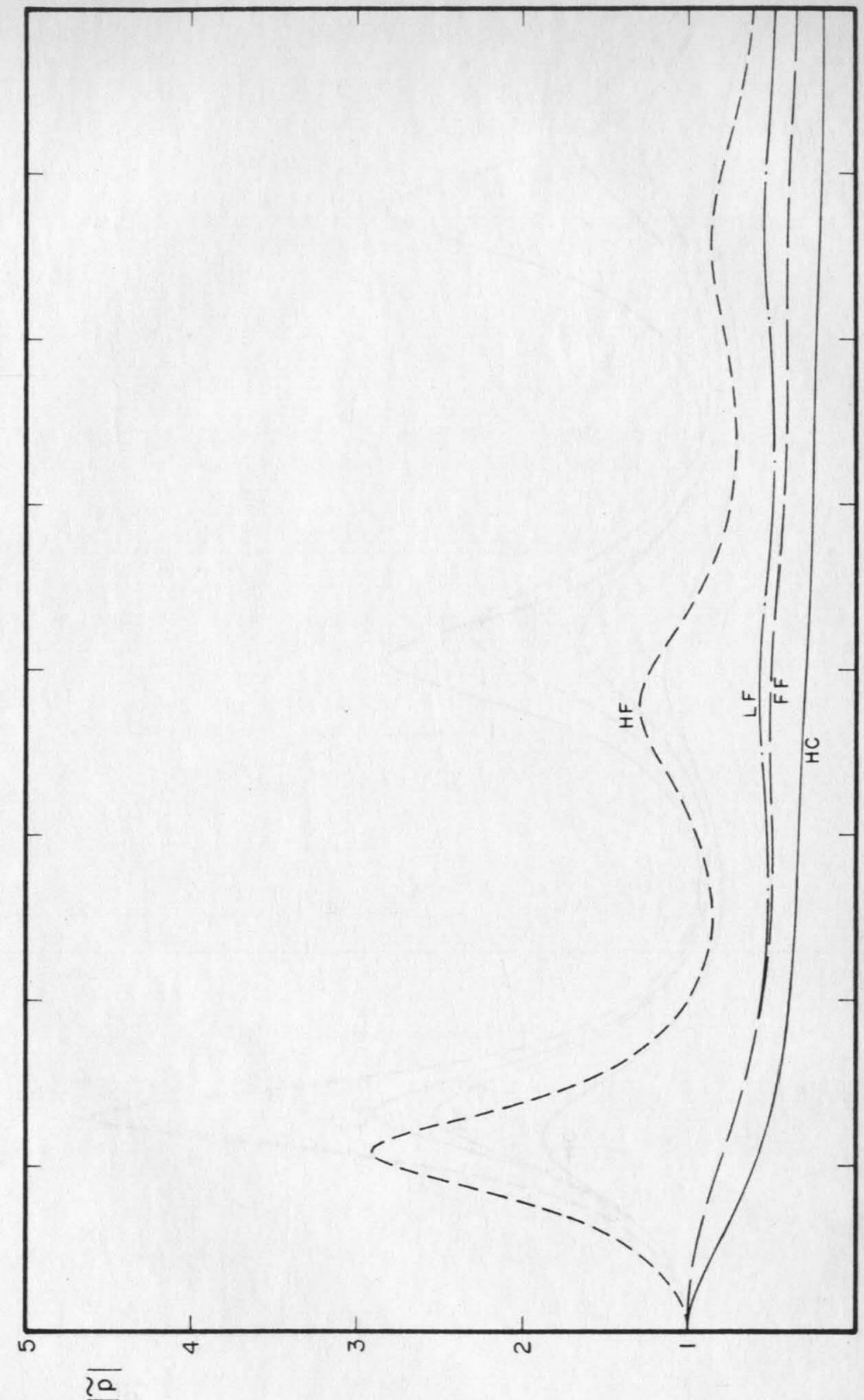

Figure 18. Frequency Response - $\upsilon = 0.0$; $\psi = 2.5$

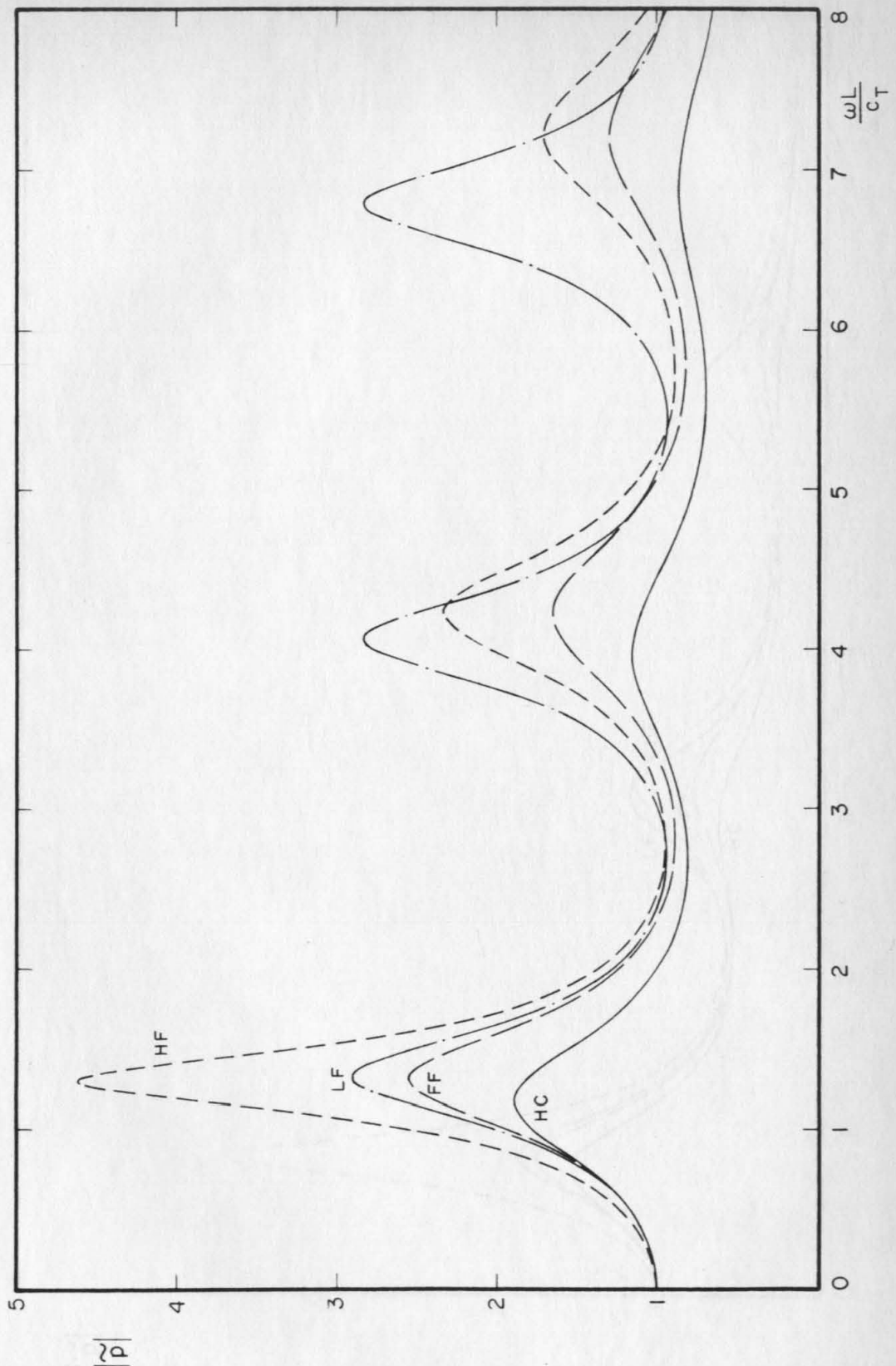

Figure 19. Frequency Response - $\nu = 0.0$; $\psi = 10$

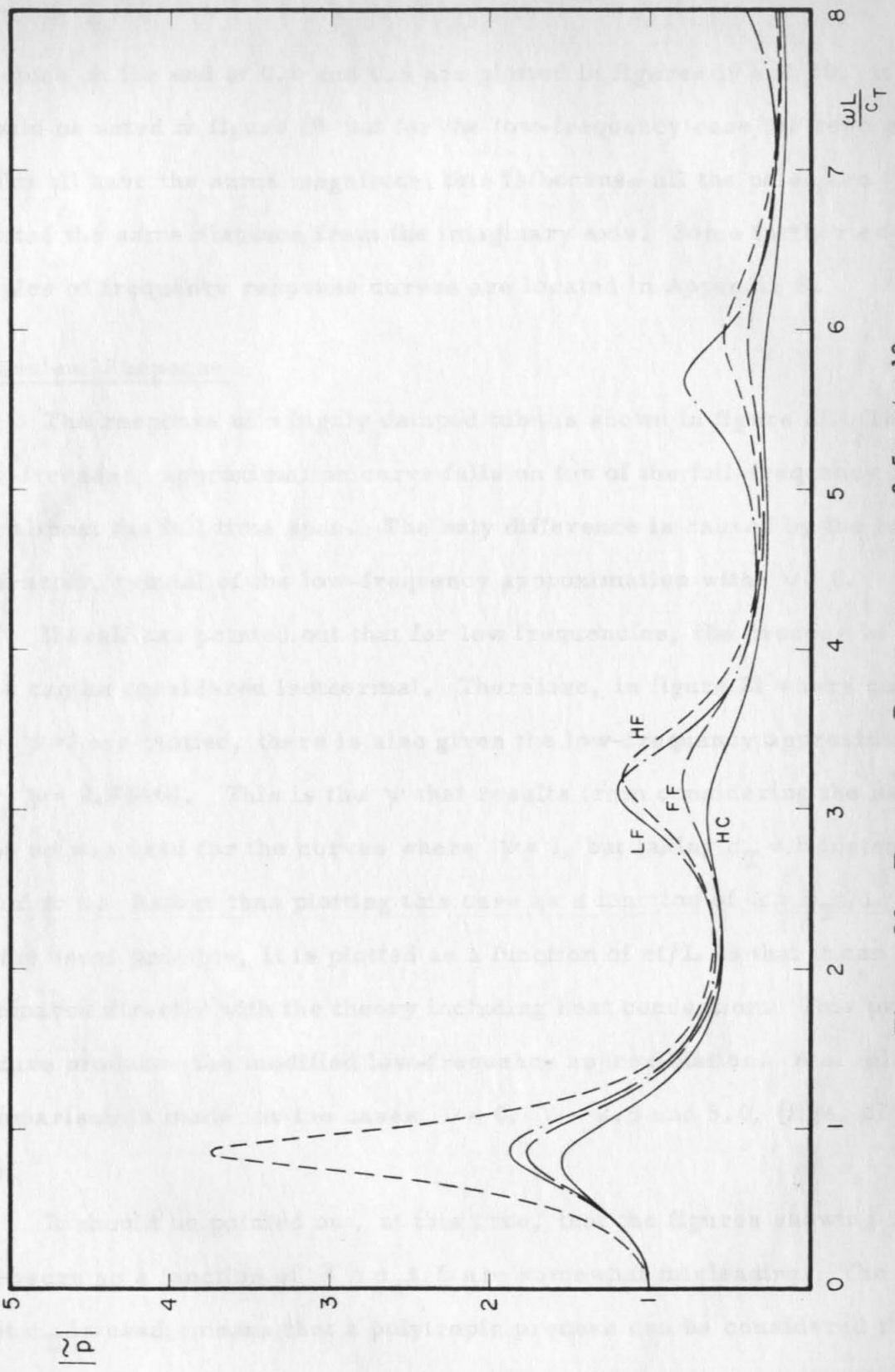

Figure 20. Frequency Response - $\upsilon = 0.5$; $\psi = 10$

volumes on the end of 0.0 and 0.5 are plotted in figures 19 and 20. It should be noted in figure 19 that for the low-frequency case the resonant peaks all have the same magnitude; this is because all the poles are located the same distance from the imaginary axis. Some further examples of frequency response curves are located in Appendix B.

Transient Response

The response of a highly damped tube is shown in figure 21. The low-frequency approximation curve falls on top of the full-frequency curve for almost the full time span. The only difference is caused by the jump character, typical of the low-frequency approximation with $\upsilon = 0$.

Iberall has pointed out that for low frequencies, the process in the tube can be considered isothermal. Therefore, in figure 21 where curves for $\psi = 1$ are plotted, there is also given the low-frequency approximation for $\psi = 0.84464$. This is the ψ that results from considering the same tube as was used for the curves where $\psi = 1$, but taking $c_T = b$ instead of equal to c. Rather than plotting this case as a function of $\tau = c_T t/L$, as is the usual practice, it is plotted as a function of ct/L so that it can be compared directly with the theory including heat conduction. This procedure produces the modified low-frequency approximation. A similar comparison is made for the cases $\upsilon = 0$, $\psi = 2.5$ and 5.0, (figs. 22 and 23).

It should be pointed out, at this time, that the figures showing the pressure as a function of $\tau = c_T t/L$ are somewhat misleading. The fact that c_T is used, means that a polytropic process can be considered that

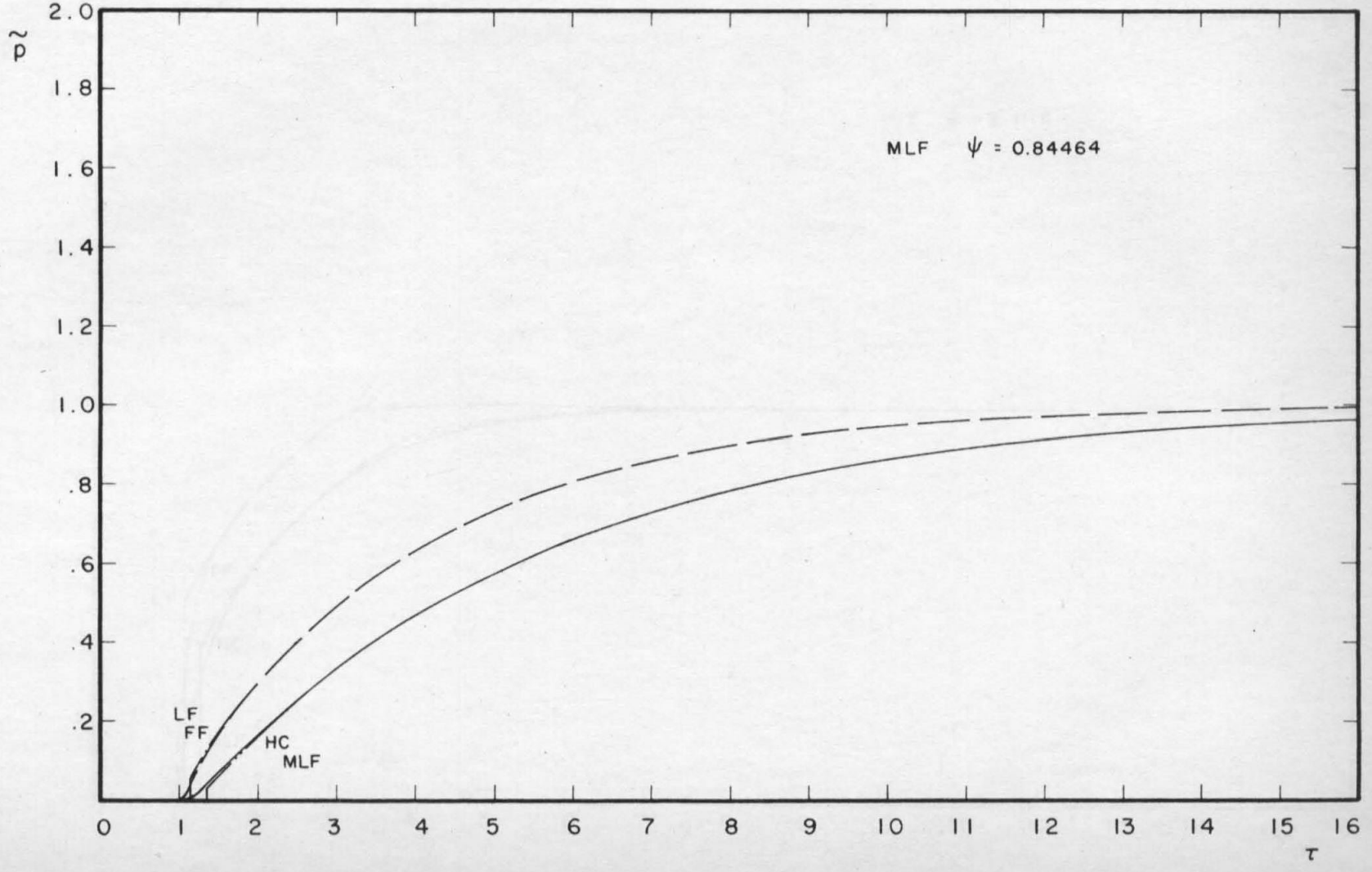

Figure 21. Transient Response - $\upsilon = 0.0$; $\psi = 1$

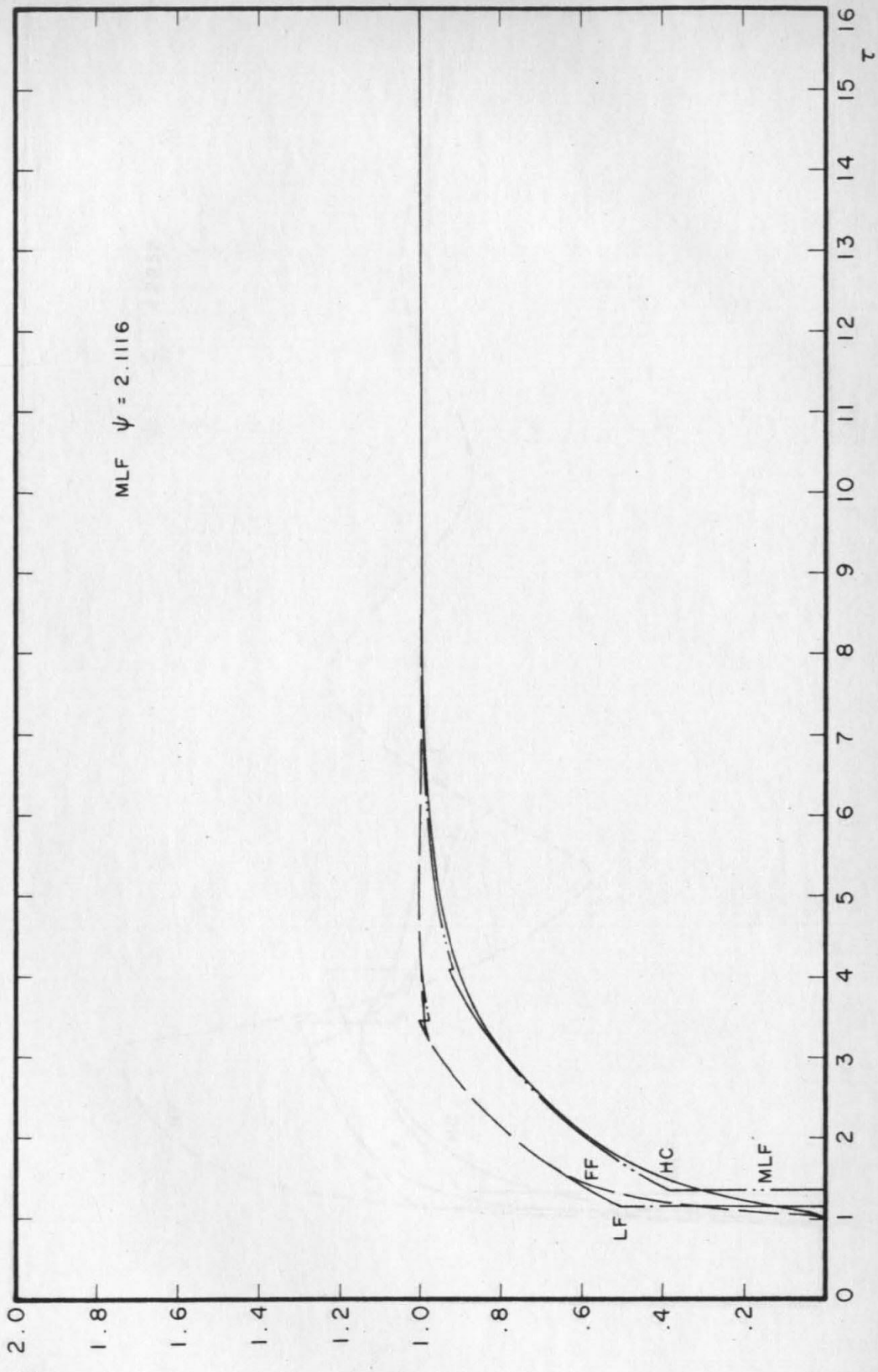

Figure 22. Transient Response - $\nu = 0.0$; $\psi = 2.5$

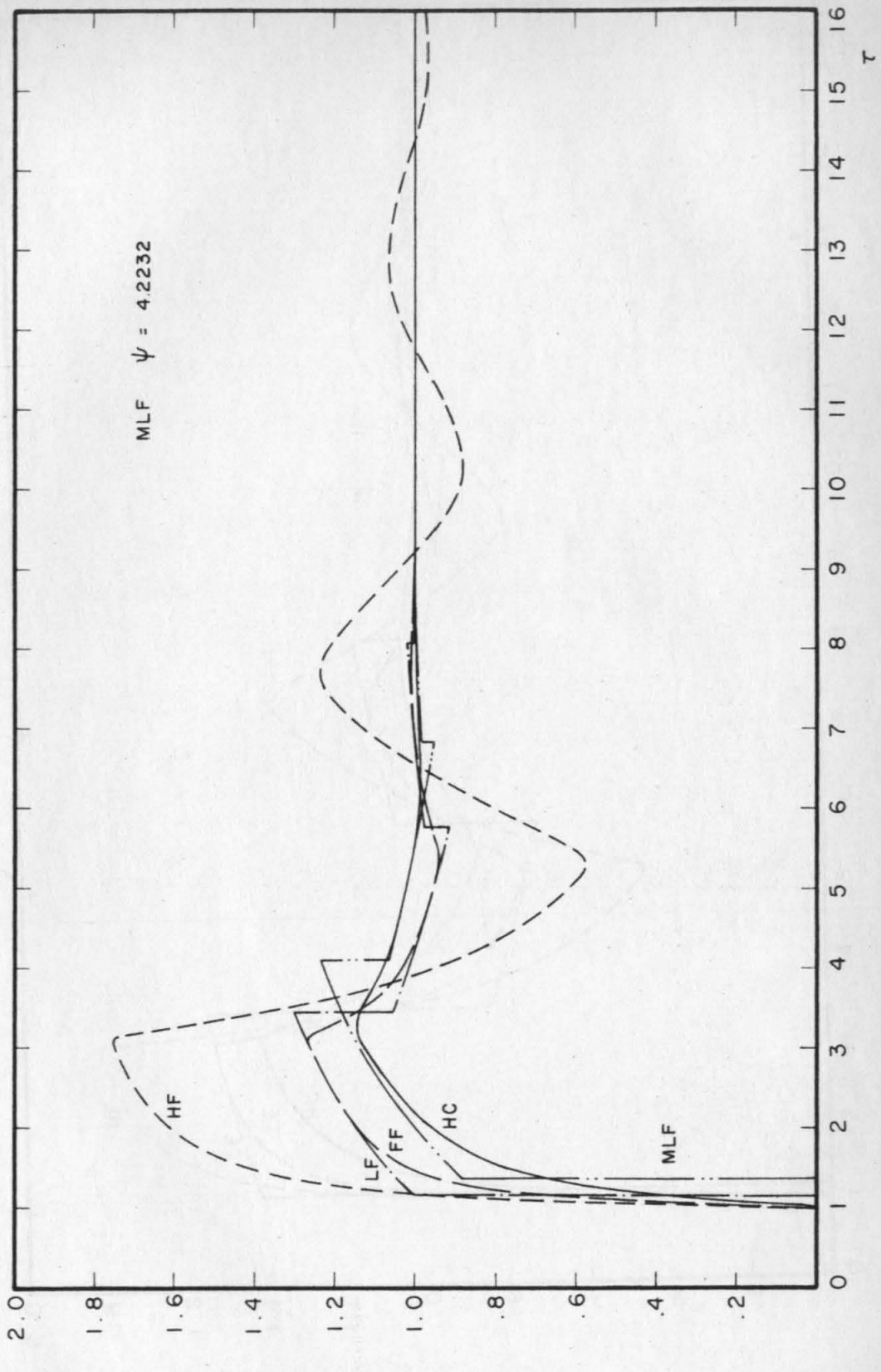

Figure 23. Transient Response - $\nu = 0.0$; $\psi = 5$

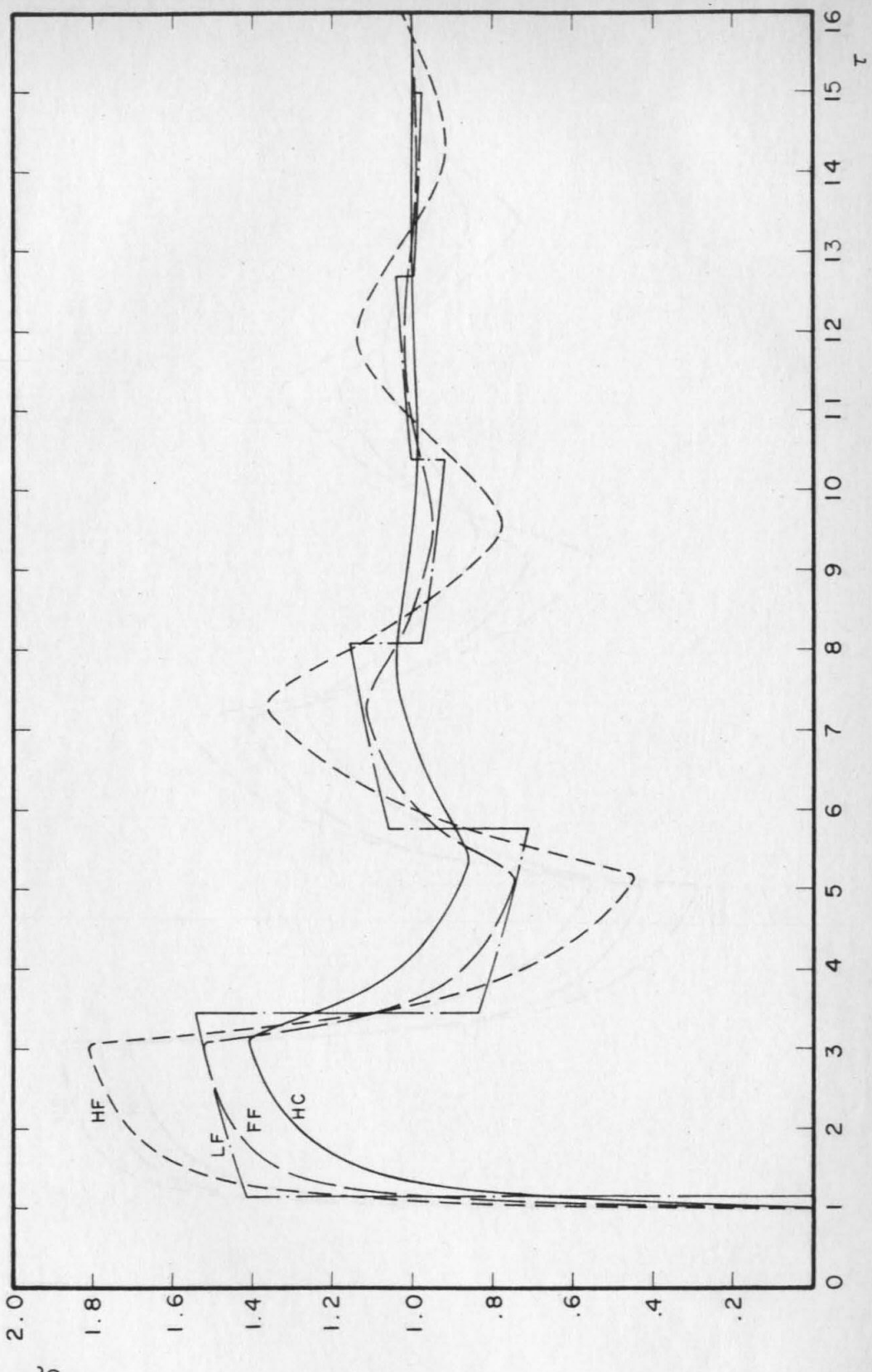

Figure 24. Transient Response - $\upsilon = 0.0$; $\psi = 10$

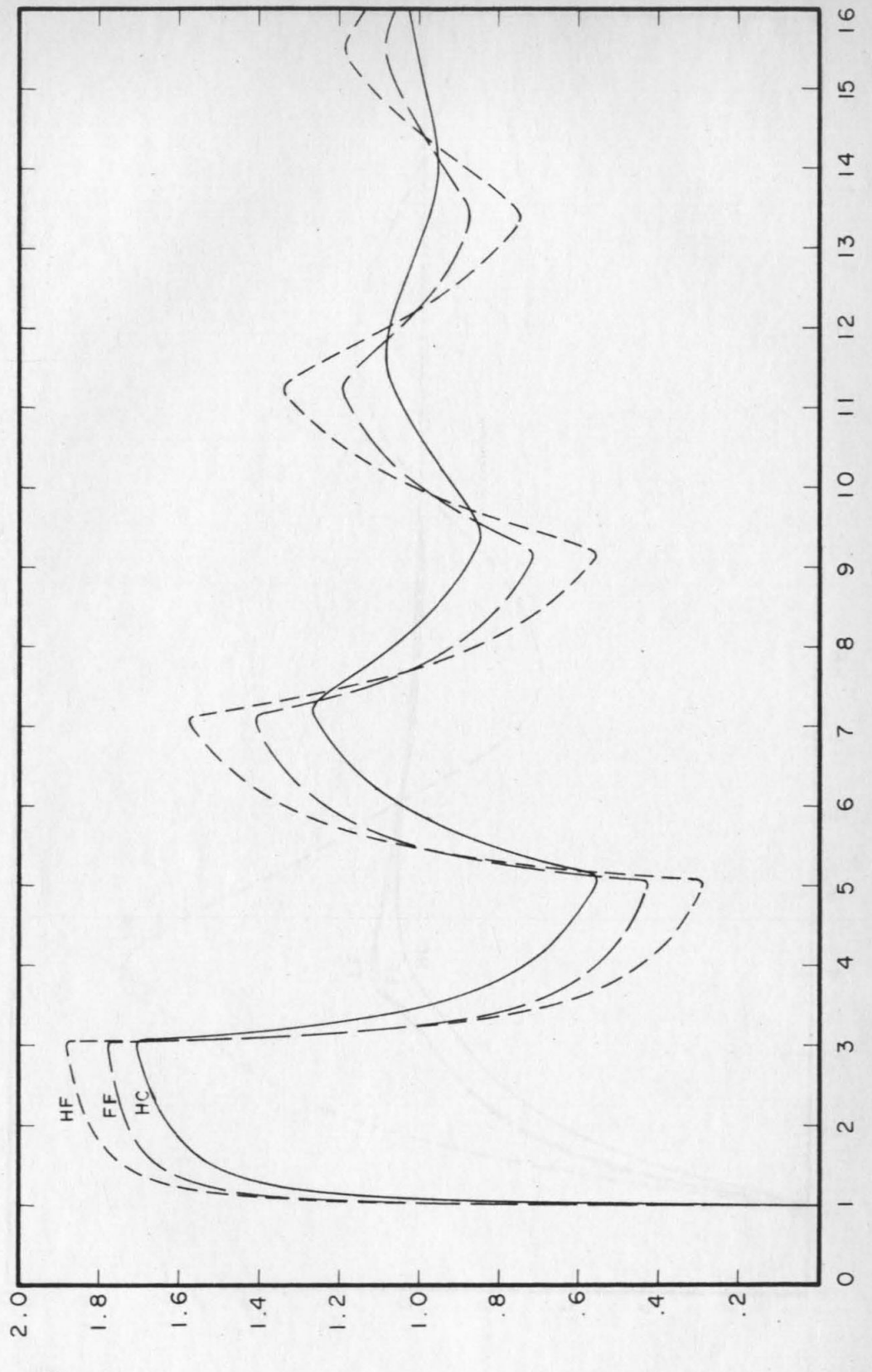

Figure 25. Transient Response - $\upsilon = 0.0$; $\psi = 30$

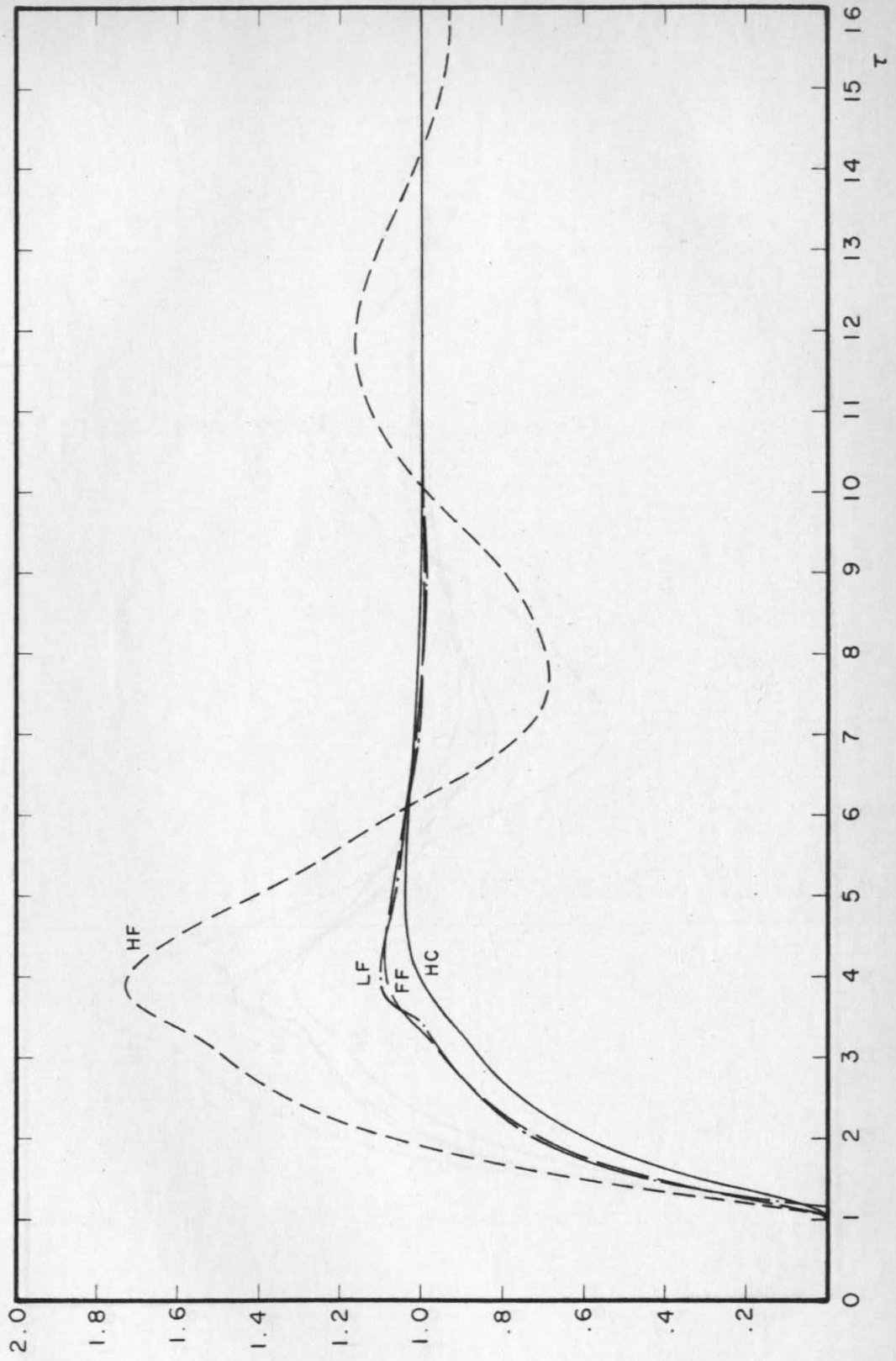

Figure 26. Transient Response - $\upsilon = 0.5$; $\psi = 5$

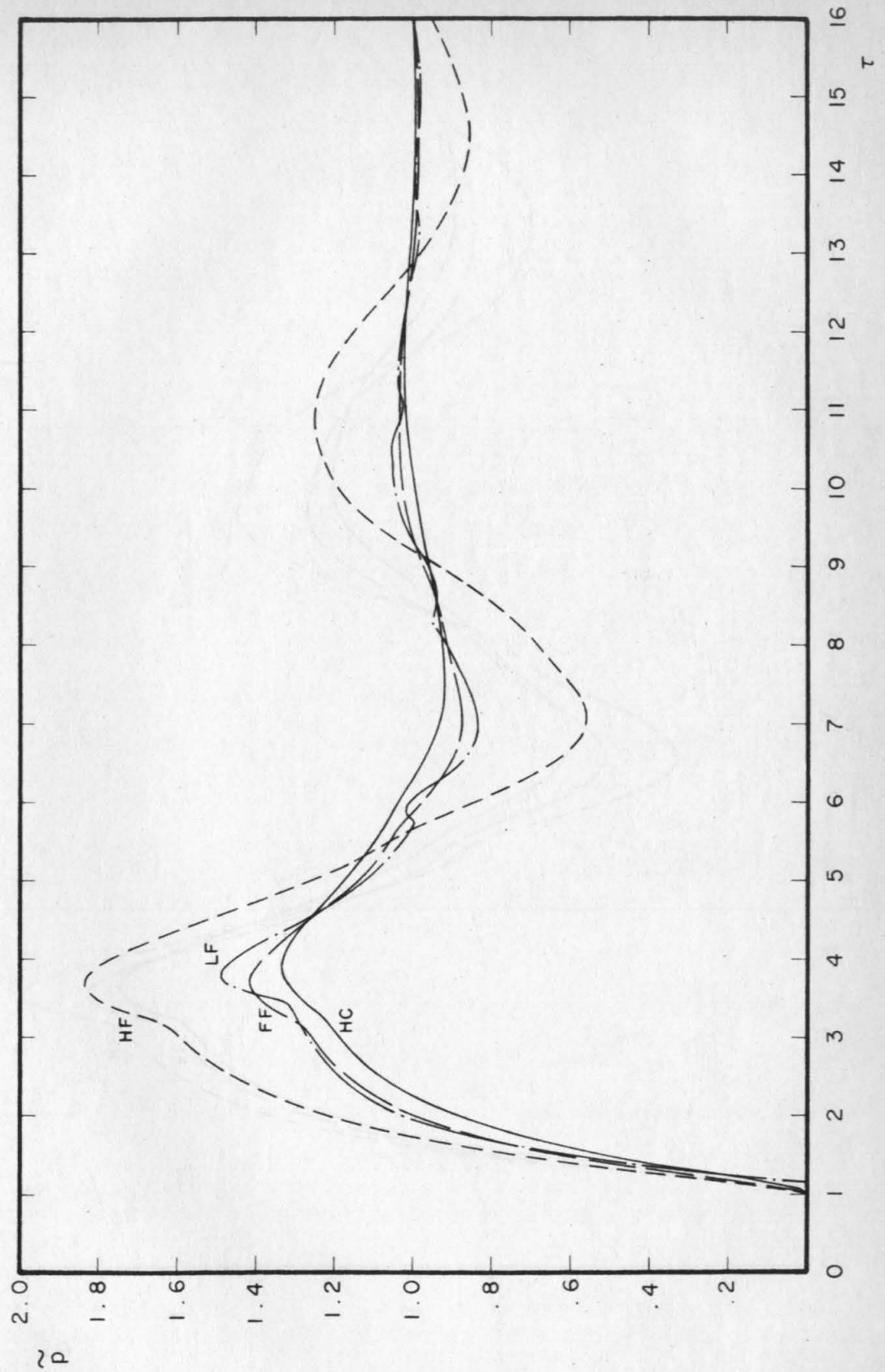

Figure 27. Transient Response - $\upsilon = 0.5$; $\psi = 10$

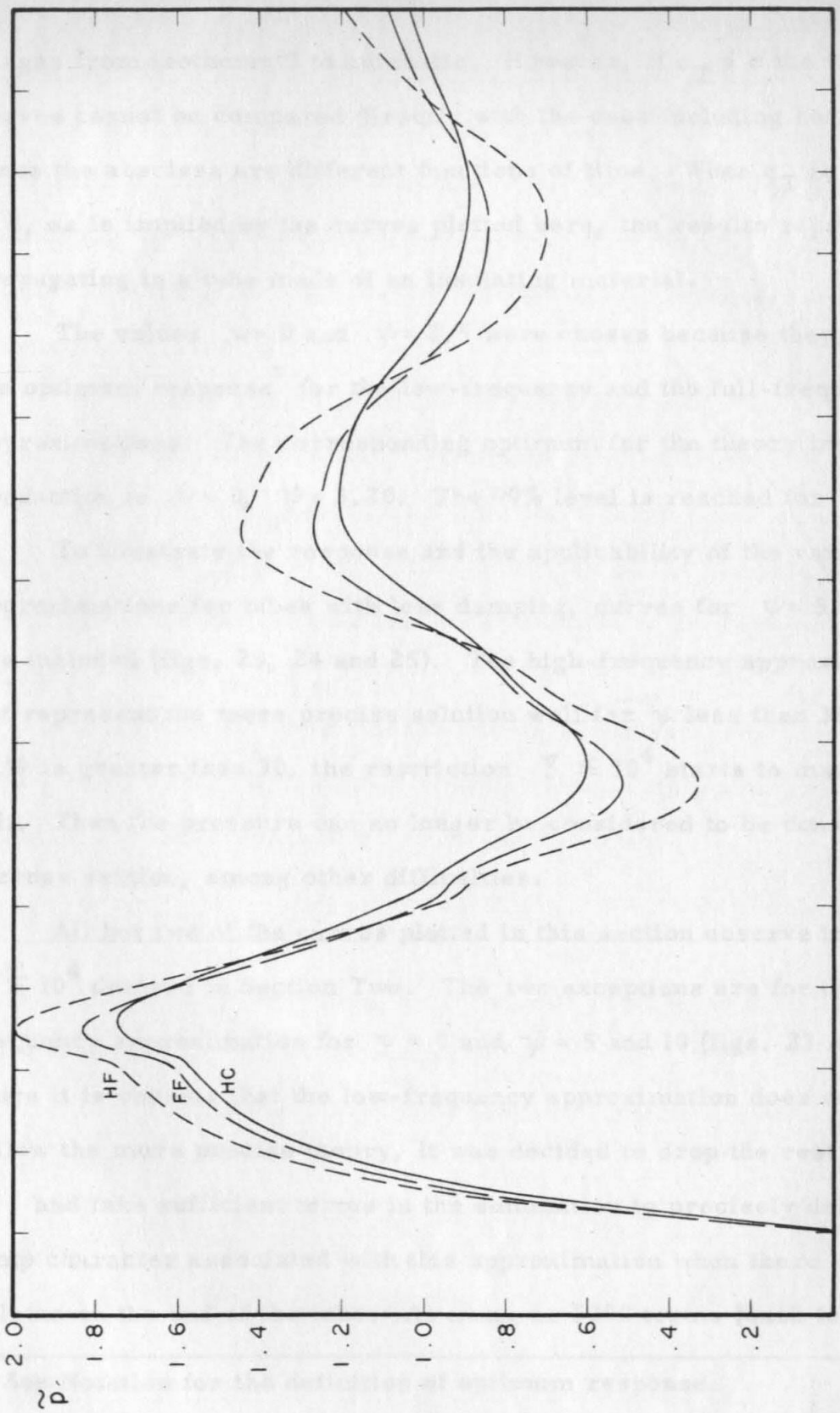

Figure 28. Transient Response - $\nu = 0.5$; $\psi = 30$

ranges from isothermal to adiabatic. However, if $c_T \neq c$ the various curves cannot be compared directly with the case including heat conduction since the abscissa are different functions of time. When c_T is set equal to c, as is implied by the curves plotted here, the results represent sound propagating in a tube made of an insulating material.

The values $\upsilon = 0$ and $\psi = 2.5$ were chosen because they produce the optimum response* for the low-frequency and the full-frequency approximations. The corresponding optimum for the theory including heat conduction is $\upsilon = 0$, $\psi = 3.20$. The 99% level is reached for $\tau = 4.0$.

To illustrate the response and the applicability of the various approximations for tubes with less damping, curves for $\psi = 5$, 10 and 30 are included (figs. 23, 24 and 25). The high-frequency approximation does not represent the more precise solution well for ψ less than 30. However, if ψ is greater than 30, the restriction $\xi \leq 10^4$ starts to make itself felt. Then the pressure can no longer be considered to be constant over a cross section, among other difficulties.

All but two of the curves plotted in this section observe the restriction $\xi \leq 10^4$ derived in Section Two. The two exceptions are for the low-frequency approximation for $\upsilon = 0$ and $\psi = 5$ and 10 (figs. 23 and 24). Since it is obvious that the low-frequency approximation does not closely follow the more precise theory, it was decided to drop the restriction on ξ, and take sufficient terms in the summation to precisely delineate the jump character associated with this approximation when there is zero volume on the end of the tube. As many as 5000 terms (each term includes

* See Notation for the definition of optimum response.

a pole and its complex conjugate) were summed, which involves $\xi = 1.36 \times 10^5$ for $\psi = 10$, and $\xi = 6.80 \times 10^4$ for $\psi = 5$. However, at the worst, the difference between the 5000-term summation and the case restricting ξ to 10^4 was just barely plottable on the scale used here. When $\upsilon \neq 0$ the low-frequency approximation no longer displays jump character.

The effect of adding a volume is shown by the curves where $\upsilon = 0.5$, (figs. 26, 27 and 28). This is a relatively small volume compared to those Iberall (5) considered, but it still has a large effect on the shape of the curves. The larger the volume, the simpler the computation because fewer terms must be included in the summation of the residues for a given degree of accuracy.

Any volume on the end of the tube is detrimental from the point of view of optimizing the system. A simple illustration of this is given by using the two term approximation for the pressure

$$\tilde{p}(1, \tau) = 1 + Ae^{\frac{\xi_o}{\psi}\tau}$$

where, for optimum response, the first pole must be at a definite position, thereby fixing ξ, which is denoted by ξ_o.

It is the response in real time that is of interest. Making the substitutions:

$$\psi = \frac{R^2 c}{\nu L}$$

$$\tau = \frac{ct}{L}$$

the pressure becomes

$$\tilde{p}(1, t) = 1 + A\, e^{\frac{\xi_o \nu}{R^2} t}$$

The minimum time constant is obtained when the absolute value of $R^2 / \xi_{oR} \nu$ is a minimum. Only the real part of ξ_o must be included in the determination of the time constant. Since ξ_{oR} was previously fixed, and presumably ν cannot be changed, R is the parameter that determines the response time. The smaller R is, the better the response. The limitations on how small R can be made are the requirement that ξ_o be held constant, and how small L can be made within the restrictions of the physical layout. Any volume on the end of the tube requires an increase in R to keep ψa, and consequently ξ_o, constant, thereby degrading the response.

IV. CONCLUSIONS

A knowledge of the volume at the end of the tube and the tube parameters is sufficient to predict the behavior of the system response. The pole loci play an important role in making this possible. Although the first residue gives a good idea of the response of the tube, a detailed evaluation of the wave shape requires a large number of terms. This is particularly true near the wave front if ψ is large, and for the low-frequency approximation with its jump character.

Optimum response* is achieved with zero volume on the end of the tube and the tube parameters chosen so that $\psi = 2.5$ if the tube is made out of an insulating material, or $\psi = 3.2$ if the tube is made of a good heat conductor. If there is a volume on the end of the tube, the response is degraded.

The high-frequency approximation does not provide a good representation of the more precise theory except for tubes with so little damping that the theory presented here is of questionable value. In particular, the pressure is no longer constant over a cross section of the tube. If the tube has no volume on the end, better results are obtained more easily by using the procedure outlined in Appendix A.

Except for the jump phenomenon exhibited when $\upsilon = 0$, the low-frequency approximation represents the more precise theory very well for ψ up to about 3.5. The low-frequency approximation can be used to describe the cases of an insulating tube or a conducting tube by equating c_T to the values b or c, respectively.

---

* See Notation for the definition of optimum response.

If the tube is made out of an insulating material, the theory including heat conduction reduces to the full-frequency approximation with c_T set equal to c.

The residue theory is, in general, by far the best method of obtaining the transient response, both from the point of view of ease of application and the speed of obtaining results. As the volume at the end of the tube is increased, the number of terms required to achieve a desired accuracy is decreased. The difference between the low-frequency approximation, the full-frequency approximation and the theory including heat conduction is also decreased. This implies that the volume, instead of the tube, becomes the major factor controlling the response of the system.

APPENDIX A

TRAVELING WAVE SOLUTION

There is another, and simpler, method of inverting the Laplace transform of the pressure

$$\tilde{p}^* = \frac{1}{\tilde{s}(\cosh\beta + \upsilon\beta \sinh\beta)} \tag{A-1}$$

in the case where $\upsilon = 0$, and it is appropriate to use the high frequency approximation. In this case equation A-1 reduces to

$$\tilde{p}^* = \frac{1}{\tilde{s} \cosh\beta} \tag{A-2}$$

The β that is used here is obtained by taking the first two terms in the high-frequency expansion of the full-frequency β,

$$\beta_{H'} = \frac{1}{\psi}\left[\xi + \sqrt{\xi}\right] \tag{A-3}$$

where the prime on the subscript indicates that this approximation is the one appropriate to the discussion in this appendix. (A comparison of the method used here, to that of Section One, will be given later.) An expression for β analogous to equation A-3, differing in not being dimensionless, is derived by Mason (13), Chapter 4, Section 3.

The pressure as a function of time is found by substituting equation A-2 into the standard Laplace inversion formula.

$$\tilde{p}(\tau) = \frac{1}{2\pi i}\int_{Br_1} \frac{e^{\tilde{s}\tau} d\tilde{s}}{\tilde{s} \cosh \beta_{H'}} \tag{A-4}$$

where the integration is along the Bromwich contour (14). Applying the expansion

$$\frac{1}{\cosh z} = 2 \sum_{n=0}^{\infty} (-1)^n e^{-z(2n+1)} \tag{A-5}$$

where

$$\text{Real } z > 0$$

and writing $\beta_{H'}$ explicitly, equation A-4 becomes

$$\tilde{p}(\tau) = \frac{1}{2\pi i} \int_{Br_1} \sum_{n=0}^{\infty} \frac{2}{\tilde{s}} (-1)^n \; e^{-(2n+1)\left[\tilde{s} + \frac{\sqrt{\tilde{s}}}{\sqrt{\psi}}\right]} e^{\tilde{s}\tau} d\tilde{s} \tag{A-6}$$

Since the series is absolutely convergent, the order of the operations of integration and summation can be reversed. The n^{th} term of equation A-6 can be written

$$\tilde{p}_n = \frac{1}{2\pi i} \int_{Br_1} \frac{2}{\tilde{s}} (-1)^n e^{-(2n+1)\tilde{s}} \; e^{-(2n+1)\frac{\sqrt{\tilde{s}}}{\sqrt{\psi}}} \; e^{\tilde{s}\tau} d\tilde{s} \tag{A-7}$$

The factor

$$e^{-(2n+1)\tilde{s}}$$

represents a shift in the time origin so that the function given by the rest of the integral is delayed by an amount

$$\tau = 2n+1$$

where

$$\tilde{p}_n(\tau) = 0 \tag{A-8}$$

for

$$0 < \tau < 2n+1.$$

The inversion

$$\tilde{p}_n(\tau) = 2(-1)^n \left[\frac{1}{2\pi i} \int_{Br_1} \frac{1}{\tilde{s}} e^{-(2n+1)\frac{\sqrt{\tilde{s}}}{\sqrt{\psi}}} e^{\tilde{s}\left[\tau-(2n+1)\right]} d\tilde{s} \right]$$

is listed by Bateman (15), pg. 177 (it is also derived, in great detail, by Weber (7) pages 321-330) as:

$$\tilde{p}_n(\tau) = 2(-1)^n \operatorname{erfc}\left(\frac{1}{2} \frac{(2n+1)}{\sqrt{\psi}\sqrt{\tau-(2n+1)}} \right) \qquad \text{(A-9)}$$

where

$$\text{Real } \tilde{s} > 0$$

and

$$\text{Real } \frac{(2n+1)^2}{\psi} > 0$$

The first restriction is satisfied along the inversion contour, and consequently, so is the restriction on equation A-5. Since ψ is a positive real constant the second restriction is also satisfied.

The total pressure as a function of time is given by the summation of the terms given in equation A-9.

$$\tilde{p}(\tau) = \sum_{n=0}^{2n+1 < \tau} 2(-1)^n \operatorname{erfc}\left(\sqrt{\frac{(2n+1)^2}{4\psi\left[\tau-(2n+1)\right]}} \right) \qquad \text{(A-10)}$$

The upper limit on the summation takes the form given here in order to satisfy equation A-8. The solution obtained from A-10 is compared with the high frequency approximation of Section One in figures A-1 and A-2.

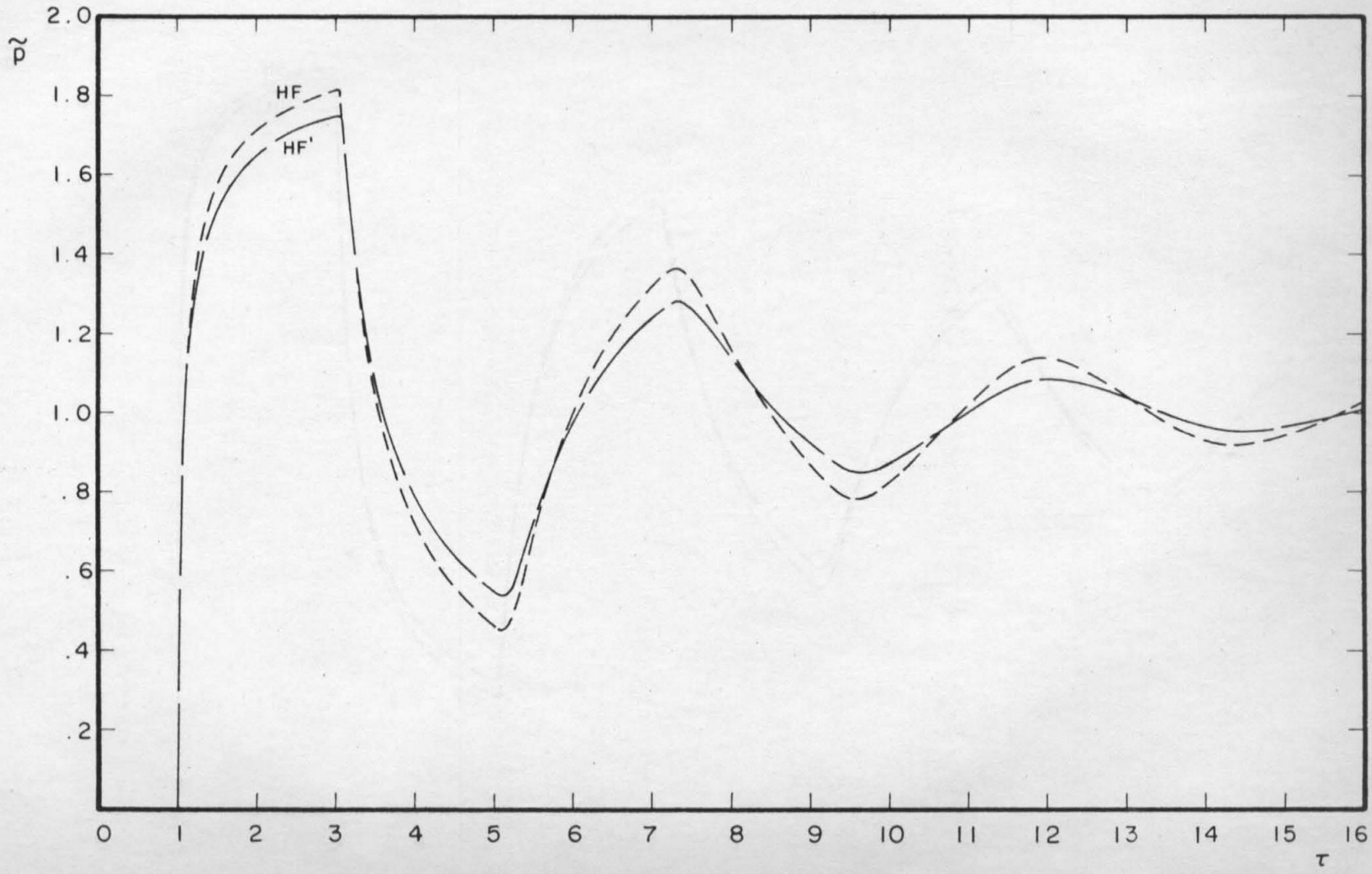

Figure A-1. Transient Response - $\upsilon = 0.0$; $\psi = 10$

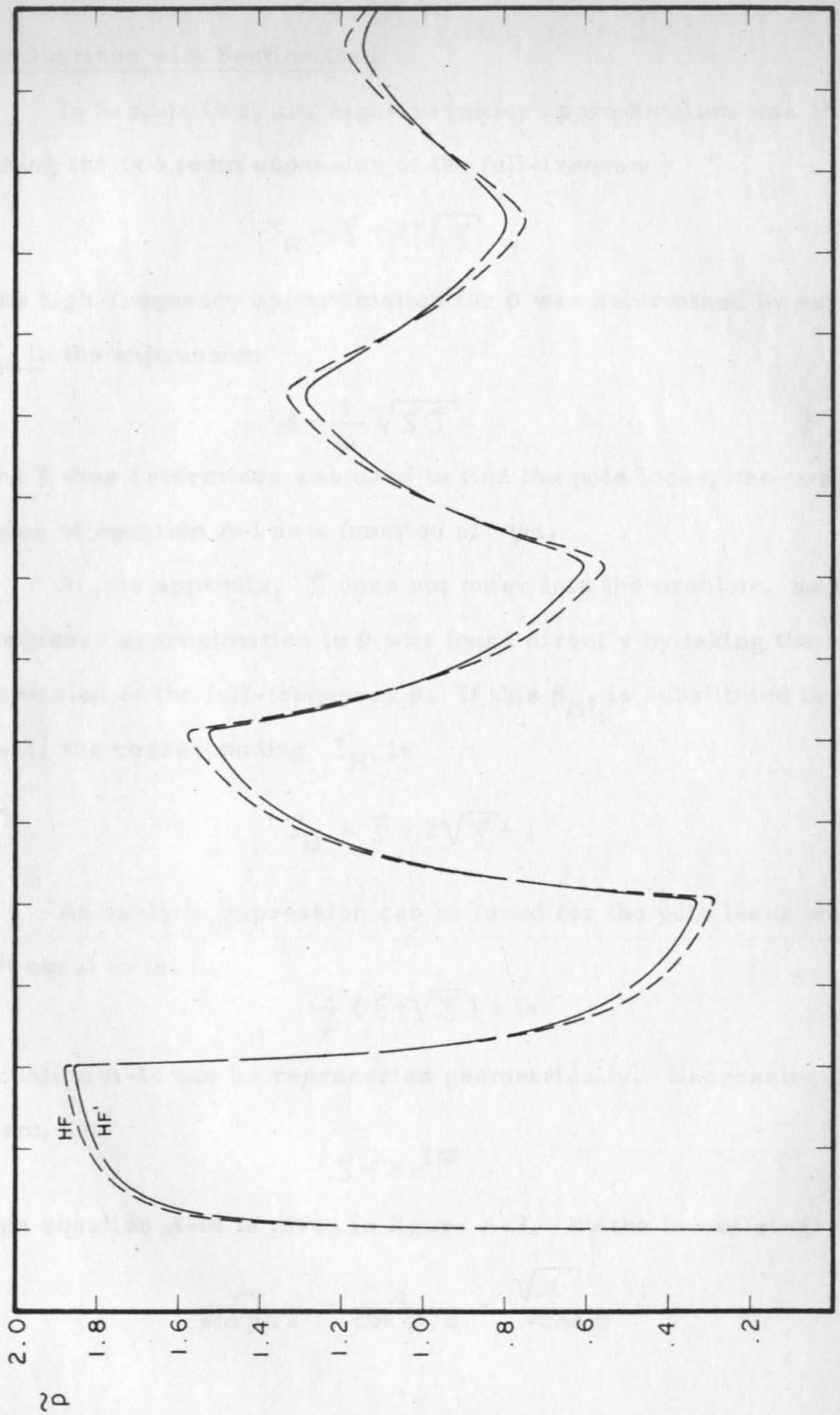

Figure A-2. Transient Response - $\upsilon = 0.0$; $\psi = 30$

Comparison with Section One

In Section One, the high-frequency approximation was obtained by taking the two term expansion of the full-frequency ζ.

$$\zeta_H = \xi + 2\sqrt{\xi} \tag{A-11}$$

The high-frequency approximation for β was determined by using this ζ_H in the expression

$$\beta = \frac{1}{\psi}\sqrt{\xi\,\zeta} \tag{A-12}$$

The β thus determined was used to find the pole locus, the position of the poles of equation A-1 as a function of ψa.

In this appendix, ζ does not enter into the problem, so the high-frequency approximation to β was found directly by taking the two term expansion of the full-frequency β. If this $\beta_{H'}$ is substituted into equation A-12, the corresponding $\zeta_{H'}$ is

$$\zeta_{H'} = \xi + 2\sqrt{\xi} + 1 \tag{A-13}$$

An analytic expression can be found for the pole locus when $\beta_{H'}$ is set equal to ia.

$$\frac{1}{\psi}\left(\xi + \sqrt{\xi}\right) = ia \tag{A-14}$$

Equation A-14 can be represented geometrically. Expressing ξ in polar form, let

$$\xi = r e^{i\varphi}$$

then equation A-14 is given in figure A-3. By the law of sines,

$$\frac{\psi a}{\sin \varphi/2} = \frac{r}{\cos \varphi/2} = \frac{\sqrt{r}}{-\cos \varphi} \tag{A-15}$$

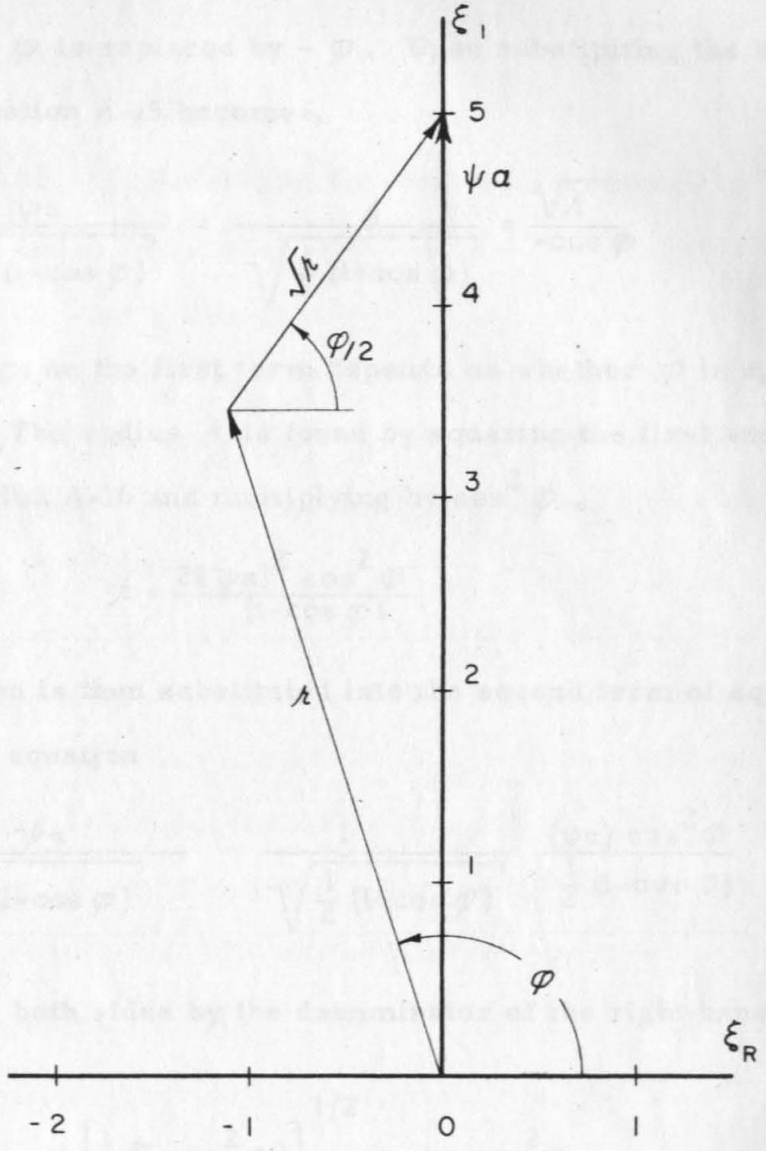

Figure A-3. Geometric Representation of Equation A-14

where for $a > 0$

$$\frac{\pi}{2} \leq \varphi \leq \pi$$

and for $a < 0$, φ is replaced by $-\varphi$. Upon substituting the half-angle identities, equation A-15 becomes,

$$\frac{\psi a}{\pm\sqrt{\frac{1}{2}(1-\cos\varphi)}} = \frac{\rho}{\sqrt{\frac{1}{2}(1+\cos\varphi)}} = \frac{\sqrt{\rho}}{-\cos\varphi} \tag{A-16}$$

where the $\pm$ sign on the first term depends on whether φ is $\pm$, respectively. The radius ρ is found by squaring the first and third terms in equation A-16 and multiplying by $\cos^2\varphi$.

$$\rho = \frac{2(\psi a)^2 \cos^2\varphi}{(1-\cos\varphi)} \tag{A-17}$$

This expression is then substituted into the second term of equation A-16 to produce the equation

$$\frac{\psi a}{\pm\sqrt{\frac{1}{2}(1-\cos\varphi)}} = \frac{1}{\sqrt{\frac{1}{2}(1+\cos\varphi)}} \quad \frac{(\psi a)\cos^2\varphi}{\frac{1}{2}(1-\cos\varphi)}$$

By multiplying both sides by the denominator of the right-hand side, this becomes,

$$\pm\left[\frac{1}{4}(1-\cos^2\varphi)\right]^{1/2} = \psi a \cos^2\varphi$$

then using trigonometric identities it reduces to

$$\frac{1}{2}\sin\varphi = \psi a \cos^2\varphi = \psi a (1-\sin^2\varphi) \tag{A-18}$$

Equation A-18 is just the quadratic equation

$$\sin^2 \varphi + \frac{1}{2\psi_a} \sin \varphi - 1 = 0$$

for which the solution is

$$\sin \varphi = \frac{1}{4\psi_a} \left[-1 + \sqrt{1 + (4\psi_a)^2} \right] \qquad \text{(A-19)}$$

The solution that would have resulted from taking a negative-sign in front of the square root symbol, was thrown out since it produces a sine of less than -1, which is clearly inadmissible.

The procedure used here produces a pole locus that differs from the one determined in Section Three. This difference is shown in figure A-4. A comparison of the contributions due to the branch cut is given in Table A-1.

The results of this appendix were checked against the results of both the direct numerical evaluation of the inversion integral, and the residue theory calculations using the ζ_H given by equation A-13 and the pole locus determined by equations A-17 and A-19. The transient response was computed at $\tau = 2$, 8 and 14 for the cases $\psi = 5$, 10 and 30. The agreement was within $\pm$ 0.0001 at each of these points.

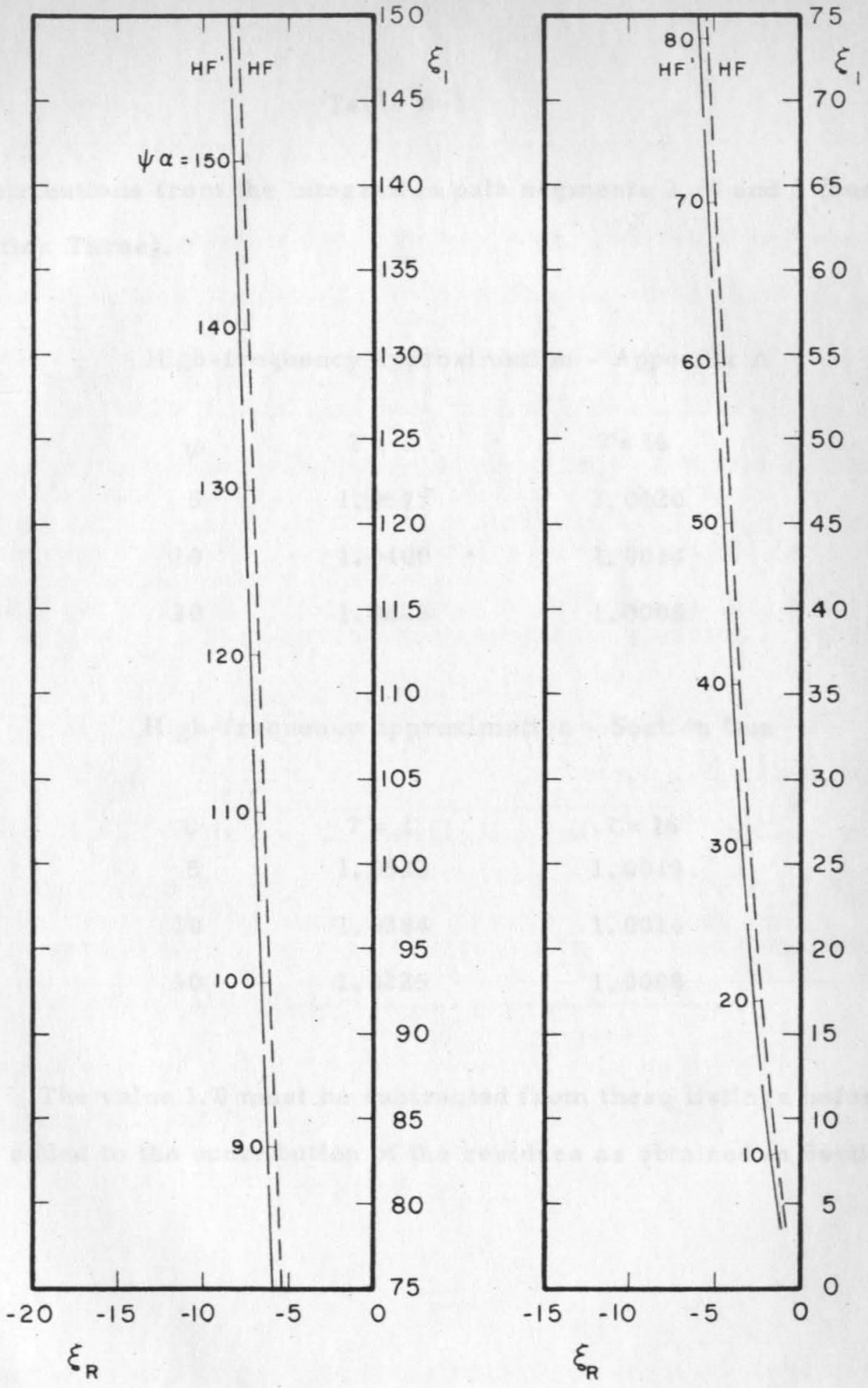

Figure A-4. Pole Locus - Overall View

Table A-1

Contributions from the integration path segments 3, 4 and 5 (see fig. 15, Section Three).

High-frequency approximation - Appendix A

ψ	$\tau = 1$	$\tau = 16$
5	1.0577	1.0020
10	1.0400	1.0014
30	1.0228	1.0008

High-frequency approximation - Section One

ψ	$\tau = 1$	$\tau = 16$
5	1.0532	1.0019
10	1.0384	1.0014
30	1.0225	1.0008

The value 1.0 must be subtracted from these listings before they are added to the contribution of the residues as obtained in Section Three.

APPENDIX B

COMMENTS ON IBERALL'S RESULTS

One of the results of the present study is a set of frequency response curves comparing the various approximate solutions for several values of the parameter ψ. Upon checking these results against the published data of Iberall (5), several discrepancies were found. In this appendix the frequency response curves of this work, for the theory which includes heat conduction, are compared with Iberall's results, as shown in figures 4 and 5 of his paper.

Iberall's expression for the frequency response of a volume-terminated tube is, (using his notation),

$$\frac{\tilde{\xi}_{OL}}{\xi_0} = \frac{\psi_T}{\psi_T \cosh \psi_T + \psi_I \sinh \psi_T} \tag{B-1}$$

and the corresponding expression given in Section Two is

$$\tilde{p}\,(1, \omega) = \frac{1}{\cosh \beta\Gamma + \frac{\upsilon\beta}{\Gamma} \sinh \beta\Gamma} \tag{B-2}$$

Equations B-1 and B-2 agree if:

$$\beta\Gamma = \psi_T \tag{B-3}$$

$$\frac{\upsilon\beta}{\Gamma} = \frac{\psi_I}{\psi_T} \tag{B-4}$$

Equations B-3 and B-4 hold if the velocity of sound in the tube c_T is set equal to the Laplace velocity of sound c, as it should be for the approxi-

mation considered here, and if

$$\frac{\upsilon}{\gamma} = \frac{\chi_{I0}}{\chi_{T0}}$$

where

$$\frac{8\gamma}{\psi^2} = \frac{\chi_{T0}}{z}$$

and

$$\xi = iz$$

where the terms on the left-hand side of these expressions are written using the notation of the present work, and terms on the right-hand side use Iberall's notation.

It should first be noted that Iberall's figures 4 and 5 are not frequency response curves, although they are plotted "as a function of a parameter proportional to frequency (χ_{T0})". They are plotted for a value of the parameter z = 6.25, where

$$z = \frac{\omega D^2}{4\nu_o}$$

If the diameter of the tube and the medium through which the sound is propagating are fixed, then the frequency is fixed. In this case, the curves are plotted as a function of the length of the tube squared. On each curve, the volume at the end of the tube is changing in such a manner that, as the length varies, χ_{I0}/χ_{T0} remains constant.

Iberall's figures 4 and 5 are reproduced here, for convenience, in figures B-1 and B-2. The true frequency response curves are given in figures B-3 and B-4. (The value of $\psi = 5.65$ was chosen so that the resonant peak for the case $\gamma = 1$, $\upsilon = 0$, would have the same maximum

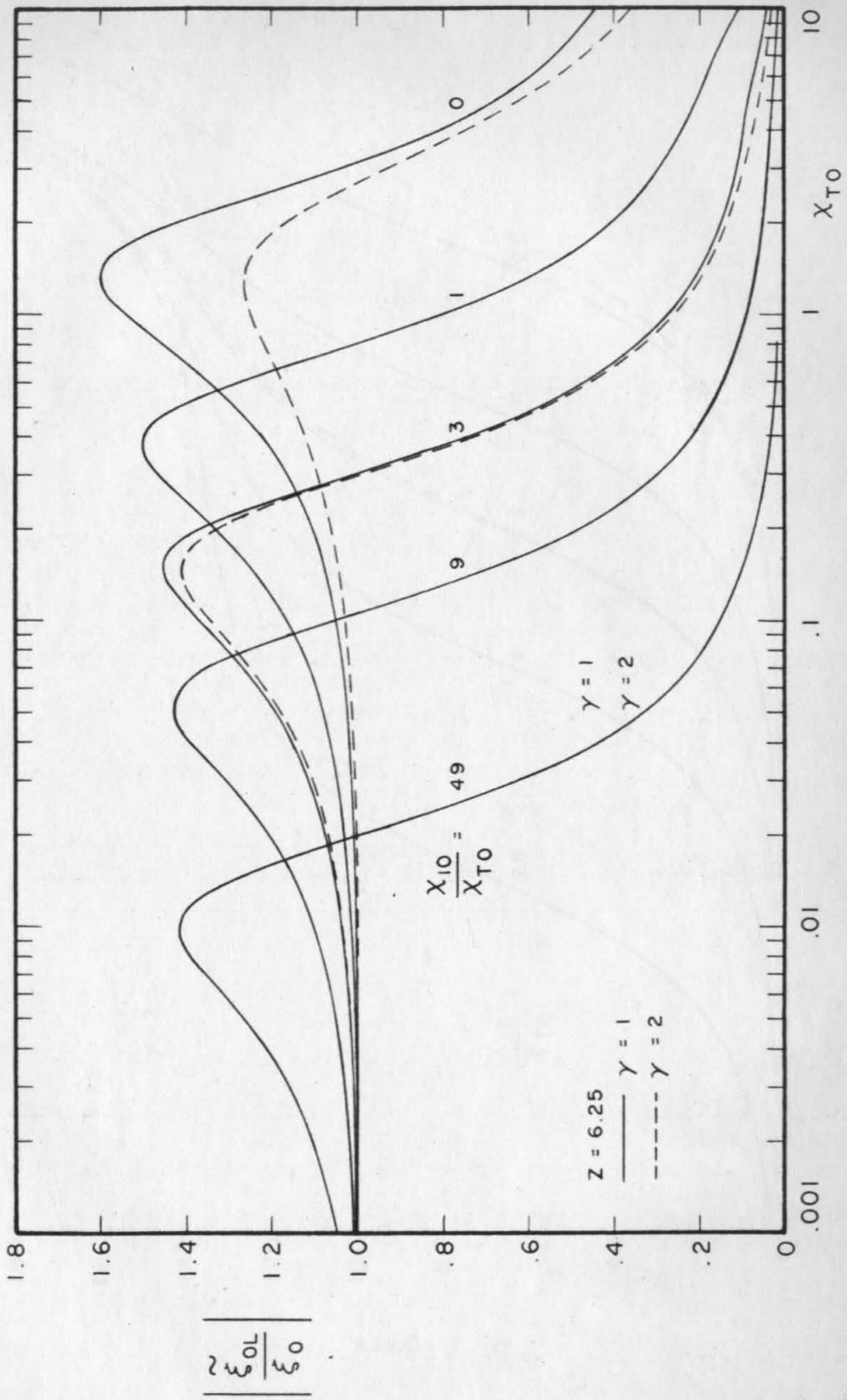

Figure B-1. Reproduction of Iberall's Fig. 4

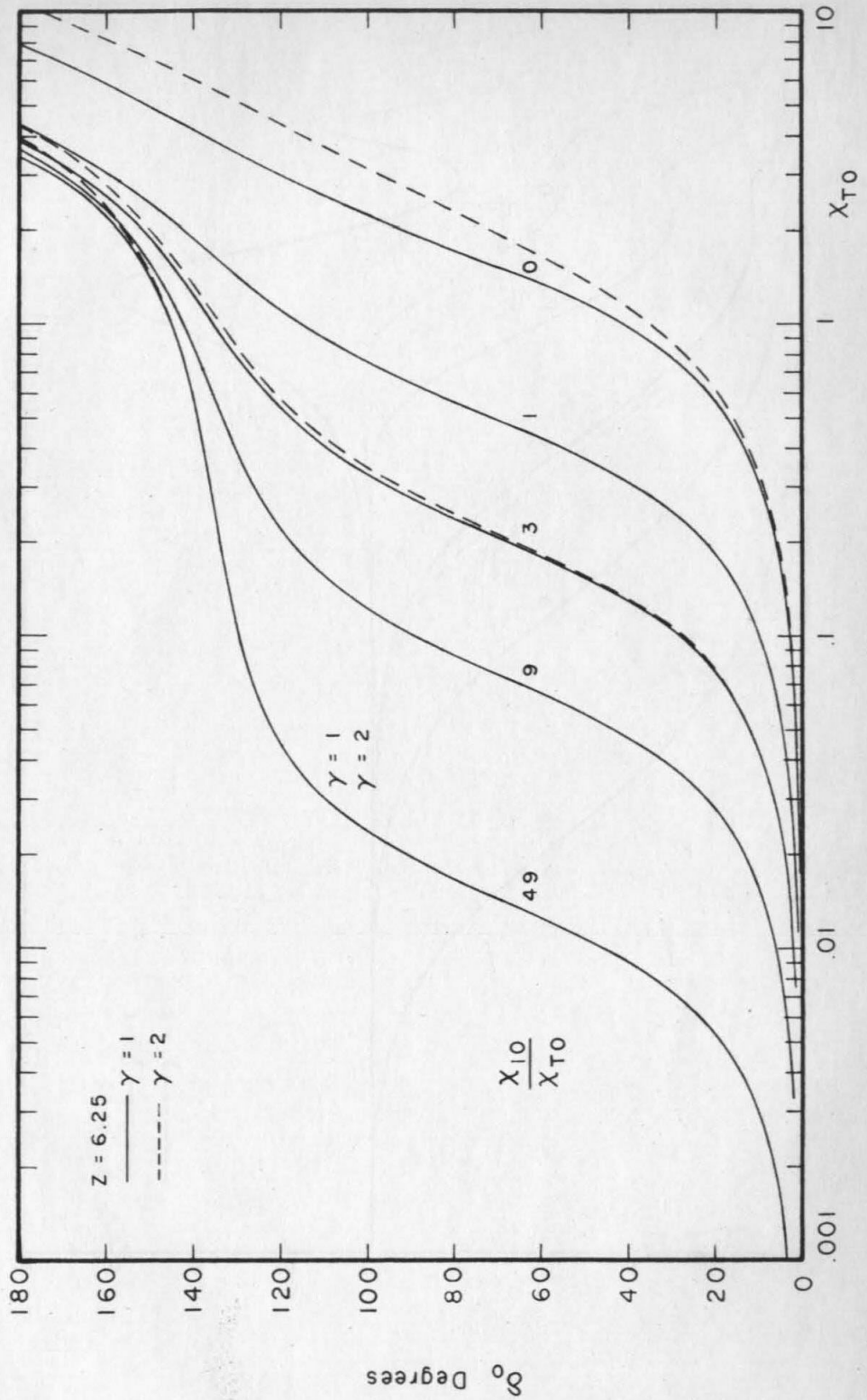

Figure B-2. Reproduction of Iberall's Fig. 5

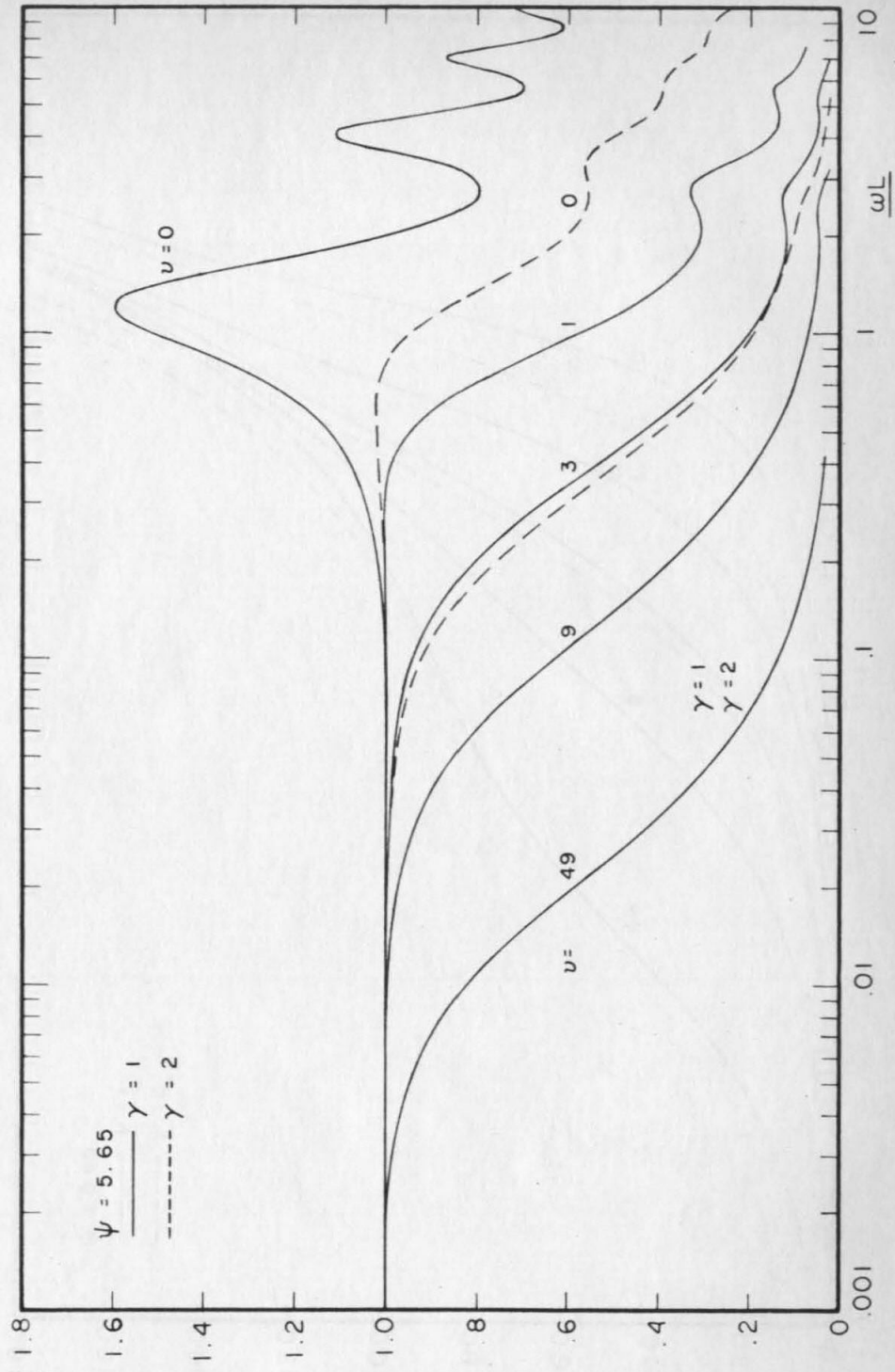

Figure B-3. Frequency Response - Amplitude

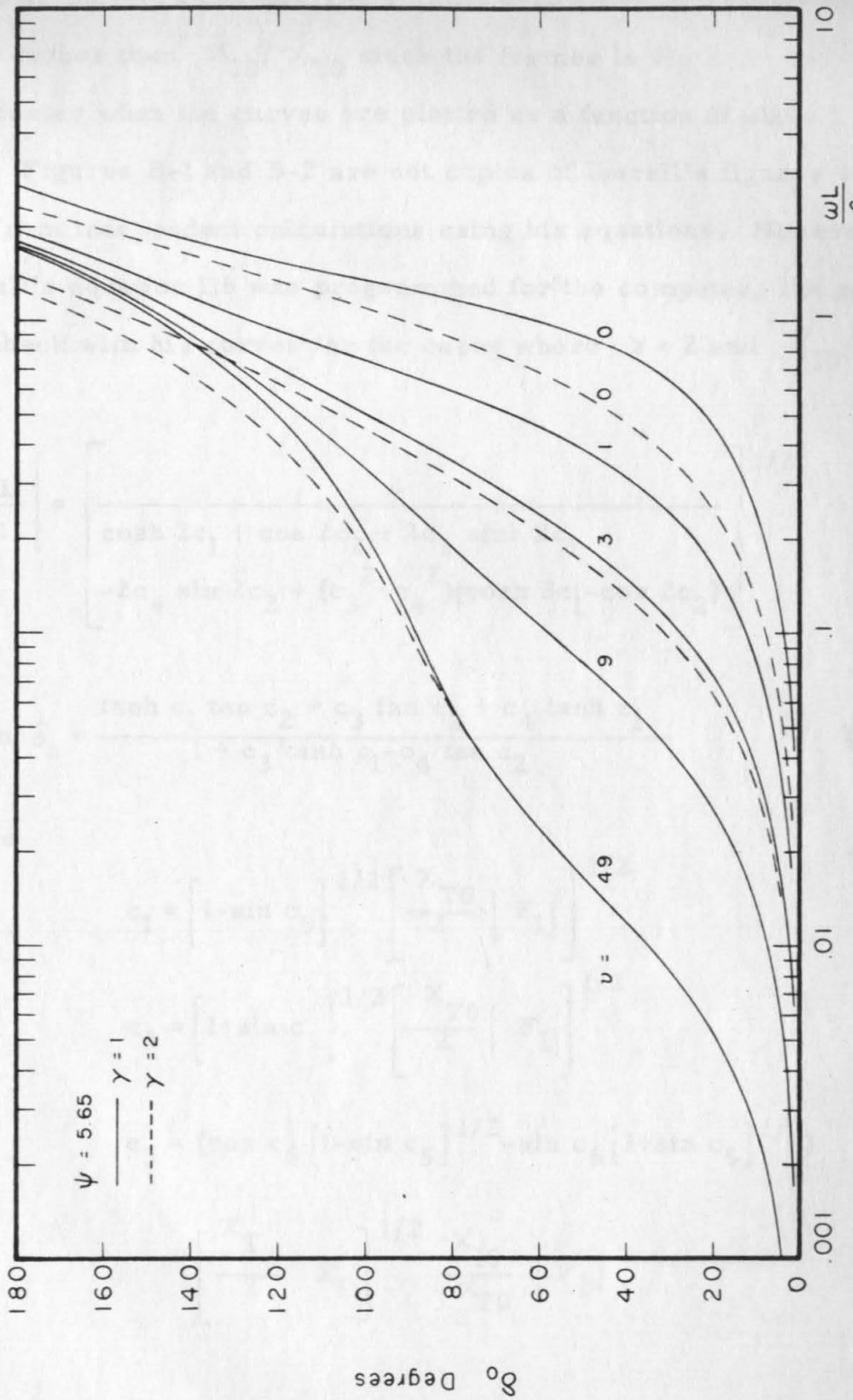

Figure B-4. Frequency Response - Phase

value as Iberall's curve. The volume parameter in figures B-3 and B-4 is υ rather than χ_{I0}/χ_{T0} since the former is the more logical parameter when the curves are plotted as a function of $\omega L/c$.)

Figures B-1 and B-2 are not copies of Iberall's figures 4 and 5, but are from independent calculations using his equations. However, when Iberall's equation 116 was programmed for the computer, the results did not check with his curves for the cases where $\gamma = 2$ and $\chi_{I0}/\chi_{T0} = 49$ or 3.

$$\left| \frac{\tilde{\xi}_{OL}}{\xi_0} \right| = \left[\frac{2}{\cosh 2c_1 + \cos 2c_2 + 2c_3 \sinh 2c_1 \\ -2c_4 \sin 2c_2 + (c_3^2+c_4^2)(\cosh 2c_1 - \cos 2c_2)} \right]^{1/2}$$

$$\tan \delta_o = \frac{\tanh c_1 \tan c_2 + c_3 \tan c_2 + c_4 \tanh c_1}{1 + c_3 \tanh c_1 - c_4 \tan c_2} \qquad \text{(Ib-116)}$$

where

$$c_1 = \left[1-\sin c_5\right]^{1/2} \left[\frac{\chi_{T0}}{2} \left| F_1 \right| \right]^{1/2}$$

$$c_2 = \left[1+\sin c_5\right]^{1/2} \left[\frac{\chi_{T0}}{2} \left| F_1 \right| \right]^{1/2}$$

$$c_3 = (\cos c_6 \left[1-\sin c_5\right]^{1/2} - \sin c_6 \left[1+\sin c_5\right]^{1/2})$$

$$\left[\frac{\chi_{T_0}}{2} F_1 \right]^{1/2} \frac{\chi_{I0}}{\chi_{T0}} \left| F_2 \right|$$

$$c_4 = (\cos c_6 \left[1 + \sin c_5\right]^{1/2} + \sin c_6 \left[1-\sin c_5\right]^{1/2})$$

$$\left[\frac{\chi_{T0}}{2} \left| F_1 \right|\right]^{1/2} \quad \frac{\chi_{I0}}{\chi_{T0}} \left| F_2 \right|$$

$$F_1 = f_1 + g_1 j$$

$$F_2 = f_2 + g_2 j$$

$$\cos c_5 = \frac{f_1}{|F_1|}$$

$$\sin c_5 = \frac{g_1}{|F_1|}$$

$$\cos c_6 = \frac{f_2}{|F_2|}$$

$$\sin c_6 = \frac{g_2}{|F_2|}$$

and

$$F_1\left(h\frac{D}{2}, \gamma\right) = \left[\frac{1 + \dfrac{2(\gamma-1)J_1\left(h\frac{D}{2}\right)}{h\frac{D}{2}\, J_0\left(h\frac{D}{2}\right)}}{\gamma}\right]\left[\frac{\dfrac{\left(h\frac{D}{2}\right)^2}{8}}{\dfrac{2J_1\left(h\frac{D}{2}\right)}{h\frac{D}{2}\, J_0\left(h\frac{D}{2}\right)} - 1}\right]$$

$$F_2\left(h\frac{D}{2}, \gamma\right) = \left[\frac{\gamma}{1 + (\gamma-1)\dfrac{2J_1\left(h\frac{D}{2}\right)}{h\frac{D}{2}\, J_0\left(h\frac{D}{2}\right)}}\right] \qquad \text{(Ib-105)}$$

$$h\frac{D}{2} = (1-j)\frac{D}{2}\left[\frac{\omega}{2\nu_o}\right]^{1/2} \qquad \text{(Ib-102)}$$

where $j = \sqrt{-1}$.

Iberall's equation 116 is reproduced here except that the error in the sign in front of the sin c_6 term in the expression for c_4 has been corrected. This error appears to be typographical since it does not account for the discrepancy between his curves and the computer results. The computer results were checked against the completely independent program used to calculate the frequency response curves, figures 18 to 20 in this work, with perfect agreement.

By multiplying the volume by a number between 1.64 and 1.66, curves are produced, for the case $\gamma = 2$, that cannot be distinguished from Iberall's curves. This range is permitted by the limited resolution of the published curves. For values of 1.63 and 1.67 or beyond, the agreement is somewhat degraded.

It can be easily shown that for a tube with a volume ratio as large as 49, the curves plotted by Iberall should be independent of γ. For the range of values of χ_{T0} plotted, $\beta\Gamma$ is small compared to unity. Therefore only the first two terms in the expansion of equation B-2 need be considered.

$$\tilde{p} = \frac{1}{1 + \frac{(\beta\Gamma)^2}{2} + \nu\beta^2}$$

or by rearranging

$$\tilde{p} = \frac{1}{1 + \beta^2\left(\nu + \frac{\Gamma^2}{2}\right)} \qquad \text{(B-5)}$$

Making the substitutions:

$$\beta^2 = \frac{i\varsigma}{8\gamma} \chi_{T0}$$

$$\upsilon = \frac{\gamma \chi_{I0}}{\chi_{T0}}$$

where ς is fixed when z is held constant, equation B-5 becomes

$$\tilde{p} = \frac{1}{1 + \frac{i\varsigma \chi_{T0}}{8} \left(\frac{\chi_{I0}}{\chi_{T0}} + \frac{\Gamma^2}{2\gamma} \right)}$$

where

$$\frac{\Gamma^2}{2\gamma} = 0.5 \qquad \text{for } \gamma = 1$$

$$= 0.4054 - i\,0.0944 \qquad \text{for } \gamma = 2.$$

The difference between these two values is $0.0946 - i\,0.0944$, which is negligible when compared with 49. Therefore, the curves could have been plotted using the simplified expression

$$\tilde{p} = \frac{1}{1 + \frac{i\varsigma}{8} \left(\frac{\chi_{I0}}{\chi_{T0}} \right) \chi_{T0}}$$

which is independent of γ.

In all fairness to Mr. Iberall, it should be pointed out that for the type of problem he gives in his example calculations, the curves he plotted, as corrected here, are easier to use than the true frequency response curves.

REFERENCES

1. Delio, G. J., G. V. Schwent, and R. S. Cesaro, Transient Behavior of Lumped-Constant Systems, NACA TN 1988, 1949.

2. Taback, I., The Response of Pressure Measuring Systems to Oscillating Pressures, NACA TN 1819, 1949.

3. Rohmann, C.P., and E.C. Grogan, On the Dynamics of Pneumatic Transmission Lines, Trans. ASME, vol. 79, May 1957, 853-874.

4. Crandall, I.B., Theory of Vibrating Systems and Sound, Van Nostrand, New York, 1926, Appendix A.

5. Iberall, A.S., Attenuation of Oscillatory Pressures in Instrument Lines, Journal of Research, Research Paper RP2115, National Bureau of Standards, vol. 45, July 1950, 85-108.

6. Schuder, C.B., and R. C. Binder, The Response of Pneumatic Transmission Lines to Step Inputs, Trans. ASME, Series D, Journal of Basic Engineering, vol. 81, Dec. 1959, 578-584.

7. Weber, E., Linear Transient Analysis, Vol. II, Two-Terminal-Pair Networks, Transmission Lines, Wiley, New York, 1956.

8. Reid, R.J., and E.M. Kops, Dynamic Response of Remote Pressure Pickups, Instruments and Control Systems, vol. 32, Aug. 1959, 1202-1204.

9. Hilsenrath, J., et.al., Tables of Thermal Properties of Gases, National Bureau of Standards Circular 564, U.S. Government Printing Office, Washington, D.C., 1955.

10. Rayleigh, J.W.S., Theory of Sound, Vol. II, Dover Publications, New York, first American edition, 1945, sections 347-350.

11. Pai, S.I., Viscous Flow Theory, Vol. I, Laminar Flow, Van Nostrand, Princeton, N.J., 1956.

12. Batchelor, G.K., and R.M. Davies, editors, Surveys in Mechanics, G.I. Taylor 70th Anniversary Volume, Cambridge University Press, London, 1956, section entitled: Viscosity Effects in Sound Waves of Finite Amplitude, by M. J. Lighthill.

13. Mason, W.P., Electromechanical Transducers and Wave Filters, Van Nostrand, New York, second edition, 1948.

14. McLachlan, N.W., Complex Variable and Operational Calculus with Technical Applications, Cambridge University Press, London, 1939.

15. Erdélyi, A., W. Magnus, F. Oberhettinger, and F. G. Tricomi, Tables of Integral Transforms, Vol. I, Bateman Manuscript Project, McGraw-Hill, New York, 1954.

The following references were used in the development of computer programs for the Bessel and erfc functions, and/or checking the accuracy of the computer results.

16. Janke, E., and F. Emde, Tables of Functions with Formulae and Curves, Dover Publications, New York, fourth edition, 1945.

17. Dwight, H.B., Tables of Integrals and Other Mathematical Data, Macmillan, New York, revised edition, 1947, (sixth printing 1952).

18. Dwight, H.B., Mathematical Tables of Elementary and Some Higher Mathematical Functions Including Trigonometric Functions of Decimals of Degrees and Logarithms, McGraw-Hill, New York, first edition, third impression (with changes), 1941.

19. U.S. National Bureau of Standards, Table of the Bessel Functions $J_0(z)$ and $J_1(z)$ for Complex Arguments, Columbia University Press, New York, 1943.

20. U.S. National Bureau of Standards, Tables of the Error Function and Its Derivatives, Applied Mathematics Series 41, U.S. Government Printing Office, Washington, D.C., 1954.